STRUCTURE-BINDING ACTIVITY RELATIONS OF AMPHIPHILIC POLYMERS AND MACROPHAGE SCAVENGER RECEPTORS: IMPLICATIONS FOR THERAPEUTIC INHIBITION OF ATHEROSCLEROSIS

by

NICOLE M. PLOURDE

A Dissertation submitted to the

Graduate School-New Brunswick

Rutgers, The State University of New Jersey

in partial fulfillment of the requirements

for the degree of

Doctor of Philosophy

Graduate Program in Chemical and Biochemical Engineering

written under the direction of

Prabhas V. Moghe

and approved by

_____

_____

_____

_____

New Brunswick, New Jersey

October 2010

ABSTRACT OF THE DISSERTATION

Structure-Binding Activity Relations of Amphiphilic Polymers and Macrophage Scavenger Receptors: Implications for Therapeutic Inhibition of Atherosclerosis

By NICOLE M. PLOURDE

Dissertation Director: Prabhas V. Moghe

Scavenger receptors mediate the uptake of oxidized low density lipoprotein (oxLDL), leading to cholesterol accumulation and the development of atherosclerosis. A promising avenue of interest in the treatment of cardiovascular disease is the use of a scavenger receptor inhibitor. To this end, a series of polymers were designed based on a mucic acid backbone, aliphatic acid arms and polyethylene glycol tail. Molecular modeling and docking approaches were used to understand the structure-activity relationship (SAR) between the polymers and scavenger receptor class A (SR-A). The polymers containing hydrophobic-bound carboxylate groups were the most favorable binders to the SR-A model as well as the most efficient inhibitors of oxLDL accumulation. Mutant SR-A models were generated by replacing charged residues with alanine. All charged residues in the region were necessary, with Lys60, Lys63 and Lys66 having the greatest effect on binding. However, binding was not mediated by charge alone and the

polymer hydrophobic domain adjacent to the carboxylate group was found to be essential.

Based on these findings from Chapter 2, the next chapter focused on the polymer backbone. Polymer models were designed to investigate the influence of backbone stereochemistry, cyclic versus linear backbone, and aromatic versus aliphatic backbone. Molecular modeling and docking results indicate the ability of the backbone to favorably position the side chains and "lock" the ligand into position. *In vitro* results followed those seen in the modeling predictions, with two polymers showing promise. Thus, minute changes in polymer structures can sensitively affect SR-A binding affinities and modulate the competitive inhibition of oxLDL uptake.

This thesis also investigated the potential of amphiphilic polymers to target scavenger receptors and deliver a hydrophobic model drug reversing cholesterol accumulation. The polymers encapsulated hydrophobic agonist (GW3965) against nuclear Liver-X receptor α (LXR), which significantly increased the drug uptake over non-polymer delivery. In combination with the encapsulated LXR-agonist, the polymers reduced oxLDL by 88% *in vitro*. Thus, the thesis findings suggest that the system of amphiphilic polymers exhibited significant tunability for scavenger receptor targeting, which can be exploited both for inhibition of cholesterol uptake as well as modulating cholesterol trafficking.

ACKNOWLEDGEMENTS

This work was supported by grants from the American Heart Association (AHA), National Institutes of Health (NIH) and National Science Foundation (NSF), awarded to Professor Prabhas V. Moghe. Partial support was provided by the Rutgers NSF IGERT Program on Biointerfaces. I first thank my advisor, Professor Prabhas Moghe, for his strong guidance, good advice and support throughout my years in his research group. I thank Drs. Evangelia Chnari and Lu Tian for establishing the groundwork for this research, and for the mentorship provided by Dr. Chnari during my first years in the lab. I thank Sarah Sparks, Dr. Jinzhong Wang, Dr. Sarah Hehir and Professor Kathryn Uhrich of Rutgers Dept. of Chemistry and Chemical Biology for the synthesis of the polymers designed and investigated in my thesis research as well as their supportive and honest thoughts and feedback. I also express thanks to Dr. Nicole Iverson, my teammate in the cardiovascular group, for her collaboration and perspective throughout my graduate work. I show great gratitude for access to computational facilities at UMDNJ-Informatics institute and the academic computing services of UMDNJ with the aid of Dr. Sandhya Kortagere and Professor William J. Welsh, without whom much of my modeling would not have been achievable. Finally, and most importantly, I thank my parents, family, friends, and my husband. I consider myself very lucky to have such caring and encouraging people in my life.

TABLE OF CONTENTS

LIST OF FIGURES

Chapter 1

Chapter 2

Chapter 3

Chapter 4

Appendix

LIST OF TABLES

CHAPTER 1: Background and Significance

1.1: Cardiovascular Disease and Atherosclerosis

Atherosclerosis is triggered by interactions between macrophages, smooth muscle cells and their extracellular matrix molecules, subsequent to the pathologic build-up of low density lipoproteins (LDL) within the vascular wall region called intima. This condition leads to coronary heart disease, which is currently the single leading cause of death in America (Center for Disease Control, 2009) and by the end of 2010, cardiovascular disease will also be the leading cause of death in developing countries (World Health Organization, 2009). Also known as "hardening of the arteries", atherosclerosis is characterized by the deposition of fatty materials, cellular waste products, and calcium build up called plaque in the inner lining of an artery which thickens, causing a reduction in lumen diameter and blood flow. As the plaque grows it is vulnerable to rupture, freeing plaque matter to form blood clots that may obstruct blood vessels and initiate the development of life threatening acute clinical syndromes such as myocardial infarction and stroke [1]. More recently atherosclerosis has been characterized as an inflammatory disease [2]. Inflammatory cells (macrophages) are present and significant in all stages of the disease from early plaque development to plaque instability and rupture [3].

The progression towards disease begins with LDL which are the major carriers of cholesterol in the blood plasma [4]. LDL particles smaller than 70 nm circulating in the blood stream can cross the intact endothelium via transcytosis and can flux in and out of

the intima [5, 6] while larger particles can enter through areas of injured endothelium or arterial branching [7].

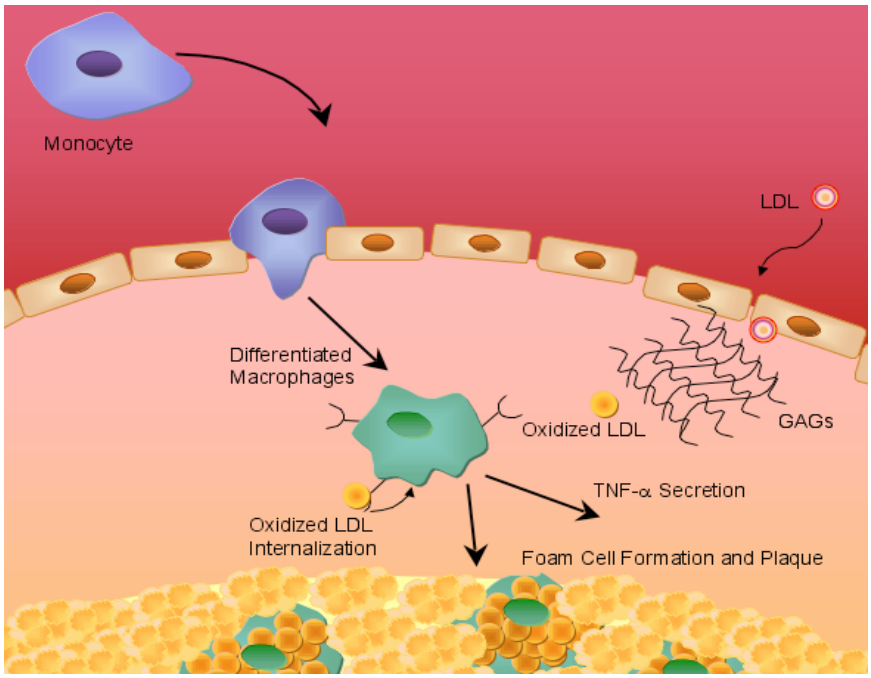

Figure 1.1: Schematic of the progression of atherosclerosis within the blood vessel wall

As shown in **Figure 1.1**, LDL enters the arterial wall where it is sequestered by extracellular matrix molecules, such as proteoglycans, and modified before release. The interaction between LDL and negatively charged proteoglycans involves apolipoprotein B, the main protein component on LDL, which contains positively charged amino acids [8]. The binding of LDL to proteoglycans in turn modifies apolipoprotein B (ApoB), rendering the molecules more susceptible to oxidation and modification and inhibiting efflux [9, 10]. However, the oxidation of LDL decreases the positive charge relative to native LDL, and thus lowers the affinity of LDL for proteoglycans [11]. Therefore, following modification, the oxidized LDL (oxLDL) is released from the proteoglycans and available to interact

with vascular cells. In addition, by-products produced during the oxidation process can cause cytotoxic damage to the vascular wall and inhibition of vasodilatation in response to nitric oxide [12, 13]. In the response-to-oxidation hypothesis, lipoprotein oxidation was proposed to be a key factor of atherosclerosis and later the response-to-retention model labeled the retention of LDL as the initiating step that lead to particle oxidation, vascular cell inflammation, and endothelial dysfunction [8, 14].

The earliest observable cellular event in the atherogenic process is the increased number of monocytes that are attracted to the endothelial surface, as a result of over-expression of adhesion molecules (VCAM-1, ICAM-1, selectins) induced by oxidative stress on endothelial cells [15, 16]. The adhered leukocytes next permeate the endothelial layer into the arterial intima, where they differentiate into macrophages [15]. Macrophages are present in variable numbers in all atherosclerotic lesions and are the most common cells found in fatty streaks [17]. LDL interacts with macrophages through various receptors subject to the degree of oxidation. Unoxidized, or native, LDL is internalized primarily by means of the LDL receptor and is controlled by feedback inhibition [18]. OxLDL uptake is mediated by scavenger receptors, which are typically not downregulated [19]. This leads to unregulated cholesterol accumulation, and results in the formation of foam cells and the formation of fatty streaks which are the earliest visible atherosclerotic lesions [20]. Activated foam cells secrete several substances, such as cytokines, growth factors and metalloproteinases, which in turn induce migration and proliferation of neighboring macrophages and smooth muscle cells [21]. As a result of these processes, fibrous cap formation and increased connective tissue synthesis are

observed [15]. The final step in the atherogenic cascade is the formation of a lipid-rich necrotic core, associated with destabilization of the advanced lesion which can lead to plaque rupture and the formation of occlusive thrombi. One key cellular event that may be associated with the formation of necrotic core is apoptosis and necrosis of the cells in the center of the plaque, as a response to accumulation of oxLDL and the resulting oxidative stress [1, 15].

1.1.1: Risk Factors

The occurrence of atherosclerosis among various individuals and groups may provide significant evidence to its pathogenesis. By and large, the propensity for atherosclerosis can be correlated to such factors as ages, family history, diet, smoking, diabetes, high blood pressure, high cholesterol, hyperlipidemia, and obesity [22]. Hyperlipidemia is the most significant factor among the major risks contributing to atherogenesis as it has been shown that elevated levels of LDL and triglyceride concentrations amplify the risk of cardiovascular disease [23]. Cholesterol and cholesterol esters derived from lipoproteins circulating in the blood accumulate in atherosclerotic plaques. Genetic disorders causing hypercholesterolemia often lead to early atherosclerosis and nearly one third of patients with premature coronary artery disease have distinctly increased quantities of LDL [23, 24]. In addition, elevated levels of LDL in the blood stream lead to a corresponding increase in uptake and arterial wall accumulation followed by activation of endothelial cells and facilitated expression of adhesion molecules [16]. Animal studies suggest that leukocyte adherence can be induced with

modification to the endothelium caused by hypercholesterolemia [15]. It is hypothesized that hypercholesterolemia in rabbits induces expression of specific adherence molecules such as VCAM-1 and E-selectin by the aortic endothelium [25]. The increased uptake and accumulation of lipoproteins in intimal macrophages initiates the cascade of events leading to the formation of atherosclerotic plaques.

1.1.2: LDL Retention within the Intima

Cholesterol has many vital physiologic roles in the body, but can be detrimental at higher concentrations, especially in the context of chronic inflammatory processes. The majority of cholesterol in the blood plasma exists as part of various lipoprotein complexes. These include chylomicrons, very low-density lipoproteins (VLDL), low-density lipoproteins (LDL) and high-density lipoproteins (HDL). However, LDL are the principal cholesterol carriers and transport cholesterol to cells throughout the body.

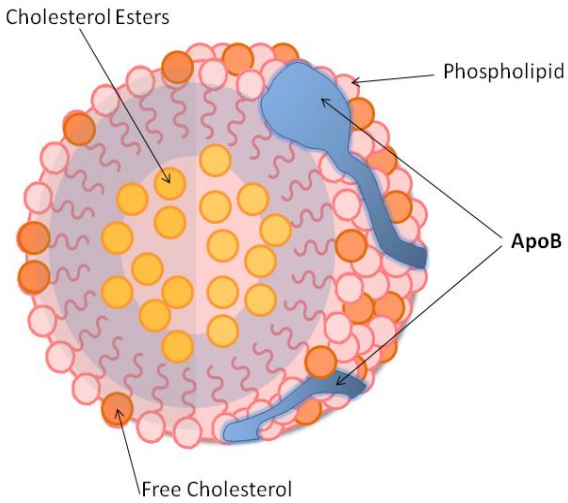

Figure 1.2: Illustration of the components that comprise an LDL particle

The LDL particle (see **Figure 1.2**) has an average diameter in the range of 17.5 – 22.5 nm can be thought of as having two distinct regions; a core and a surrounding surface layer [26]. As a result of these subcomponents, specifically lipid composition and ApoB conformation, the LDL particles are in a constant dynamic state in terms of structure and physical properties [27].

LDL particles circulating in the blood stream can cross the intact endothelium via transcytosis or can enter through areas of injured endothelium or arterial branching [7]. Subsequent to LDL entering the arterial wall, it can become trapped and sequestered in the extracellular matrix (ECM), which forms the space in contact with smooth muscle cells and macrophages. The primary matrix molecules within the vascular intima responsible for LDL retention are the glycosaminoglycans (GAGs), which when linked to core proteins form proteoglycans (PGs).

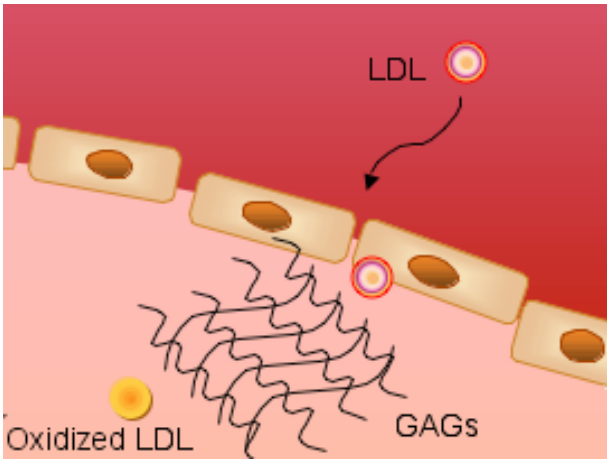

Figure 1.3: LDL entering the artery wall is sequestered by GAGs

The GAGs (see **Figure 1.3**) play various roles in the vascular wall, but are made up of carbohydrate chains consisting of negatively charged repeating disaccharide units, which form reversible ionic interactions with positively charged residues in LDL,

specifically ApoB [28-31]. It has been demonstrated that the occurrence of LDL-GAG complexation increases the cholesterol accumulation in macrophages due to irreversible changes that occur in the conformation of ApoB after binding to GAGs which leaves LDL vulnerable to modifications that inhibit their efflux [9, 10]. LDL-GAG binding results in a virtually irreversible structural modification to the LDL surface and renders the LDL vulnerable to oxidation. It is well known that the accumulation of oxLDL within the vascular intima intensifies the development of atherogenesis and can also induce foam cell formation [20]. Upon oxidation of LDL, the lysine residues of ApoB are neutralized, reducing the positive charges, and lowering the affinity of oxLDL for GAGs [11]. The uptake of oxLDL by macrophages is also a result of modified lysine residues which are recognized by scavenger receptors [32]. This suggests that the same ApoB modifications which decrease LDL-GAG binding lead to an increase in LDL uptake via scavenger receptors.

1.1.3: Oxidized LDL

It was first suggested that oxLDL was an important factor in atherogenesis when it was demonstrated that oxLDL was detrimental to arterial cells [33]. Pro-inflammatory effects of oxLDL on vascular cells include increases in proliferation [34], expression of inflammatory cytokines [35], toxicity [36], increased expression of metalloproteinases [37], inhibition of expression of inducible nitric oxide synthase [38], and effects on macrophage lipid metabolism and accumulation [39-41]. OxLDL has the ability to be rapidly taken up by macrophages which leads to the formation of foam cells [19, 20]. However, oxLDL also

possess many other characteristics that have been demonstrated to advance atherogenesis. For circulating monocytes, oxLDL itself is a chemoattractant, due to the generation of lysophosphatidylcholine from conversion of LDL into its oxidized form, while also stimulating endothelial cells to release monocyte chemoattractant protein-1 and macrophage colony-stimulating factor, which attract circulating monocytes to areas of accumulated oxLDL and can stimulate them to differentiate into macrophages [42, 43]. In addition, unlike native LDL, oxLDL is cytotoxic to endothelial cells, which triggers a loss of endothelial integrity, and has also been shown to stimulate matrix metalloproteinase (MMP) secretion, which may play a role in plaque instability by weakening the fibrous cap of atherosclerotic plaques [44, 45]. Lipid hydroperoxides break up into small reactive aldehydes which attack the α-amino groups on ApoB, increasing the net negative charge of the LDL particle.

1.1.4: Macrophages and LDL Metabolism

Through a series of reactions, intimal macrophages take up and metabolize LDL. Cellular cholesterol metabolism is controlled by multiple pathways including enzymes, such as phospholipases, which metabolize phospholipids through acylhydrolases, lysophospholipases or phosphodiesterases, [46-48] and transcription factors [49], including AP-1[50, 51], NF-K B[50], PPAR[52] and LXR[53]. The uptake is mediated by the process of receptor-mediated endocytosis or phagocytosis of cell membranes containing cholesterol (see **Figure 1.1**[19, 54]). Once endocytosed, LDL protein and cholesterol ester components are transported to the lysosomes. The lysosomes liberate the cholesterol

which then enters the cytoplasm by passing across the lysomal membrane. Here enzymes re-esterify the cholesterol and lastly it is stored in the cytoplasm in the form of cholesterol ester droplets, or it is excreted from the cell, depending on the presence of a cholesterol acceptor [55, 56].

In contrast to native LDL, oxLDL is not degraded as rapidly. Macrophages, in general, will not accumulate large amounts of lipid in the form of native LDL, however oxLDL uptake will lead to lipid accumulation and foam cell formation [19]. It has been shown that modified ApoB of oxLDL is unaffected by acid proteolysis and as a result accumulates in lysosomes and also may inactivate lysosomal acid hydrolases [57-60]. In addition, native LDL and oxLDL differ as to the manner in which they are taken up by macrophages. Unoxidized, or native, LDL is internalized primarily by means of the LDL receptor via clathrin-mediated endocytosis and is controlled by feedback inhibition, which means that cell surface receptors are down-regulated as the intracellular cholesterol levels increase. OxLDL uptake is mediated by scavenger receptors.

1.1.5: Scavenger Receptors and oxLDL

A key breakthrough in the study of modified lipoproteins was made by Goldstein, Brown, and associates when they showed that incubating macrophages with acetylated low density lipoprotein (AcLDL) produced intracellular accumulation of cholesterol and resulted in foam cell formation, which implied the presence of a macrophage receptor for chemically modified LDL which could possibly play an important role in atherogenesis [19]. The phrase “scavenger receptor’’ was coined to describe the activity

of macrophages that mediates the uptake of modified LDL in cell culture. These receptors recognize a broad range of ligands, hence the term "scavenger receptor". However, the overlapping binding behavior between the receptor classes can make it challenging to characterize their respective behaviors in terms of ligand uptake. For example, most scavenger receptors bind an array of polyanionic ligands [61].

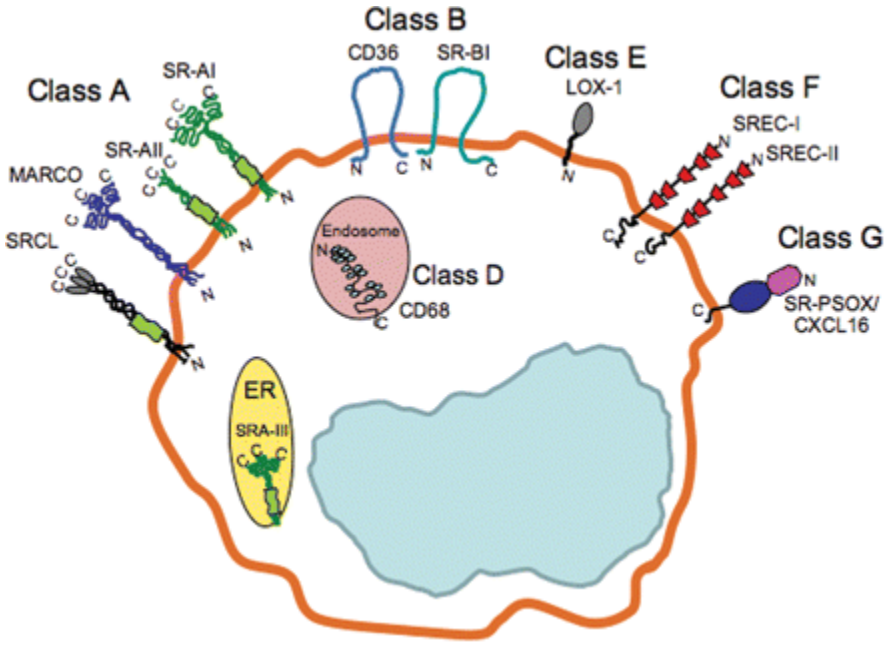

Figure 1.4: Examples of the seven macrophage scavenger receptor classes. Of these, SRA and CD36 are key to atherogenesis. [62]

A number of different scavenger receptors for oxLDL have been identified and the receptors are grouped into classes A through G, according to their structure as illustrated in **Figure 1.4** [62]. These include SR-AI/II/III, macrophage receptor with collagenous structure (MARCO), SR-BI, CD36, SR-C, CD68, LOX-1, and SR-PSOX. The significance of some of these oxLDL receptors has not been fully quantified *in vivo*; however SR-A and CD36 have been established to be central to atherogenesis. Kunjathoor et al. demonstrated, through the use of transgenic mice lacking both SR-A

and CD36 scavenger receptors that together, the receptors accounted for nearly 90% of total oxLDL uptake by macrophages [63]. In addition, Nakagawa-Toyama and colleagues completed an investigation of CD36 and SR-A expression in human atherosclerotic lesions suggesting that CD36 expression is highest in the center of the atheroma, within macrophage foam cells, and SR-A is expressed in cells closer to the lumen of the artery [64]. Beside SR-A and CD36, a recent class of scavenger receptors has also emerged as an endothelial cell target, called LOX-1. LOX-1 activity was recently proposed as a novel predictive marker of coronary heart disease and stroke [65]. Upon recognition of oxLDL, LOX-1 initiates oxLDL internalization and degradation as well as inducing a variety of pro-atherogenic cellular responses, such as reduction of nitric oxide (NO) release [66], secretion of monocyte chemoattractant protein-1 (MCP-1) [67], production of reactive oxygen species [68], expression of matrix metalloproteinase-1 and -3 [69], monocyte adhesion [67], and apoptosis [70].

SR-A

SR-A is principally expressed on macrophages, although the receptors have also been identified on endothelial and smooth muscle cells [71]. Class A receptors can bind modified LDL (both acLDL and oxLDL), polynucleic acids, bacteria and bacteria fragments, and certain carbohydrate-based ligands [72]. Early assessments on the ability of SR-A deficient macrophages to take in oxLDL implied that the receptor was responsible for at least 50% of OxLDL uptake [73]. Despite this partial prevention of oxLDL uptake by macrophages, SR-A knockout mice show a considerable decrease in atherosclerotic lesions in the apoE–/– and LDLR–/– mouse models [73, 74].

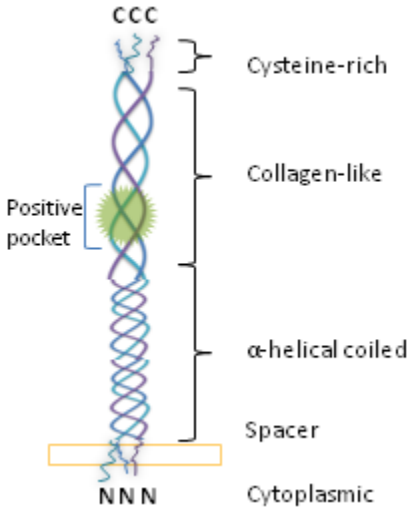

Figure 1.5: Illustration of the SR-A scavenger receptor and five distinct domains

The SR-A structure (**Figure 1.5**) consists five distinct segments totaling 451 amino acid residues: a cysteine-rich C-terminal region, a collagen-like region, a segment of α-helical coiled-coils, a single transmembrane domain, and an N-terminal cytoplasmic domain [75]. It has been reported that a cluster of four lysines within the collagen-like region is responsible for ligand recognition, as changing these basic amino acids to neutral residues eliminated ligand binding [76]. This is especially noteworthy as SR-A is known to principally bind to anionic ligands. The cycle of SR-A begins when the receptor binds to oxLDL at the cell surface and the complexes (SR-A + oxLDL) cluster in vesicles and clathrin-coated pits before becoming internalized and delivered to the endosomes. Once in the endosomes, the acidic pH causes the receptor to release the ligand and the receptor is then likely recycled to the cell surface [77].

1.2: Treatment of Atherosclerosis

Therapeutic treatments are widely used to combat cardiovascular diseases and can be either curative or preventative in nature. Curative treatments target existing arterial blockages to restore blood flow to an obstructed vessel and include balloon angioplasty and bypass surgery. Preventative treatments commonly target the control of lipoproteins, in an effort to prevent LDL accumulation and the formation of the fatty streak either through a reduction in LDL synthesis (cholesterol-reducing drugs), or management of LDL transport in the arterial wall.

1.2.1: Preventative Treatments

Research indicates that a 10% increase in serum cholesterol levels will result in 27% increase in risk of coronary heart disease [78]. Evidence has verified that elevated cholesterol levels increase the probability of coronary heart disease and that by reducing cholesterol levels there is an analogous decrease in risk [79, 80]. There are five main categories of cholesterol lowering medications: statins, bile resins acid, nicotinic acid, fibrates and ezetimibe. Nearly all are obtainable only by prescription, while nicotinic acid, a form of vitamin B3 (niacin), is available over–the–counter. HMG CoA reductase inhibitors, or statins, operate by reducing liver cholesterol synthesis and triggering upregulation of liver LDL receptors. This, consequentially, increases the uptake of LDL and decreases plasma LDL levels [81]. Bile acid resins help to increase the excretion of bile acids (the substance to which the liver converts cholesterol) from the intestines. The liver responds by increasing the conversion of cholesterol into bile acids,

which in turn causes an upregulation of LDL receptors and increases the removal of LDL from circulation [82]. Nicotinic acid decreases the amount of VLDL particles secreted from the liver and fewer particles are available to be converted into LDL [82]. Fibrates are effective by reducing triglyceride production and increasing the rate at which circulating triglycerides are removed from the blood stream. They are less effective at reducing LDL cholesterol levels while modestly increasing HDL cholesterol levels in most patients. Ezetimibe is a member of a class of selective inhibitors that prevents the absorption of cholesterol by inhibiting the migration of dietary and biliary cholesterol across the intestinal wall without preventing the absorption of other soluble food nutrients [83].

1.2.2: Issues Related to Cholesterol Reducing Drugs

While preventative medication can successfully lower cholesterol synthesis and reduce accumulation, there are numerous associated side effects. Polyneuropathy, a form of nerve damage, is the simultaneous malfunction of many peripheral nerves throughout the body and can be caused by statins. Although rare, this condition causes pain, tingling, loss of feeling, weakness and damage that may be long lasting or even permanent [84]. A popular statin, Lipitor, recently came under increased scrutiny as the medication's maker, Pfizer Inc., has been sued by users experiencing lasting muscle damage [85]. There are additional side effects connected with statins as well. Especially at the highest doses prescribed as part of an aggressive lipid management strategy, statins can adversely affect liver function.

A rare, but potentially terminal side effect of statins and some fibrates is rhabdomyolysis [86]. In rhabdomyolysis, muscle cells break down and release their contents into the bloodstream which, in rare cases, can lead to organ failure and death [87]. Various other cholesterol reducing drugs have reportedly caused muscle aches, allergic reaction, abdominal pain, headache, heartburn, blurred vision, drowsiness, weakness or fatigue and nausea but are seen in low frequencies [82].

Questions have been raised about the possibility that pharmacologic intervention aimed at reducing cholesterol levels may increase the risk for nonvascular diseases. This has led to uncertainty of the benefits of drug therapy, especially for those without known coronary heart disease [88, 89]. Thus, there is a critical need to develop integrative approaches to prevent escalation of atherosclerosis, which arises from the accumulation of oxLDL and the subsequent uncontrolled uptake by macrophages. The target should not only be cholesterol synthesis, but also the mechanism by which macrophages interact with modified lipoproteins.

1.2.3: Cardiovascular Disease and Nanomedicine

There are numerous medications currently available that help patients lower their cholesterol levels in addition to surgical procedures used to treat patients with vessel blockages. Unfortunately, these options are not problem-free and are plagued with adverse side effects. “Nanomedicine” as termed by the National Institutes of Health (Bethesda MD, USA) is a field that offers potential solutions to traditional cardiovascular disease treatment options. Recent advances in nanotechnology for

cardiovascular health are abundant and include the application of nanosensors to monitor nitro-oxidative species (oxidative stress) produced in the failing heart [90], microarrays and microchips for the study of complex traits associated with cardiovascular diseases providing new insights into possible pathogenetic mechanisms and new therapeutic approaches [91], electrospun nanofibers as potential materials for tissue engineered vascular grafts [92-94], and carbon nanotubes as possible implant materials for their anticoagulant function and antithrombotic properties [95, 96].

Nanotechnology can also be used to improve drug efficacy through targeted delivery. Most systemically introduced drugs circulate through the entire body, leading to difficulty in maintaining an optimal concentration in disease-specific areas because of metabolism and excretion of drugs, as well as toxicity in nonrelated tissues [97]. By encapsulating drugs in nanospheres [98] or erodible self-assembled structures [99] specificity in drug release can be introduced.

One avenue of particular interest is the use of a nanolipo-blocker to prevent oxLDL uptake via scavenger receptors. Native LDL does not stimulate foam cell formation while binding of oxLDL to macrophage scavenger receptors leads to unregulated cholesterol accumulation which results in foam cell formation [20, 100]. Therefore, any approach directed at lowering LDL accumulation within the vascular intima should prevent this uncontrolled uptake via scavenger receptors. As described previously, SR-A and CD36 appear to be of primary importance in atherogenesis, demonstrated by mice lacking either receptor show considerable reduction in lesion formation [63, 101]. Previous investigations have been completed on synthetic compounds

that can bind to scavenger receptors, potentially blocking modified LDL entry into cells [102-105]. Synthetic oxidized phospholipids (oxidized phosphocholine) cross-linked to a hexapeptide or bovine serum albumin (BSA) have been used as pattern recognition ligands for CD36 and have been shown to viably inhibit the binding of oxLDL to CD36 expressing cells [102]. In addition, sulfatide derivatives for the targeting of SR-A have been synthesized and investigated and have been shown to reduce acetylated LDL binding and uptake in a concentration-dependent manner [103]. Although these previous efforts to develop scavenger receptor inhibitors to block modified LDL uptake are encouraging, the role of a 3-D organized presentation of the targeting groups to increase efficiency of the inhibitors had not been investigated. Additionally, the previously synthesized particles are not multifunctional, but instead target a single scavenger receptor, while the remaining scavenger receptors are free to bind and internalize oxLDL.

Nanoscale Amphiphilic Polymers

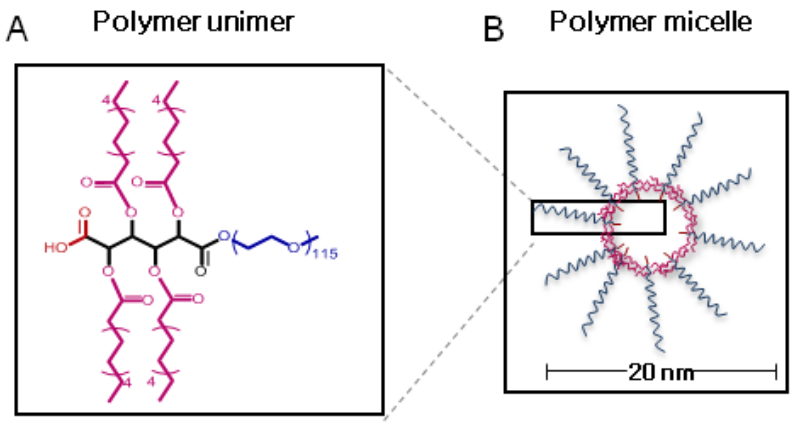

Figure 1.6: AScM unimers (A) aggregate to form micelles (B) in solution

Tian, et al., a former collaborator on this project in the laboratory of Dr. Kathryn Uhrich, previously described a unique class of polymers, amphiphilic scorpion-like macromolecules (AScM) [106]. The AScM (**Figure 1.6**) is composed of unimers that self organize into micelles with the ability to bind to macrophage scavenger receptors and reduce the uptake of oxLDL [107, 108]. Additionally, AScMs may have the potential to be hydrophobic drug carriers as the polymers have low critical micelle concentration (CMC), low cytotoxicity, high drug loading efficiency, and sustained release [106, 109].

The unimers of AScM are identified as M12P5 which corresponds to a mucic acid (M) with aliphatic acid chains of 12 carbons (12) and polyethylene glycol (PEG) chains (P) with a molecular weight of 5 kDa (5). These building blocks are naturally occurring or biocompatible compounds and are joined via biodegradable ester bonds. PEG contributes to the polymer's hydrophilicity and is used to prevent the non-specific adsorption of proteins, mucic acid is a multi-hydroxylated saccharide providing reaction sites for further polymer modification, and aliphatic acid chains control the polymer hydrophobicity. The branched hydrophobic core aids in micellar stability, as seen by the low CMC, as well as increases the micelle's capacity to self-assemble. The nanoassemby also has a small aggregation diameter (~20 nm) [106]. Previous studies have focused on anionic AScMs that spontaneously form micelles at concentrations above the CMC (10^{-7}M) [106]. In addition, the micellar organization of the nanoparticle is able to encapsulate, and potentially deliver a drug of interest to scavenger receptor expressing cells [109].

AScM polymers have two therapeutic advantages. They not only have the capacity to prevent the internalization of oxLDL by competing with oxLDL for access to scavenger receptors, but the polymers also compete with GAGs for binding to native LDL, thus facilitating the uptake of native LDL before extensive oxidation occurs [107, 110]. In preliminary studies, the AScM was functionalized with a carboxylic acid, such that the micellar polymer displays anionic charges in an organized and clustered configuration. Previous findings by Dr. Evangelia Chnari from the Moghe laboratory show that anionic AScMs reduced oxLDL uptake in murine IC21 macrophages by up to 75% after 5 hr, and both SR-A and CD36 receptors were involved in the uptake of the polymers and highly oxidized LDL (hoxLDL) [107, 108]. AScMs have also been shown to be effective in binding to native LDL (nLDL) and mildly oxidized LDL (moxLDL) [110]. As LDL particles become more highly oxidized, they were shown to no longer form complexes with the polymers.

The primary interaction of the polymers with differentially oxidized LDL (nLDL, moxLDL and hoxLDL) and scavenger receptors (SR-A and CD36) is one of charge-based electrostatic interactions. Native LDL has a net positive charge but becomes less positive as the particle is oxidized. As a result, the anionic AScM complexes with native LDL, and to some extent, moxLDL, but not hoxLDL. In addition, the anionic nanopolymers can bind to scavenger receptors, like SR-A, which has a positive pocket.

Drug Encapsulation for Expanded Targeting

The micellar structure of the AScM polymers has the ability to encapsulate, and potentially deliver a drug of interest to scavenger receptor expressing cells for

internalization [109]. The amphiphilic composition of the polymers allows for hydrophobic drugs to be protected from solution and increase their solubility, therefore, increasing the drug concentration in a solvent such as blood. Moreover, the nanoscale size of the micelles could potentially allow for delivery that mimics the naturally occurring transport system similar to viruses and lipoproteins [111].

Both lipid metabolism and inflammatory reactions are potential targets for the treatment and prevention of atherosclerosis. A number of liver-X receptor (LXR) target genes have been linked to the regulation of reverse cholesterol transport, where excess cholesterol is transported to the liver via HDL particles [112]. LXR belongs to a family of nuclear membrane proteins that become transcriptionally activated through ligand binding [112]. In addition, LXRs block NF-kB signaling, where NF-kB is required for the induction of TNF-α and IL-6, which are inflammatory cytokines [113-115]. One model drug of interest for encapsulation in the AScM polymers is GW3965, which is an agonist of LXR. LXR agonist treatment with GW3965 has been shown to reduce the formation of foam cells in macrophages by increasing cellular cholesterol efflux and has been shown to reduce lesion formation in apoE-/- and LDLR -/- mice by 50% [114].

CHAPTER 2: Structure-Binding Activity Relations of Polymers with the Atherogenic Domain of Human Macrophage Scavenger Receptor A

This Aim has been published as the following: Plourde, N. M.; Kortagere, S.; Welsh, W.; Moghe, P. V., Structure-activity relations of nanolipoblockers with the atherogenic domain of human macrophage scavenger receptor A. Biomacromolecules 2009, 10, (6), 1381-91.

2.1: Specific Aim 1

Oxidized low density lipoprotein (oxLDL) uptake by macrophages is mediated by scavenger receptors and leads to unregulated cholesterol accumulation. Polymers functionalized with anionic groups inhibit oxLDL uptake via the scavenger receptor A (SR-A). However, the factors necessary for effective binding were not well understood. In order to understand the structure-activity relationship (SAR) between the polymers and SR-A, molecular modeling and docking approaches were employed. A homology model of SR-A was constructed and six polymer models were docked to the SR-A homology model to investigate charge placement and clustering. Polymer models with the most favorable binding energy were also found to be the most effective oxLDL inhibitors in THP-1 macrophages. Mutant SR-A models were generated by replacing charged residues with alanine. All charged residues in the region were necessary, with Lys60, Lys63 and Lys66 having the greatest effect on binding. I hypothesize that structural studies aided by theoretical modeling and docking can be used to design promising polymer candidates with optimal binding properties.

2.2: Rationale

Atherosclerosis is triggered by complex interactions between macrophages, smooth muscle cells and extracellular matrix molecules, following the pathologic build-up of oxidized low density lipoproteins (oxLDL) within the vascular wall region [116]. OxLDL uptake is mediated by scavenger receptors, which unlike the receptors for native LDL, are not down-regulated [20]. This leads to unregulated cholesterol accumulation and results in the formation of foam cells and fatty streaks, which are the earliest visible atherosclerotic lesions [20, 100]. The two principal receptors involved in oxLDL uptake are SR-A and a class B scavenger receptor-CD36, and account for the majority of modified LDL uptake (75-90%) and degradation, as demonstrated by knockout mice lacking both SR-A and CD36 receptors [63]. A characteristic of SR-A is the mediation of uptake and degradation of modified proteins and several polyanionic ligands in the absence of structural similarities [32, 117, 118]. Ligand binding is thought to be mediated through electrostatic interactions between the arginine and lysine residues in the collagenous domain and negative charges on the ligands [75]. Interactions of ligands with CD36 are generally hydrophobic and only somewhat mediated by charge [119]. A cluster of amino acids has been proposed to be membrane-associated and form hydrophobic pockets on the CD36 receptor [120].

One promising avenue of interest in the treatment and prevention of cardiovascular disease is the use of a scavenger receptor inhibitor to prevent oxLDL uptake via scavenger receptors. OxLDL (and not native LDL) stimulates foam cell formation through binding to macrophage scavenger receptors, which leads to

unregulated cholesterol accumulation [20, 100]. A unique class of multifunctional polymers, amphiphilic scorpion-like macromolecules (AScM) have been described previously and explored *in vitro* [106]. The polymers are micellar aggregates of unimers identified as M12P5 which corresponds to a mucic acid (M) with aliphatic acid chains of 12 carbons (12) and polyethylene glycol (PEG) chains (P) with a molecular weight of 5 kDa (5) (**Figure 1.6**). These building blocks are naturally occurring or biocompatible compounds and are connected via biodegradable ester bonds. PEG contributes to the polymer's hydrophilicity and is used to prevent the non-specific adsorption of proteins. Mucic acid is a multi-hydroxylated saccharide providing reaction sites for further polymer modification, and aliphatic acid chains control the polymer hydrophobicity. The branched hydrophobic core aids in polymer stability, as seen by the low critical micelle concentration (CMC) ($1.25 * 10^{-7}$ M), as well as increases the micelle's capacity to self-assemble [106]. The micelle also has a small aggregation diameter (~20 nm). It is hypothesized that the collagenous region of macrophage SR-A is responsible for polymer binding as it has been shown to be the region responsible for oxLDL binding and contains a cluster of positively charged amino acids which bind to anionic ligands [76, 121-123].

Although previous studies provide information on the correlation between particle design and the prevention of oxLDL uptake [107, 108, 110, 124], the mechanistic contribution of sub-domains of the macromolecules are not well understood thus making the current trial and error pipeline from polymer design to *in vitro* testing time consuming and inefficient. Therefore, the present SAR studies are targeted at

understanding the nature of interactions between the collagen domain of the scavenger receptor SR-A and the modeled polymers. The results from this study will further enable the screening of numerous virtually designed polymers and obviate the need to synthesize structures with suboptimal binding properties. Analysis will involve both *in vitro* studies as well as atomistic molecular modeling simulations of macrophages and polymer interactions.

2.3: Materials and Methods

2.3.1: Polymer Synthesis and Characterization

Structures were prepared as previously described by colleagues in the Dr. Kathryn Uhrich laboratory [106, 108, 124]. The major reactants included 5000 Da heterobifunctional poly(ethylene glycol) (NH2-PEG-COOH) (Nektar, San Carlos, CA), 4-(Dimethylamino)pyridinium p-toluenesulfonate (DPTS) and carboxylate-terminated poly(ethylene glycol) (PEG-COOH 5000 MW) (Sigma, St. Louis, MO). All PEG reagents were dried by azeotropic distillation with toluene. All other reagents and solvents were purchased from Aldrich and used as received.

Chemical structures and compositions were confirmed by 1H and 13C NMR spectroscopy with samples (~ 5-10 mg/ml) dissolved in CDCl3-d solvent on Varian 400 MHz spectrometers, using tetramethylsilane as the reference signal. IR spectra were recorded on a Mattson Series spectrophotometer (Madison Instruments, Madison, WI) by solvent (methylene chloride) casting on a KBr pellet. Negative ion-mass spectra were recorded with a ThermoQuest Finnigan LCQTMDUO System (San Jose, CA) that includes

a syringe pump, an optional divert/inject valve, an atmospheric pressure ionization (API) source, a mass spectrometer (MS) detector, and the Xcalibur data system. Meltemp (Cambridge, Mass) was used to determine the melting temperatures (Tm) of all the intermediates.

Gel permeation chromatography (GPC) was used to obtain molecular weight and polydispersity index (PDI). It was performed on Perkin-Elmer Series 200 LC system equipped with Pl gel column (5 μm, mixed bed, ID 7.8 mm, and length 300 mm) and with a Water 410 refractive index detector, Series 200 LC pump and ISS 200 Autosampler. Tetrahydrofuran (THF) was the eluent for analysis and solvent for sample preparation. Sample was dissolved into THF (~ 5 mg/ml) and filtered through a 0.45 μm PTFE syringe filter (Whatman, Clifton, NJ) before injection into the column at a flow rate of 1.0 ml/min. The average molecular weight of the sample was calibrated against narrow molecular weight polystyrene standards (Polysciences, Warrington, PA).

2.3.2: Cell Culture

Human THP-1 monocytes (ATCC) were grown in suspension with RPMI-1640 medium (ATCC) and supplemented with 10 % FBS, in an incubator with 5 % CO_2 at 37 °C. The cells were seeded at a concentration of 10^5 cells/cm^2 and differentiated into macrophage cells by 14 hrs incubation in 16 nM phorbol myristate acetate. After the 14 hr differentiation period the cells were incubated for an additional 58 hr in RPMI-1640 medium and experiments were performed within three days.

2.3.3: Polymer Association with Macrophage Cells

The role of scavenger receptors in polymer uptake by THP-1 human macrophages was ascertained by incubating the cells with 10 μg/mL primary antibodies to SR-A and CD36 (R&D Systems) for 45 min at 37 °C to block receptor availability. To avoid any nonspecific reaction between the IgG isotypes and the macrophage cells, isotype controls were included where the SR-A and CD36 antibodies were replaced with purified mouse IgG_1 and purified rat IgG_{2b} respectively (Invitrogen). Texas-red conjugated polymers were prepared as previously described [125, 126]. Differentiated THP-1 cells were incubated were incubated with 10^{-6} M fluorescently labeled polymers in serum-free RPMI for 2 hr at 37 °C in the presence of additional antibodies or controls to guarantee continuous receptor blocking. Cells were washed, fixed with 4% paraformaldehyde and imaged on a Nikon Eclipse TE2000-S fluorescent microscope to determine fluorescently tagged polymer attachment. The images were analyzed with ImageJ 1.42q (NIH) and fluorescence data was normalized to cell count.

2.3.4: LDL Oxidation

OxLDL was prepared within five days of each experiment. BODIPY-labeled human plasma derived LDL (Molecular Probes, OR) was oxidized by 18 hr of incubation with 10 μM $CuSO_4$ (Sigma) at 37 °C with 5 % CO_2 [127, 128]. After 18 hr the oxidation was stopped with 0.01 % w/v EDTA.

2.3.5: OxLDL Accumulation in Macrophages

The internalization of oxLDL by THP-1 macrophage cells was assayed by incubating BODIPY-labeled oxLDL (10 ug/ml) with cells for 5 hr at 37 °C and 5% CO2. Conditions included a control of RMPI-1640 medium and a non-micellar control of carboxy-terminated PEG. Cells were washed, fixed with 4% paraformaldehyde and imaged on a Nikon Eclipse TE2000-S fluorescent microscope to determine fluorescently tagged oxLDL accumulation. The images were analyzed with ImageJ 1.42q (NIH) and fluorescence data was normalized to cell count. The levels of oxLDL uptake were normalized to those obtained in the absence of polymers.

2.3.6: Statistical Analysis

Each *in vitro* experiment was performed at least twice and three replicate samples were investigated in each experiment. 5 images per well were captured and analyzed. The results were then analyzed using analysis of variance (ANOVA). Significance criteria assumed a 95% confidence level ($P<0.05$). Standard error of the mean is reported in the form of error bars on the graphs of the final data.

2.3.7: Polymer Models

The polymers were built according to their chemical structures illustrated in **Figure 2.1** using the build module in molecular operating environment (MOE) (Chemical Computing Group, Inc., Montreal, Canada). The model polymer molecules were

parameterized for Amber99 [129] force field and energy minimized until convergence (grad = 0.001) was attained.

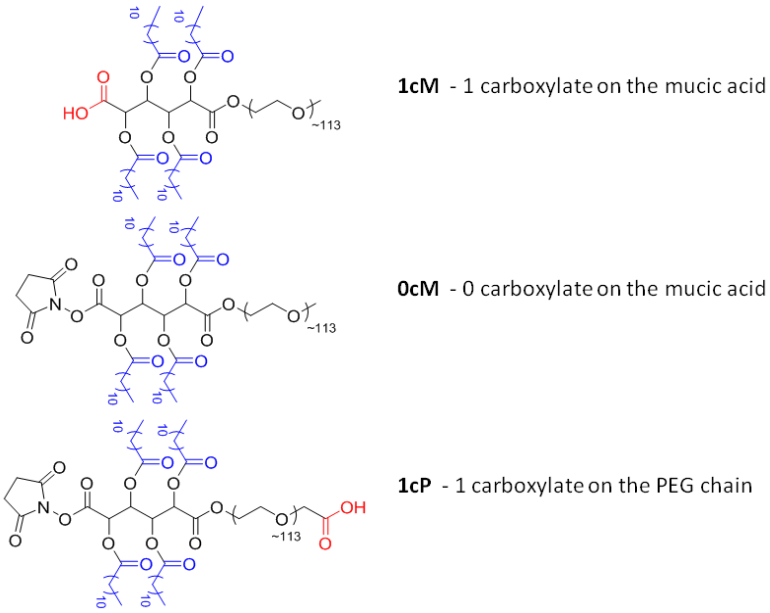

Figure 2. 1: Chemical structure of each of the polymers synthesized and tested. The nomenclature corresponds to the anionic structure.

2.3.8: SR-A Homology Model and Mutants

The primary sequence of the human SR-A receptor was retrieved from the National Center for Biotechnology Information (NCBI) Entrez protein database (P21757-Macrophage scavenger receptor types I and II) and the sequence was matched with similar sequences of proteins from the Protein Data Bank (PDB) using NCBI Basic Local Alignment Search Tool (BLAST) [130]. Pairwise sequence alignment of the template sequences with the SR-A collagen-like domain sequence was completed using CLUSTALW [131]. For further analysis, the secondary structures of both SR-A and collagen type I, chain A [132] (1Y0FA) were determined through PSIPRED, which maps sequences

into regions of helices, coils, or strands [133, 134]. The structures were mapped similarly throughout the collagen-like domain, and the corresponding region of collagen type I chain A the regions contained coils with high prediction confidence. The PDB file for collagen type I chain A contained only the protein backbone therefore the side chains were modeled using SYBYL (Ver 8.0 Tripos Inc., St. Louis, Missouri, USA) and energy minimized using steepest descent method until convergence was attained. The 3D homology model of the SR-A collagen-like domain was generated using the program MODELLER [135] with collagen type I chain A as template. MODELLER program utilizes spatial constraints derived from template structures for the generation of 3D model structures of proteins [135]. The resulting 3D model can be obtained by 1) calculating distance and dihedral angle restraints from the aligned target and template 3D structure, 2) utilizing an objective function of combined spatial restraints and CHARMM energy terms to impose proper stereochemistry [136], and 3) optimizing the objective function in Cartesian space through applying the variable target function method [137] utilizing techniques of conjugate gradients and molecular dynamics with simulated annealing [135]. The resulting PDB file of the collagen-like region of SR-A was parameterized for Amber99 [129] force field and energy minimized until convergence (grad = 0.001) was attained and further refined using molecular dynamics simulation using AMBER [138] program at 300K with a production run of 500 ps. Further, mutants were generated by substituting segments of the known binding region in the human collagen-like domain important for oxLDL binding (three lysines and two arginines [76, 121-

[123, 139]) with alanines using SYBYL8.0 and refined applying the same process described previously for the wild-type.

2.3.9: Docking and Scoring

The polymer models were docked to collagen-like domain of SR-A using GOLD v3.2 [140]. The GOLD program employs a genetic algorithm for docking flexible ligands into partially flexible receptor sites. The binding cavity was defined as residues Arg45 – Ser68 with an active site radius of 15 A° such that all residues important for oxLDL binding were included. Dockings were performed with standard default settings; population size of 100, selection pressure of 1.1, number of operations was 100,000, number of islands was 5, and a niche size of 2. Twenty independent docking runs were performed for each polymer. In the absence of any general rule to choose the number of conformations in GOLD, I have used 20 runs that optimized the computational time required to dock and score non-redundant conformations. The docked pairs were ranked based on each GoldScore, which is a scoring function based on H-bonding energy, van der Waals energy and ligand torsion strain. In most cases the best ranking conformation of the polymer illustrated the most preferred conformation to interact with scavenger receptor. The binding energy was computed for the refined complexes using **Equation 1**.

$$\Delta E_{binding} = \Delta E_{complex} - \Delta E_{SR-A} - \Delta E_{Polymer} \qquad \textbf{Equation 1}$$

Where $\Delta E_{complex}$ is the energy of the polymers docked to collagen-like domain of SR-A,

$\Delta E_{SR\text{-}A}$ is the energy of the homology model of the scavenger receptor collagen-like domain, and $\Delta E_{Polymer}$ is the energy of the polymer. Each structure (polymer model, homology model of the SR-A collagen-like domain, and the docked conformation of the pair) was parameterized using Amber99 [129] force field and energy minimized until convergence (grad = 0.001) was attained. These minimized energies were used to estimate the binding energy from **Equation 1**.

2.4: Results

2.4.1: Identification of Scavenger Receptors Involved in Cell-Polymer Interactions

To identify which receptor(s) were involved in the interaction between macrophage cells and polymers, the role of scavenger receptors were investigated through the use of selective blocking with antibodies. Similar to knockout studies, the

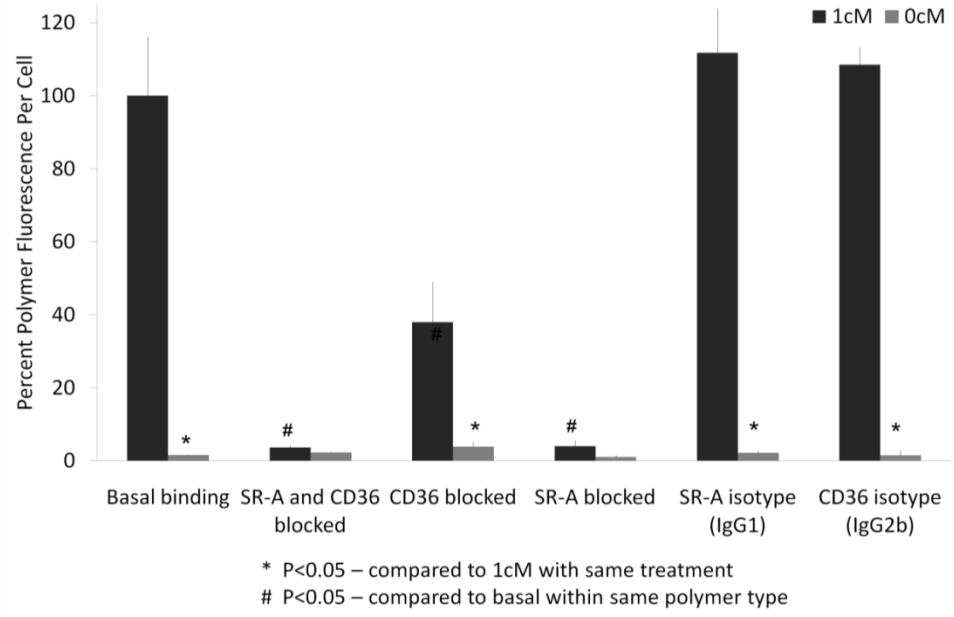

Figure 2.2: Reduction of polymer binding through receptor blocking illustrates receptor-mediated pathways involved in anionic and neutral polymer uptake by THP-1 macrophages

importance of each receptor can be inferred from the binding observed with receptor blocking compared to binding detected without receptor blocking. The polymers tested had one carboxylate on the mucic acid (**1cM**) as the anionic polymer and zero carboxylates on the mucic acid (**0cM**) as the neutral control (**Figure 2.1**). The basal binding of **0cM** was minimal and no variation was observed in the scavenger receptor blocking conditions (**Figure 2.2**). Further, no change was seen between the blocking and non-blocking conditions, implying that the trivial binding noted was not SR-A specific. In addition, when both SR-A and CD36 receptors were antibody-blocked, binding of both **1cM** and **0cM** was minimal and no significant difference was detected between the two conditions.

2.4.2: Structure Activity Relations of Polymers with SR-A

The role of the positioning and clustering of the anionic (carboxylate) group of the polymers on the inhibition of oxLDL uptake in THP-1 macrophages was examined (**Figure 2.3**). The first generation of polymers to be investigated included **1cM** and **0cM** as well as 1 carboxylate on the PEG chain (**1cP**), as seen in (**Figure 2.1**), and 1 carboxylate on PEG without aliphatic chains (**PEG-COOH**). Results of oxLDL accumulation followed a similar trend as that observed with mouse macrophages and polymers 108. The PEG-COOH macromolecules, which did not self-assemble into micelles, produced minimal inhibition of oxLDL uptake by macrophages. Uncharged polymers (**0cM**) had a limited effect in inhibiting oxLDL accumulation, which was dramatically enhanced in the presence of either anionic polymer (**1cM** and **1cP**). **1cM**

was the most efficient inhibitor and resulted in a 67% reduction in oxLDL accumulation by macrophage cells.

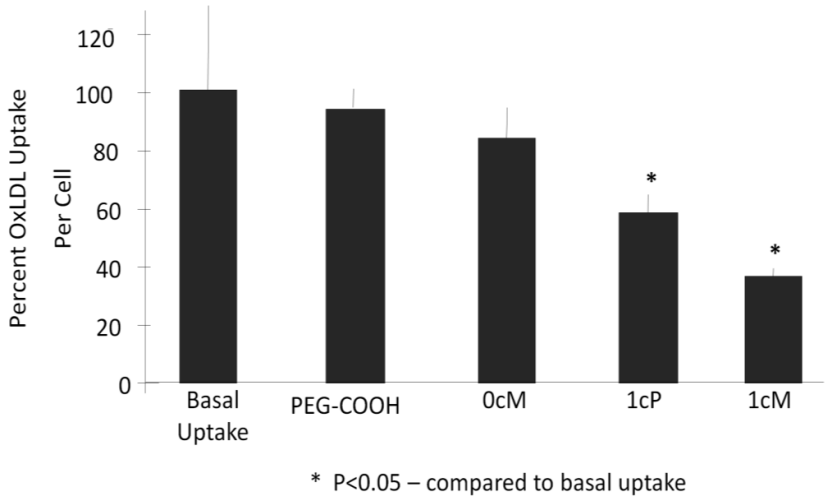

Figure 2.3: Reduction of oxLDL accumulation in the presence of various polymers illustrates the structure-activity relationship of polymers with THP-1 macrophage cells

2.4.3: Molecular Modeling of Polymers and Scavenger Receptor

The model polymers, described above, were scaled to contain PEG chain repeats of 20 in place of 115 and aliphatic chains of 2 repeats in place of 4. Two forms of first generation models were chosen to understand the structural interactions of polymer with SR-A. The first model consisted of a single unimer of the polymer aggregate with varying charge locations corresponding to **0cM**, **1cM**, **1cP** and **PEG-COOH**, as seen in **Figure 2.1**. The second model contained two **1cM** unimers covalently linked at the aliphatic chain on position 5 and represented a segment of a 1cM polymer aggregate to approximate the behavior of a multi-unimer polymer.

The three dimensional (3D) structure of SR-A is unknown. For our studies, a multi-step process was used to match the SR-A sequence with a similar sequence of known structure in order to predict scavenger receptor structure. Residues 812-877 of the collagen-like region of SR-A was modeled, as anionic ligand binding is mediated through the collagenous domain [75]. The amino acid sequence for SR-A was matched with similar sequences of proteins using a BLAST [130] search of the protein data bank (PDB). Two matches with the highest score were the structure of collagen type I, chain A[132] (1Y0FA) and the high resolution crystal structure of an active recombinant fragment of human lung surfactant protein D[141] (1PW9), with bit scores of 32.0 and 25.4 respectively. The scores are based on the alignment of similar or identical residues and gaps introduced to align the sequences; higher scores indicate better alignment [130].

In the region of interest, the alignment between collagen type I chain A and the SR-A collagen-like domain contained two identical matches and two "similar" matches. In addition, the structure of collagen was functionally similar to the collagenous domain of SR-A more so than the fragment of human lung surfactant protein D and therefore collagen type I chain A was chosen as the template for future studies (**Figure 2.4).**

```
Collagen-like   ------------------------------QGPPGPPGEKGDRGPTGESGPRGFPGPIGP 30
1Y0FA           AGAXGTPGPQGIAGQRGVVGLXGQRGERGFXGLXGPSGEXGKQGPSGASGERGPXGPMGP 840
                                              *  **.** *.:**:* ** **  **:**

Collagen-like   PGLKGDRGAIGFPGSRGLPGYAGRPGNSGPKGQKGEKGSG-------------------- 70
1Y0FA           XGLAGPXGESGREGAXGAEGSXGRDGSXGAKGDRGETGPAGPXGAXGAXGAPGPVGPAGK 900
                 ** *  *  *  *:  *  *  ** *. *.**:**.*..
```

Figure 2.4: ClustalW pairwise alignment of SR-A collagen-like region and collagen type I chain A (1Y0FA) with the regions necessary for oxLDL binding highlighted in gray boxes.

For further analysis, the secondary structures of both SR-A and collagen type I chain A were determined using PSIPRED [33], which mapped sequences into regions of helices, coils, or strands [133, 134]. The collagen-like domain of SR-A and the corresponding region of collagen type I chain A contained coils with high prediction confidence. The 3D model of the SR-A collagen-like domain was generated using the program MODELLER [135] and refined using energy minimization and molecular dynamics simulations using AMBER [138] program (see **Materials and Methods**).

2.4.4: Docking and Scoring of First Generation Polymers

The modeled polymers were docked to SR-A collagen-like domain homology model using GOLD v3.2 [140]. The docked pairs were ranked based on each GoldScore. The five residues reported to be responsible for oxLDL binding to SR-A [76, 121] were used to define the binding pocket. **Figure 2.5** illustrates the consensus binding of 20 independent docking runs. There was no consensus orientation or specificity seen with the 20 docking runs of the **0cM** polymer model. However, the hydrophobic aliphatic chains occasionally remained close to the positive pocket. It was noted that only **1cM** and **PEG-COOH** appeared to be oriented in a way so as to facilitate binding in the essential region, specifically Lys60, and not **1cP** or **0cM**. PEG did not appear to be predominantly involved in binding. The docking of the second model of two 1cM unimers covalently linked (**1cM-link**) at the aliphatic chain on position 5 can be seen in **Figure 2.6**. It is noteworthy that when docked, the 2 unimers oriented such that the PEG chains were positioned away from the SR-A collagenous domain and the aliphatic

chains formed a “core-like” structure around the binding pocket, specifically Arg53 and Lys60.

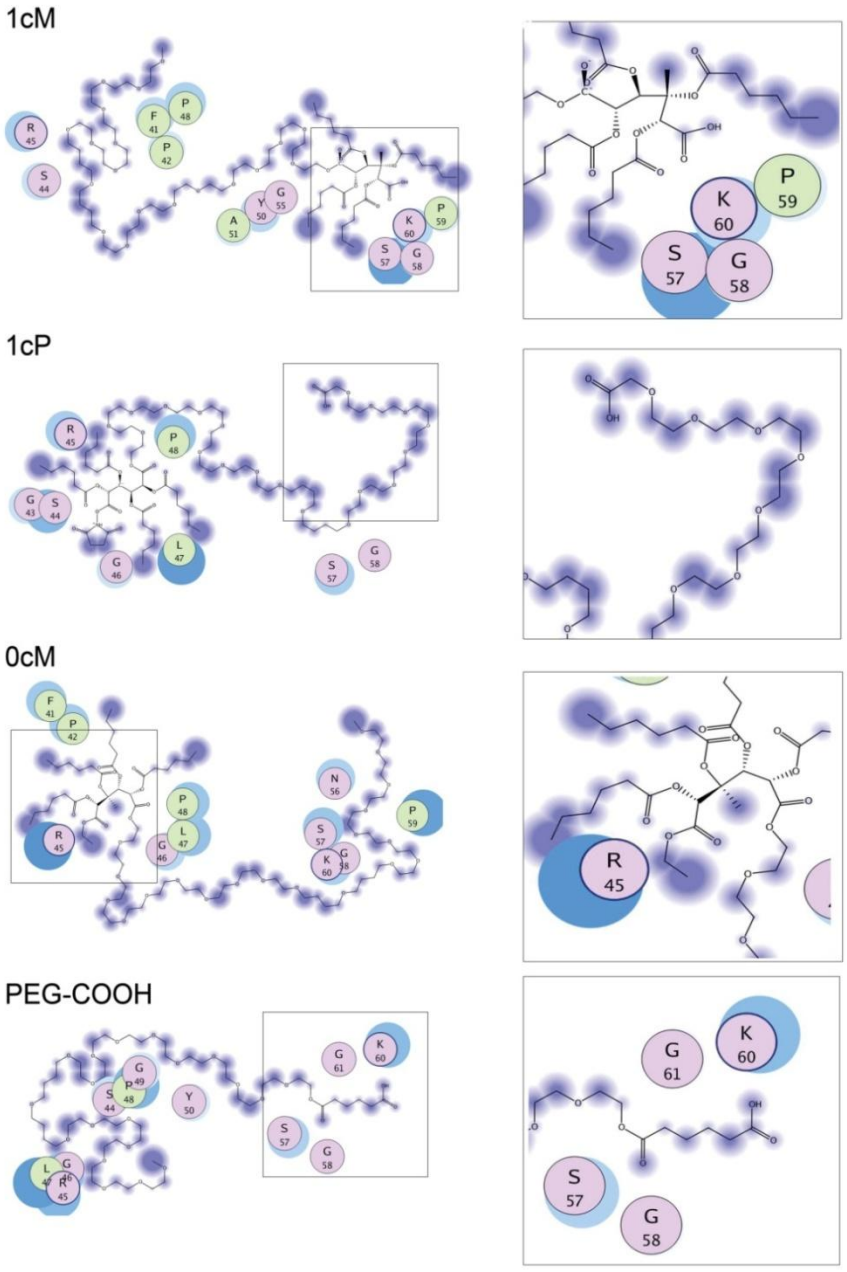

Figure 2.5: Schematic representation of the docked interactions of SR-A collagen-like domain homology model residues (as seen in the colored circles) with polymer models: Residue characteristics are illustrated through color: Purple = polar, green = hydrophobic, blue border = basic, and red border = acidic.

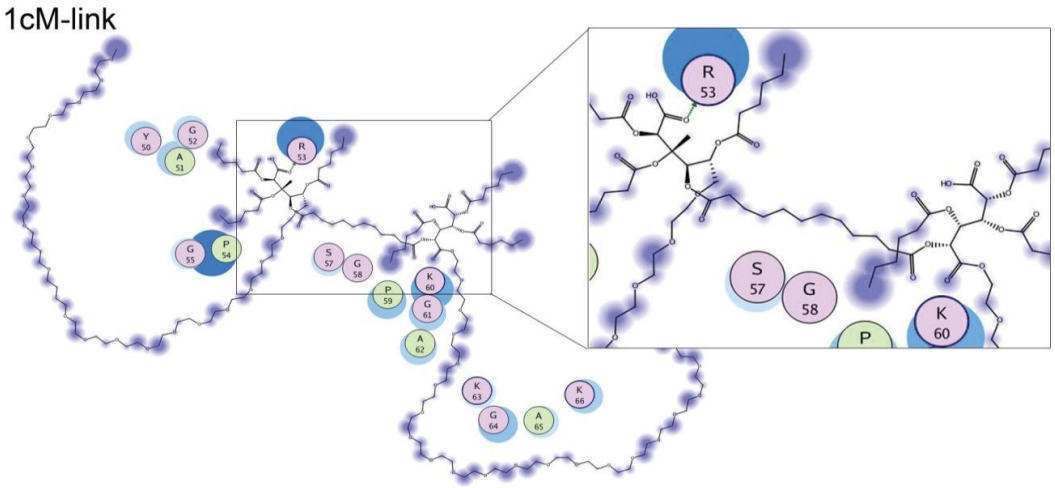

Figure 2.6: Schematic representation of the docked interactions of SR-A collagen-like domain homology model residues with polymer model of 2 covalently bonded 1cM unimers representing a section of a 1cM aggregate. Residue characteristics are illustrated through color: Purple = polar, green = hydrophobic, blue border = basic, and red border = acidic.

The binding energy was computed for each refined complex using **Equation 1** and the results are tabulated in **Table 1**. The energy values reinforce docked observations, in that the polymer models with the most favorable energies were also positioned in a way so as to facilitate binding.

First Generation Polymer	ΔE binding (kcal/mol)
1cM	-42.07
PEG-COOH	-23.83
1cP	20.45
0cM	38.88
1cM-link	283.46

Table 2.1: Values of the binding energy of first and second generations of polymer models when docked with SR-A collagen-like domain homology model

The energy of the second model of **1cM-link** was very unfavorable, the two unimers would not be covalently linked in actuality but would instead be a fraction of a dynamic micelle.

2.4.5: Docking and Scoring of Multiply-Charged (MC) Polymers

A second generation of polymer configurations was investigated based on the design of the first generation of polymers. Two multiply-charged (MC) polymers each containing 2 carboxylate groups were designed to investigate the role of charge clustering and charge location and to assess the ability of the model to predict polymer effectiveness *in vitro* (**Figure 2.7**).

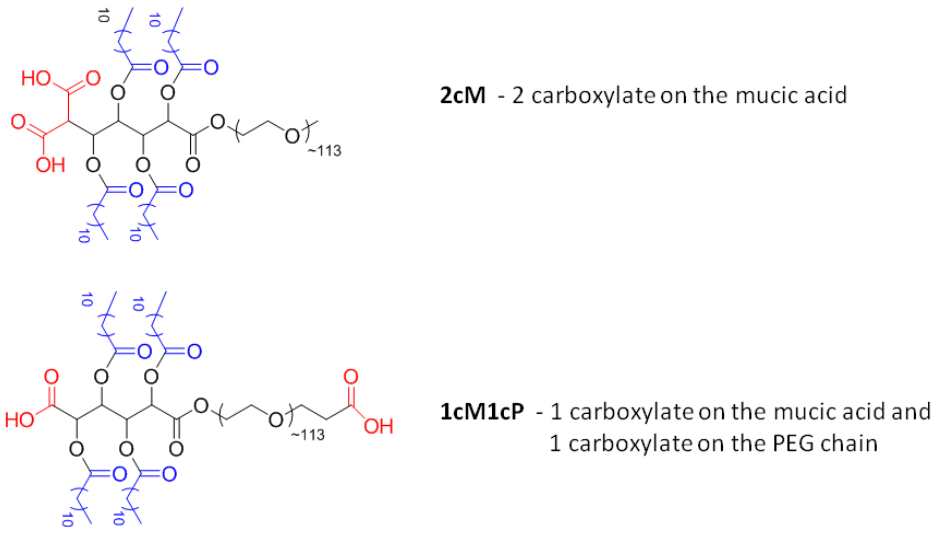

Figure 2.7: Chemical structure of each of the second generation MC-polymers synthesized and tested. The nomenclature corresponds to the anionic structure.

Based on the finding that one carboxylate on the mucic acid provided both strong model binding and was an efficient inhibitor of oxLDL *in vitro* (**1cM**), a MC-

polymer containing two carboxylates on the mucic acid (**2cM**) was modeled. Further, a second MC-polymer containing one carboxylate on the mucic acid and one carboxylate on the PEG chain (**1cM1cP**) was modeled to investigate the effect of multiple charge placement. As described above, the MC-polymers were scaled to contain PEG chain repeats of 20 in place of 115 and aliphatic chains of 2 repeats in place of 4. The modeled MC-polymers were docked to SR-A collagen-like domain homology model using GOLD v3.2 [140] and the docked pairs were ranked based on each GoldScore. **Figure 2.8** illustrates the consensus binding of 20 independent docking runs. It can be noted that the flexibility of the PEG chain in the **1cM1cP** allowed for at least two predominant binding modes as shown in configurations A and B. In the first mode (**Figure 2.8A**), which occurred in 70% of the docking runs, the MC-polymer had a more linear conformation, in which the carboxylates interacted with Arg45 and Gly55. In the second mode (**Figure 2.8B**), which was observed in 30% of docking runs, the MC-polymer was seen to fold inwards such that the two carboxylates were proximal and interacted with neighboring residues Pro48, Tyr50, Ala51, Arg53 and Pro54. In contrast, in the **2cM** polymer the positioning of the two carboxylate groups on the mucic acid resulted in binding between no more than 1 residue and 1 anionic group, as seen in **Figure 2.8C** with Arg53.

The binding energy was computed for each refined complex using **Equation 1** and the results are tabulated in **Table 2.2**. Of the polymer models examined, **1cM1cP** had the most favorable binding energy. The binding of the **2cM** polymer model to the collagen-like domain was unfavorable and similar to the value of **0cM** binding.

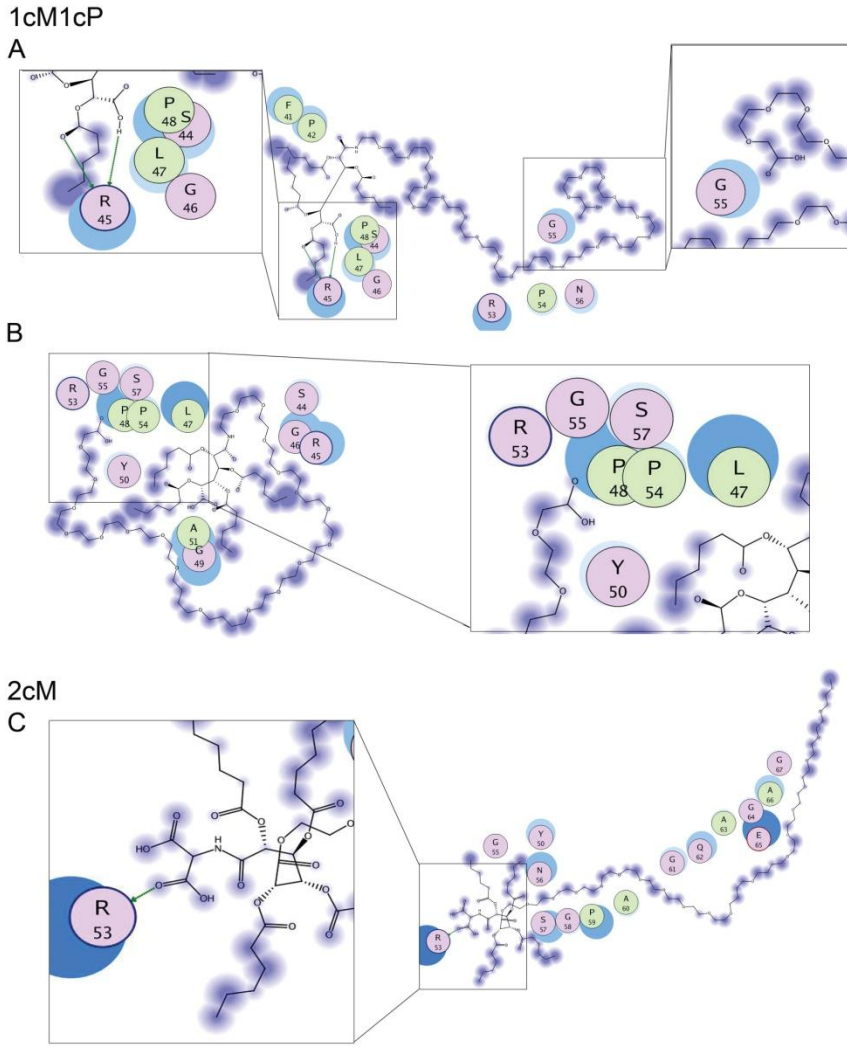

Figure 2.8: A) In 70% of docking runs, the 1cM1cP model was found to bind as mode A to distant residues, B) in 30% of runs as seen in mode B, polymer folded inward and bound the same or adjacent residues. C. Schematic representation of the interaction of 2cM with SR-A. Residue characteristics are illustrated through color: Purple = polar, green = hydrophobic, blue border = basic, and red border = acidic.

Second Generation MC-polymer	ΔE binding (kcal/mol)
2cM	40.92
1cM1cP	-59.99

Table 2.2: Values of the binding energy of second generations of MC-polymers models when docked with SR-A collagen-like domain homology model

The binding energies trend well with the experimental oxLDL uptake data and were validated by the *in vitro* results in **Figure 2.9**. Here, the MC-polymers were compared to the previous gold standard, **1cM**, and basal uptake in the presence of no particles. The role of the positioning and clustering of the anionic groups of the MC-polymers on the inhibition of oxLDL uptake in THP-1 macrophages was examined via incubation of the cells with 10^{-6} M polymers and fluorescent oxLDL for 5 hr at 37 ºC.

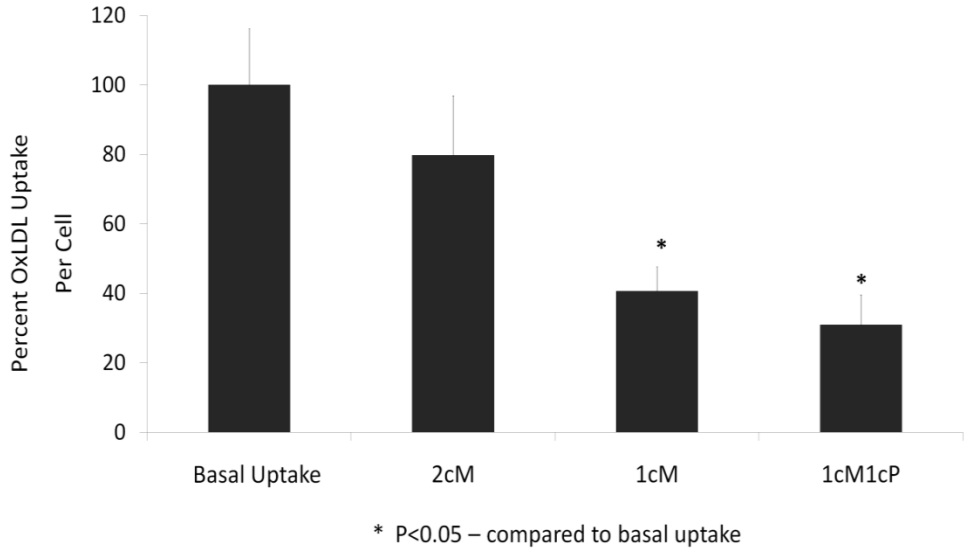

Figure 2.9: The reduction of oxLDL accumulation in the presence of MC-polymers compared to the previously identified most inhibitory polymer configuration (1cM).

The **2cM** polymer inhibited minimal uptake of oxLDL. However, in vitro **1cM1cP** was as effective as, but no more successful than **1cM**. The additional carboxylate on the PEG enhanced binding but did not translate to a more effective oxLDL inhibitor.

2.4.6: Docking and Scoring of Mutants

In an effort to understand the role of the 5 conserved residues on polymer binding, mutants were generated by substituting segments of the known binding region (three lysines and two arginines [76, 121-123]) with alanines. Initially, 3 mutant models were generated; **mutant 1** (replacement of Arg45, Arg53, Lys60, Lys63 and Lys66 with alanine), **mutant 2** (replacement of Arg45 and Arg53 with alanine) and **mutant 3** (replacement of Lys60, Lys63 and Lys66 with alanine). The **1cM** model was chosen as the test polymer because the **1cM** had strong interactions with the SR-A collagen-like domain homology model and also had close correlation to the *in vitro* oxLDL uptake results. **Figure 2.10** illustrates the consensus binding of 20 independent docking runs between the mutants and **1cM**. In **mutant 1** model all the five charged residues were removed and yet binding was still observed consistently between the carboxylate group and residues Gln62 and Glu65. This finding led to the generation of two additional mutants: **mutant 4** (replacement of Gln62 and Glu65 with alanines) and **mutant 5** (replacement of Arg45, Arg53, Lys60, Lys63, Lys66, Gln62 and Glu65 with alanines). In **mutants 2, 3**, and **4**, after the removal of charged residues of interest, binding was retained through interactions with the remaining positive amino acids (Lys60, Lys63 and Lys66 in **mutant 2**, Arg45 and Arg53 in mutant 3, and Arg45, Arg53, Lys60, Lys63 and Lys66 in **mutant 4**). In **mutant 5** there was no specificity observed and the replacement of all seven residues in the region of interest resulted in the abolishment of specific binding, however the aliphatic chains did again seem to associate with the glycine residues.

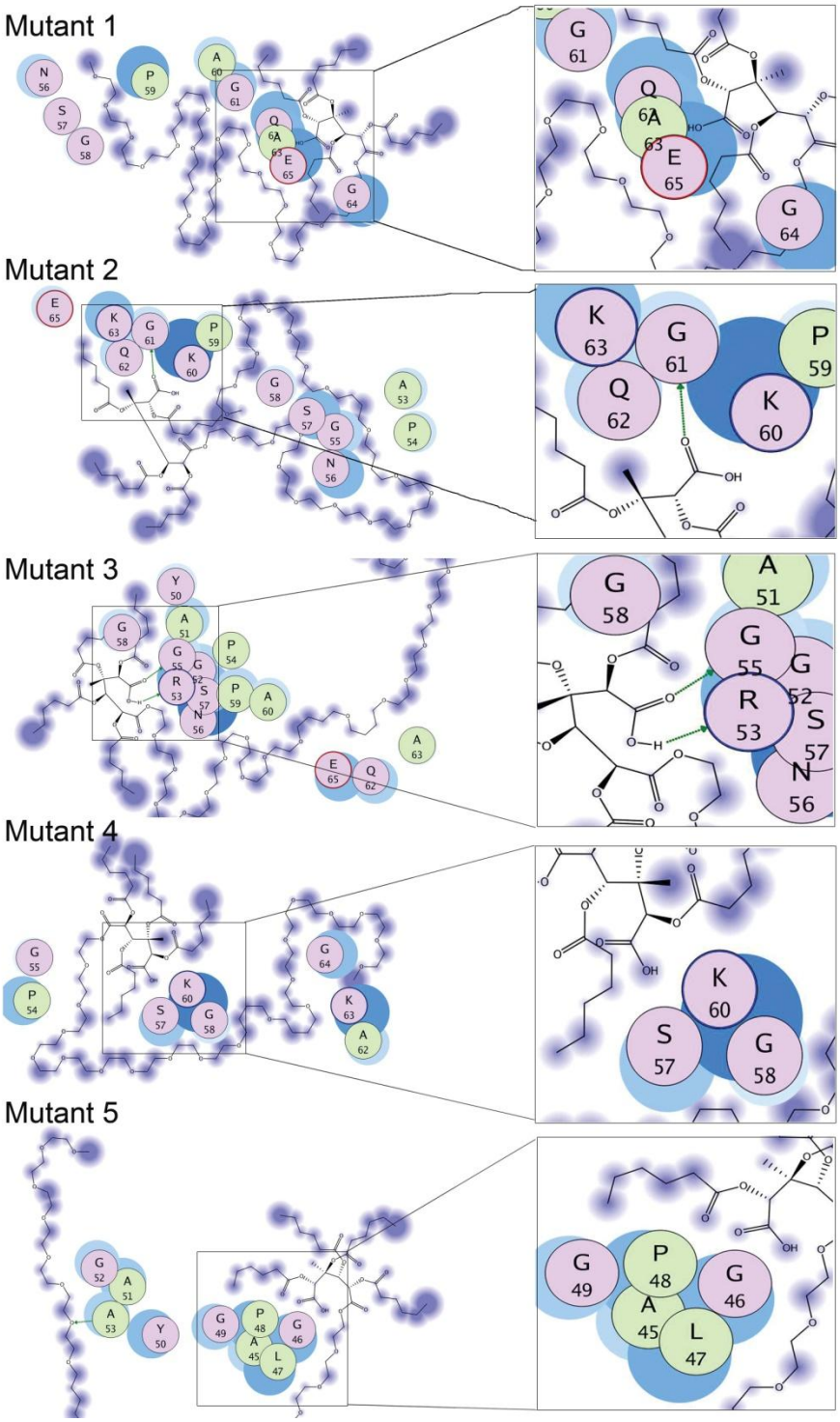

Figure 2.10: Schematic representation of docked interactions of 1cM polymer model with SR-A collagen-like domain homology model mutants in which specific residues were replaced with alanine. Residue characteristics are illustrated through color: Purple = polar, green = hydrophobic, blue border = basic, and red border = acidic.

The binding energy (**Table 2.3**) was computed for each refined mutant-1cM complex using **Equation 1**. The most favorable binding was seen with the wild-type SR-A collagen-like domain homology model followed by **mutants 4** and **2**. The percent change in the binding energy from wild-type SR-A correlated with the number of residues mutated from binding pocket.

SR-A Mutation	ΔE binding (kcal/mol)	Percent change from Wild-type SRA	Residues mutated
Wild type	-42.07	0	0
Mutant 1	1.15	102.73	5
Mutant 2	-31.09	26.10	2
Mutant 3	65.61	255.95	3
Mutant 4	-32.19	23.48	2
Mutant 5	30.87	173.38	7

Table 2.3: Values of the binding energy of the 1cM model when docked with SR-A collagen-like domain homology model mutants as well as the percent change in binding energy from wild-type SR-A collagen-like domain homology model versus the number of residues mutated. mutant 1(Arg45, Arg53, Lys60, Lys63, and Lys63), mutant 2 (Arg45 and Arg53), mutant 3 (Lys60, Lys63, and Lys63), mutant 4 (Gln62 and Glu65), mutant 5 (Arg45, Arg53, Lys60, Lys63, Lys63, Gln62 and Glu65).

The correlation between number of residues removed and percent change in the binding energy from wild-type SR-A was linear, with the exception of a sharp spike that correspond to **mutant 3** (replacement of Lys60, Lys63 and Lys66 with alanines).

2.5: Discussion

Polymers designed to block scavenger receptors and inhibit oxLDL accumulation were examined using both *in vitro* and molecular modeling SAR studies to investigate the interaction between a polymer and SR-A. To the best of our knowledge, this is the

first ever modeling SAR study of a nanoparticle or scavenger receptor and has opened the door to numerous future studies. The first generation of polymers to be investigated included **1cM**, **0cM**, **1cP** and 1 carboxylate on PEG without aliphatic chains (**PEG-COOH**). The **1cM** and **1cP** were used to observe the effect of charge location on polymer binding and uptake and the **0cM** served as the neutral control particle. **PEG-COOH** was used as a non-micellar control as it contained the same functional group and PEG chain length, but did not form micelles in solution. The polymer containing hydrophobic-bound carboxylate groups (**1cM**) was the most efficient inhibitor and resulted in a 67% reduction in oxLDL accumulation by macrophage cells. In contrast, the **1cP**, which had the anionic groups conjugated to the hydrophilic domain caused only 41% induced reduction in oxLDL uptake. Given that **1cM** and **1cP** have similar charge densities as demonstrated previously through zeta potential measurements [124], this finding implied that the interaction between the receptor and polymer was not solely charge-based. The enhanced binding may be due to hydrophobic and charge interactions acting in concert for improved inhibitory ability, but could not be confirmed by uptake studies. Hence, molecular modeling and docking simulations were performed to further understand the SAR of the polymers with SR-A

Results indicate that the collagenous domain homology model interactions with polymer models correlated well with *in vitro* studies of THP-1 macrophage and polymer interactions, shown by models with the most favorable (lowest) docked energy having the same chemistry as the polymers that reduced cholesterol accumulation to the greatest extent. There was no consensus orientation or specificity seen with the 20

docking runs of the **0cM** polymer model. However, the hydrophobic aliphatic chains occasionally remained close to the positive pocket. This lack of directed specificity with sporadic positioning near the charged residues in the collagenous domain may explain the finding that **0cM** exhibits limited blocking of oxLDL accumulation, which was far less than anionic polymers. It was noted that only **1cM** and **PEG-COOH** appeared to be oriented in a way so as to facilitate binding in the essential region, specifically Lys60. However, only the **1cM**, and not the **PEG-COOH**, prevented the accumulation of oxLDL in the *in vitro* studies. The aliphatic chains seemed to stabilize the long molecule and acted as an anchor between the carboxylate group on the **1cM** polymer model and the SR-A collagenous domain homology model. This may be due to interactions between the aliphatic chains and several glycine residues in the SR-A collagenous domain. The bulk of these chains are far removed from the anionic moiety which appeared to instead hinder the binding of **1cP** while their removal (as illustrated with **PEG-COOH**) restored binding. PEG did not appear to be predominantly involved in binding; however it was necessary *in vitro* for micelle formation and protected the anionic moiety from non-specific adsorption of proteins [142]. The docking of the second model of two 1cM unimers covalently linked at the aliphatic chain on position 5 (**1cM-link**) when docked, the 2 unimers oriented such that the PEG chains were positioned away from the SR-A collagenous domain and the aliphatic chains formed a “core-like” structure around the binding pocket, specifically Arg53 and Lys60. Thus it is hypothesized that the multi-unimer polymer aggregate binds to the SR-A in a mode where the carboxylates in the micelle core act in concert to interact with the charged region (Arg45 to Glu65) of the

collagenous domain of SR-A. The binding energies also trend well with the experimental oxLDL uptake data. While the accumulation of oxLDL is not a direct measurement of ligand binding it can be inferred that the polymers with the most favorable binding energy bind at a higher rate than polymers with less favorable binding energies and therefore would block more oxLDL from accumulating within the THP-1 macrophages. The **1cM** polymer model had both the most favorable binding energy and also prevented the most oxLDL from accumulating *in vitro*. It should be noted that while the energy of the second model of two 1cM unimers covalently linked at the aliphatic chain was very unfavorable, the two unimers would not be covalently linked in actuality but would instead be a fraction of a dynamic micelle. The covalent bond limited the degrees of freedom, however the polymer mode of binding as a micellar aggregate cannot be ruled out. This was reinforced by the finding that while the **PEG-COOH** polymer had similar binding energy to the **1cM**, it was far less successful at reducing the accumulation of oxLDL *in vitro*. The **PEG-COOH** lacked only the aliphatic side chains of the **1cM** and did not form micelles in solution [108]. This evidence indicated the necessity of aliphatic arms in a polymer for efficient binding and possibly to the need for a multi-unimer polymer aggregate.

In light of the close correlation between the *in vitro* oxLDL accumulation data in THP-1 macrophages and the *in silico* binding energy results, a second generation of polymer configurations were investigated based on the design of the first generation of polymers. Two multiply-charged (MC) polymers each containing 2 carboxylate groups were designed to investigate the role of charge clustering and charge location and to

assess the ability of the model to predict polymer effectiveness *in vitro*. It can be noted that the flexibility of the PEG chain in the **1cM1cP** allowed for at least two predominant binding modes. In contrast, in the **2cM** MC-polymer the positioning of the two carboxylate groups on the mucic acid resulted in binding between no more than 1 residue and 1 anionic group. In comparison with the **1cM** model, the **1cM1cP** model had additional interactions with both adjacent and remote residues. These additional large favorable interactions could account for the increase in the binding energy in comparison with **1cM** model. The binding of the **2cM** polymer model to the collagen-like domain was unfavorable and similar to the value of **0cM** binding. This seems inconsistent with the previous finding that carboxylates located on the mucic acid result in favorable binding (**1cM**) and that increased charge results in increased binding (**1cM1cP**). There are several explanations for this phenomenon. First, in the **2cM** model the carboxylate groups are positioned closely together. This limited the degrees of freedom of the two carboxylates to move and bind more than one residue, compared to the **1cM1cP**. Second, internal hydrogen bonding was observed between the carboxylates and the nitrogen at position 4 or the oxygen at position 5 which resulted carboxylates unavailable for binding to SR-A. Third, compared to the other polymer models, the **2cM** was less hydrophobic due to the additional anionic charge near the hydrophobic moiety.

The creation of mutant models demonstrated the importance of all residues in the collagen-like domain region of interest (residues 45-65) for binding to **1cM**. Mutants were generated by substituting segments of the known binding region (three

lysines and two arginines [76, 121-123]) with alanines. Initially, 3 mutant models were generated; **mutant 1** (replacement of Arg45, Arg53, Lys60, Lys63 and Lys66 with alanine), **mutant 2** (replacement of Arg45 and Arg53 with alanine) and **mutant 3** (replacement of Lys60, Lys63 and Lys66 with alanine). The **1cM** model was chosen as the test polymer because the **1cM** had strong interactions with the SR-A collagen-like domain homology model and also had close correlation to the *in vitro* oxLDL uptake results. In **mutant 1** model all the five charged residues were removed and yet binding was still observed consistently between the carboxylate group and residues Gln62 and Glu65. This finding led to the generation of two additional mutants: **mutant 4** (replacement of Gln62 and Glu65 with alanines) and **mutant 5** (replacement of Arg45, Arg53, Lys60, Lys63, Lys66, Gln62 and Glu65 with alanines). In **mutants 2, 3**, and **4**, after the removal of charged residues of interest, binding was retained through interactions with the remaining positive amino acids (Lys60, Lys63 and Lys66 in **mutant 2**, Arg45 and Arg53 in mutant 3, and Arg45, Arg53, Lys60, Lys63 and Lys66 in **mutant 4**). These results were encouraging and implied the ability of the **1cM** polymer to bind to multiple locations within the SR-A collagen-like domain, providing a strengthened ability to block oxLDL binding and uptake. In **mutant 5** there was no specificity observed and the replacement of all seven residues in the region of interest resulted in the abolishment of specific binding, however the aliphatic chains did again seem to associate with the glycine residues. While there was no *in vitro* site-directed mutagenesis study to reinforce these findings as yet, the ability of the wild-type model to trend with experimental results supports these findings. The most favorable binding was seen with

the wild-type SR-A collagen-like domain homology model followed by **mutants 4** and **2**. The correlation between number of residues removed and percent change in the binding energy from wild-type SR-A was linear, with the exception of a sharp spike that correspond to **mutant 3** (replacement of Lys60, Lys63 and Lys66 with alanines). This suggested the important role of the lysines in binding between **1cM** and SR-A as mutation of these residues had the greatest effect on binding energy. It should be noted that the binding energies of **PEG-COOH** and **1cM1cP** with the mutants followed an identical trend indicating the specific binding of these polymer models, but the **1cP**, **0cM**, **2cM** and **1cM-link** had no correlation (data not shown). This is not surprising as only **1cM**, **1cM1cP** and **PEG-COOH** appeared to be oriented in a way to facilitate binding in this region.

Site-directed mutagenesis experiments could be performed to confirm this hypothesis. Furthermore, the important role of the charged residues as demonstrated by the mutant binding energies may provide opportunities for polymer refinement using information gained from this SAR of polymers with SR-A. Future studies may focus on the development and use of coarse-grained molecular models to more completely characterize the system of polymer and SR-A interactions.

CHAPTER 3: Design and Structure-Binding Activity Relations of Polymers with the Atherogenic Domain of Human Macrophage Scavenger Receptor A: The Influence of Backbone Chemistry

3.1: Specific Aim 2

Based on the findings from Chapter 2, newer polymers were designed by altering the basic **1cM** structure that had proved effective in the past. Whereas in the previous model only the effect of charge number and placement could be varied and critical role for amphiphilicity was recognized, this aim focuses on the role of polymer backbone. Polymer models were designed to investigate the influence of mucic acid backbone stereochemistry **(1cS)**, the influence of a cyclic versus linear backbone (**0cG** and **0cGl**), and the influence of aromatic versus aliphatic backbone (**1cAr**). In order to understand the structure-activity relationship (SAR) between the polymers and SR-A, molecular modeling and docking approaches were employed. Polymer models were docked to the previously constructed SR-A homology model to investigate the significance of the polymer backbone on receptor binding. Modeling realizations indicate the ability of the polymer backbone to position the side chains and "lock" the polymer ligand into position. To validate the model predictions, polymers were synthesized by our collaborators from the Uhrich laboratory and experimental studies of binding of the new polymers to SRA-transfected HEK cells showed that results followed those seen in the modeling predictions, with **1cAr** and **0cGl** showing promise. Thus, minute changes in polymer backbone can sensitively affect SR-A binding affinities and consequently modulate the competitive inhibition of oxLDL uptake.

3.2: Rationale

Nanoscale amphiphilic polymers have been reported to possess high biocompatibility, stability and tunability. The most promising polymeric unimers are comprised of a hydrophobic core based on the sugar, mucic acid, alkylated along its backbone *via* hydrolytically degradable ester bonds. The polymers form micelles of ~10-20 nm in solution and have been shown to significantly inhibit scavenger receptor-mediated uptake of highly oxidized low density lipoprotein (oxLDL) [107, 110, 143]. A number of structure-function relationship studies on these systems have been previously performed and suggested the importance of the polymer backbone and the position of the aliphatic arms. This work aims to design nanoscale polymers with features enabling optimal binding to the scavenger-receptor A (SR-A) of human macrophages and to evaluate the role that the stereochemistry and rigidity of the polymers has on the oxLDL uptake inhibition.

Molecular modeling and docking studies of the atherogenic domain of human macrophage SR-A with a number of variations of the parent polymer, **1cM** were carried out. Polymers with favorable and unfavorable binding were chosen for testing and synthesized by Dr. Sarah Hehir in the laboratory of Prof. Kathryn Uhrich. This range of polymers with good-to-poor binding energies allowed for validation of the model.

3.3: Materials and Methods

3.3.1: Polymer and SR-A Modeling

The polymers were modeled according to their chemical structures illustrated in **Figure 3.1** using the build module in molecular operating environment (MOE) (Chemical Computing Group, Inc., Montreal, Canada). The model polymer molecules were parameterized for Amber99 [129] force field and energy minimized until convergence (grad = 0.001) was attained. The creation of the SR-A homology model was described in the previous chapter and the resulting publication [143]. Briefly, The 3D homology model of the SR-A collagen-like domain was generated using the program MODELLER [135] with collagen type I chain A as template.

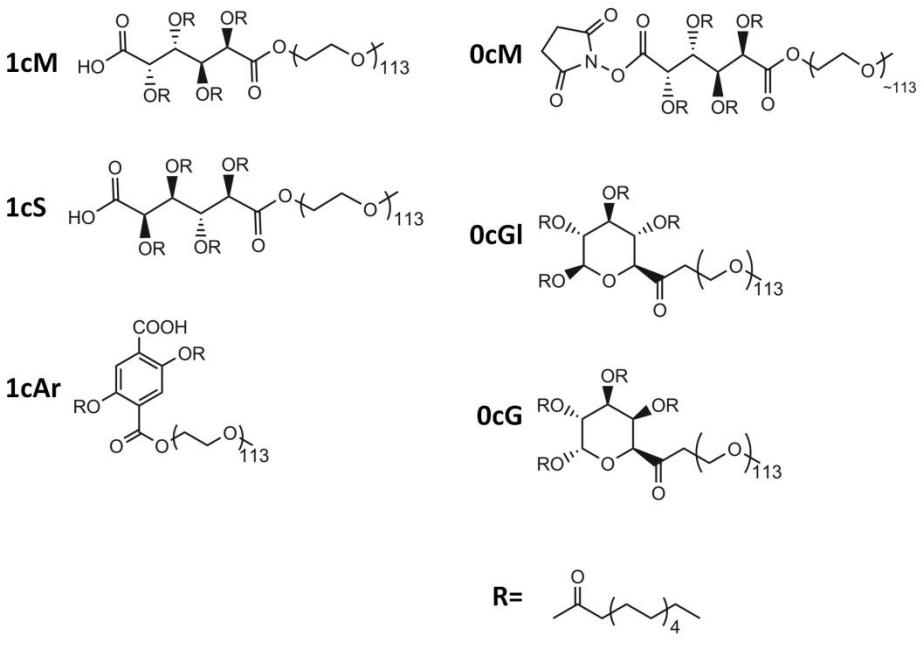

Figure 3.1: Schematic of the new structures designed to study the role of polymer backbone

3.3.2: Docking and Scoring

The polymer models were docked to collagen-like domain of SR-A using GOLD v3.2 [140]. The GOLD program employs a genetic algorithm for docking flexible ligands into partially flexible receptor sites. The binding cavity was defined as residues Arg45 – Ser68 with an active site radius of 15 A° such that a range of residues important for oxLDL binding was included. Dockings were performed with standard default settings; population size of 100, selection pressure of 1.1, number of operations was 100,000, number of islands was 5, and a niche size of 2. In the absence of any general rule to choose the number of conformations in GOLD, 20 independent docking runs were performed for each polymer, which optimized the computational time required to dock and score non-redundant conformations. The docked pairs were ranked based on each GoldScore, which is a scoring function based on H-bonding energy, van der Waals energy and ligand torsion strain. In most cases the best ranking conformation of the polymer illustrated the most preferred conformation to interact with scavenger receptor. The binding energy was computed for the refined complexes using **Equation 1**.

$$\Delta E_{binding} = \Delta E_{complex} - \Delta E_{SR-A} - \Delta E_{Polymer} \qquad \textbf{Equation 1}$$

Where $\Delta E_{complex}$ is the energy of the polymers docked to collagen-like domain of SR-A, $\Delta E_{SR\text{-}A}$ is the energy of the homology model of the scavenger receptor collagen-like domain, and $\Delta E_{Polymer}$ is the energy of the polymer. Each structure (polymer model, homology model of the SR-A collagen-like domain, and the docked conformation of the

pair) was parameterized using Amber99 [129] force field and energy minimized until convergence (grad = 0.001) was attained. These minimized energies were used to estimate the binding energy from **Equation 1**.

3.3.3: Polymer Synthesis and Characterization

Polymer synthesis and characterization was performed by Dr. Sarah Hehir and Li Gu in the laboratory of Prof. Kathryn Uhrich. Reagents for AM synthesis were purchased from Sigma-Aldrich. ^{1}H-NMR spectra were obtained using a Varian 400 MHz or 500 MHz spectrophotometer with TMS as internal reference. Molecular weights (Mw) were determined using gel permeation chromatography (GPC) with respect to PEG standards (Sigma-Aldrich) on a Waters Stryagel HR 3 THF column (7.8 x 300 mm. Dynamic light scattering (DLS) analysis was carried out on a Zetasizer nanoseries nano ZS90 (Malvern instruments). CMC studies were carried out on a Spex fluoromax-3 spectrofluorometer (Jobin Yvon Horiba) at 25 ºC.

*Polymers were synthesized through modification of a previously described procedure [106]. For **1cS**, the stereochemistry was altered by substituting saccharic acid for mucic acid in the backbone. Saccharic acid is commercially available. Polymers were prepared by acylation and DCC coupling to PEG. For **1cAr**, dihydroxyterephthalic acid was acylated and coupled to PEG. For **0cG** and **0cGl**, the synthesis involved acylation of galacturonic acid and glucuronic acid respectively with lauroyl chloride followed by DCC/dimethylaminopyridiniumtosylate (DPTS) coupling to PEG.*

3.3.4: Cell Culture

Studies of polymer interactions were conducted using a tet-inducible cell line with controlled expression of SR-A, Human embryonic kidney (HEK) cells stably transfected with human scavenger receptor A (gift from Dr. Steven R. Post), which are referred to as HEK-SRA. Cells were propagated in high glucose DMEM (Invitrogen) supplemented with 10% FBS, 1% penicillin/streptomycin, 15 ug/mL Blasticidin and 100 ug/mL HygromycinB at 37°C in 5% CO_2. SR-A expression was induced with addition of 0.5 ug/ml tetracycline overnight and throughout the experiment.

3.3.5: LDL Oxidation

As described previously [110], oxidized low density lipoprotein LDL (oxLDL) was generated by incubating 50 µg/ml LDL purified from human plasma (Molecular Probes Eugene, OR) with 10 µM $CuSO_4$ at 37 °C for 18 hr exposed to air. [11, 144] Oxidation was terminated with 0.01% w/v EDTA (Sigma, St. Louis, MO).

3.3.6: OxLDL Accumulation in HEK-SRA Cells

The internalization of oxLDL by HEK-SRA cells was assayed by incubating BODIPY-labeled oxLDL (10 ug/ml) with cells for 24 hr at 37 °C and 5% CO_2 in serum containing DMEM. Conditions included a control of medium alone without polymer intervention, and non-induced cell controls. Cells were washed, fixed with 4% formaldehyde and imaged on a Nikon Eclipse TE2000-S fluorescent microscope to determine fluorescently tagged oxLDL accumulation. The images were analyzed with ImageJ 1.42q (NIH) and

fluorescence data was normalized to cell count. The levels of oxLDL uptake were normalized to those obtained in the absence of polymers.

3.3.7: Statistical Analysis

Each *in vitro* experiment was performed at least twice and three replicate samples were investigated in each experiment. 5 images per well were captured and analyzed. The results were then analyzed using analysis of variance (ANOVA). Significance criteria assumed a 95% confidence level ($P<0.05$). Standard error of the mean is reported in the form of error bars on the graphs of the final data.

3.4: Results

3.4.1: Molecular Modeling of Polymers

The model polymers, described above, were scaled to contain PEG chain repeats of 20 in place of 115; however the aliphatic side chains were full length to better understand the role of the hydrophobic domain. Polymer models were designed to investigate the influence of mucic acid backbone stereochemistry **(1cS)**, the influence of a cyclic versus linear backbone (**0cG** and **0cGl**), and the influence of aromatic versus aliphatic backbone (**1cAr**).

3.4.2: Docking and Scoring of Polymers to SR-A

The modeled polymers were docked to SR-A collagen-like domain homology model using GOLD v3.2 [140]. The docked pairs were ranked based on each GoldScore.

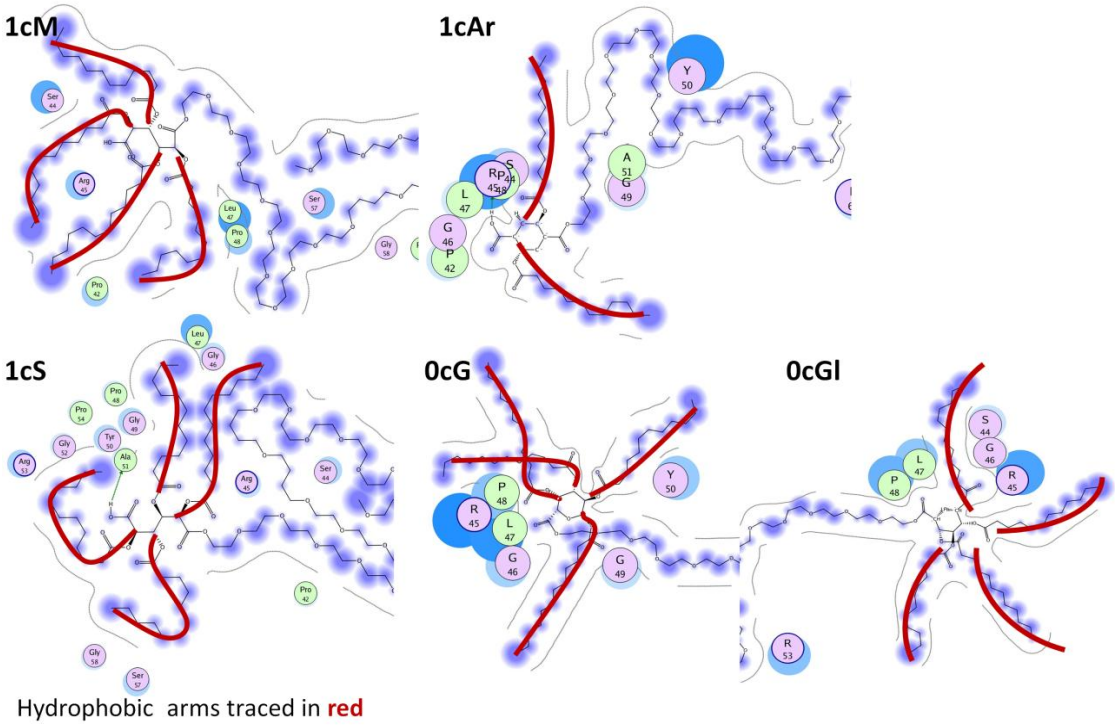

Figure 3.2: Schematic representation of the docked interactions of SR-A collagen-like domain homology model residues (as seen in the colored circles) with polymer models: 1cM (1 carboxylate on the mucic acid), 1cS (1 carboxylate on saccharic acid), 1cAr (1 carboxylate on aromatic), 0cG (zero carboxylate on galacturonic acid) and 0cGl (zero carboxylate on glucuronic acid). Residue characteristics are illustrated through color: Purple = polar, green = hydrophobic, blue border = basic, and red border = acidic.

The five residues reported to be responsible for oxLDL binding to SR-A [76, 121] were used to define the binding pocket. **Figure 3.2** illustrates the 2D representations of the consensus binding of 20 independent docking runs. It was noted that all of the unimers appeared to be oriented in a way so as to facilitate some binding in the oxLDL binding pocket, specifically Arg45 and Arg53. The most notable difference between the polymers was the positioning of the aliphatic acid chains, highlighted in red. The **1cM**, **1cAr** and **0cGl** hydrophobic arms align with and encircle the SR-A residues. However, in

the **1cS** and **0cG**, the arms overlap and a have looser structure that appears to be independent of the binding pocket residues.

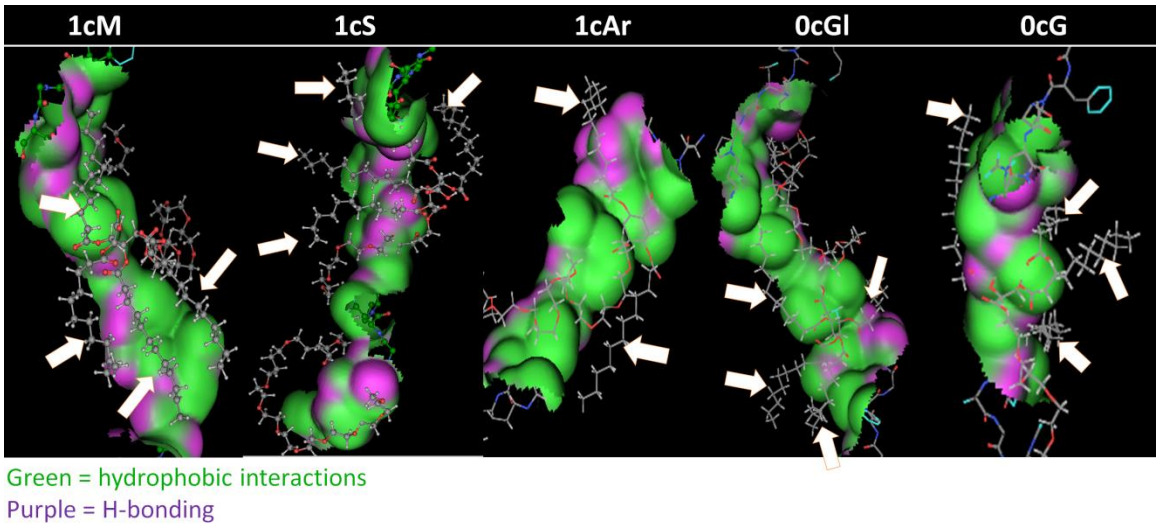

Figure 3.3: 3D schematic of polymer models docked to SR-A collagen-like domain. Hydrophobic arms are indicated by arrows. Green shading represents hydrophobic interactions and purple designates hydrogen bonding. In the polymer model gray represents carbon, oxygen - red, hydrogen - white, and nitrogen - blue.

Based on these findings that the arms may be playing a larger role in binding, the 3D interactions were captured and can be seen in **Figure 3.3**. As implied by the 2D representation, the arms in **1cM**, **1cAr**, and **0cGl** wrap closely around the SR-A homology model and the hydrophobic interactions are shaded in green. The **0cG** unimer also has significant hydrophobic interactions, however not all arms are involved. However, in **1cS** the hydrophobic interactions are minimal and there is much free space between the arms and the protein.

The binding energy was computed for each refined complex using **Equation 1** and the results are graphed in **Figure 3.4**. The energy values reinforce docked

observations, in that the polymer models with the most favorable energies were also positioned in a way so as to facilitate binding.

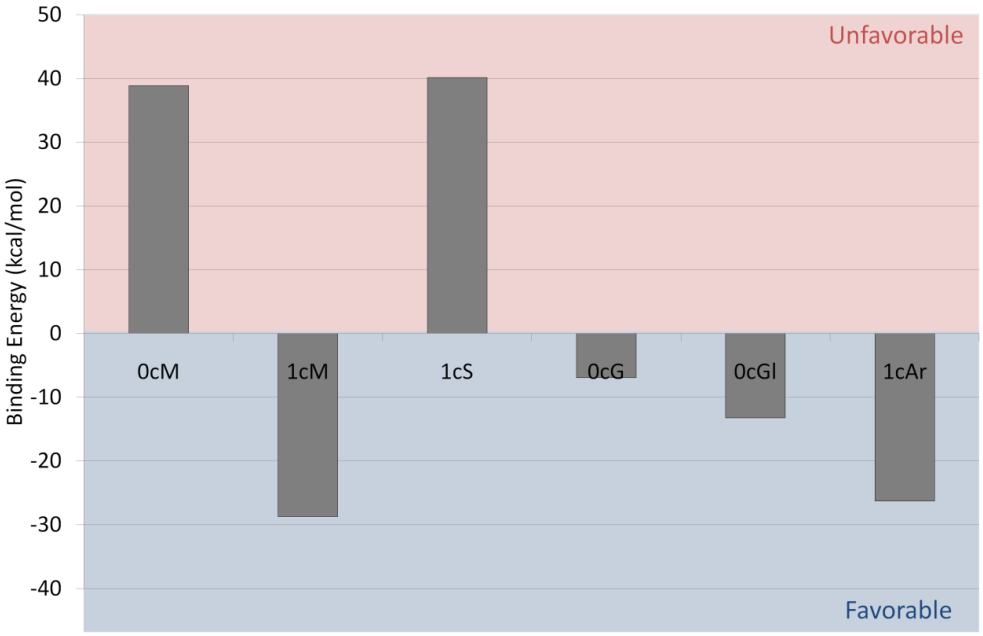

Figure 3.4: Graph of the binding energies of polymer models when docked with SR-A collagen-like domain homology model.

3.4.3: OXLDL Accumulation in HEK-SRA Cells

In **Figure 3.5** the polymers were compared to the polymer previously shown to have the highest binding efficacy **1cM,** neutral control polymer **0cM**, and to basal uptake in the absence of polymers, or without tetracycline induction. The role of charge as well as the position and type of polymer backbone on the inhibition of oxLDL uptake in HEK-SRA cells was examined via incubation of the cells with 10^{-6} M polymers and fluorescent oxLDL for 24 hr at 37 °C. The uptake inhibition seen is primarily SR-A mediated as this is the only scavenger receptor expressed in the engineered cell line.

Both the **1cM** and **1cAr** we able to reduce oxLDL accumulation to nearly the same levels elicited by the SR-A free control cells (23% oxLDL uptake in basal non-induced cells compared to, 35% and 38% in **1cM** and **1cAr** respectively). The binding energies trend well with the competitive inhibition of the experimental oxLDL uptake and were validated by the *in vitro* results.

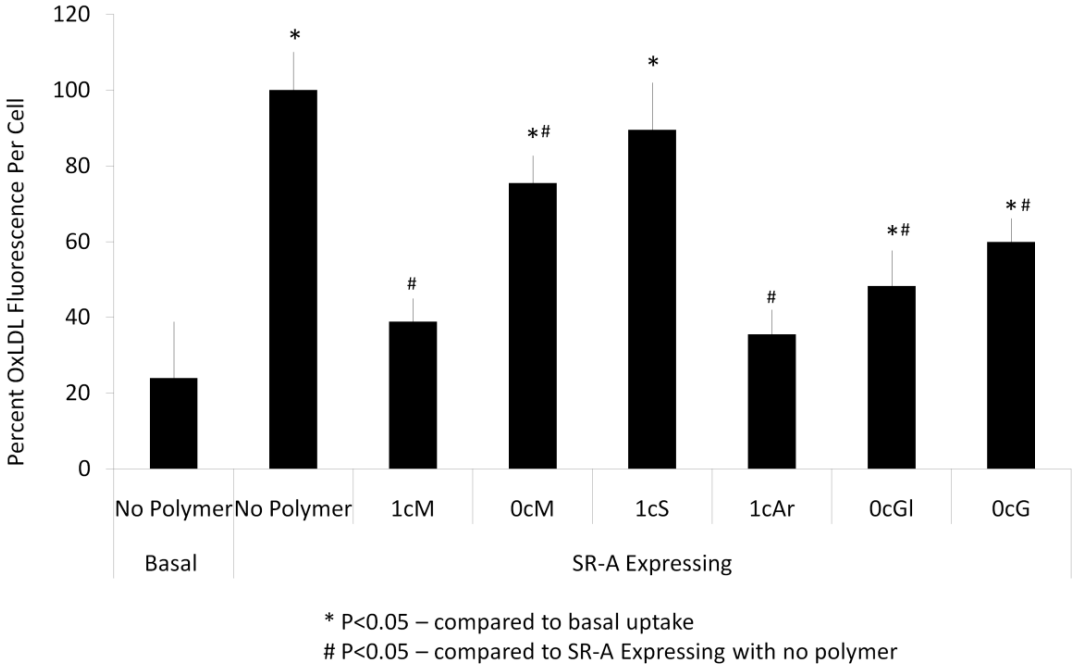

Figure 3.5: The reduction of oxLDL accumulation in the presence polymers compared to the previously identified most inhibitory polymer configuration (1cM).

3.5: Discussion

Polymers designed to block scavenger receptors and inhibit oxLDL accumulation were examined using both molecular modeling and *in vitro* SAR studies with engineered cells to investigate the interaction between backbone-modified polymers and SR-A.

Four new polymer models were designed to investigate the influence of mucic acid backbone stereochemistry (**1cS**), the influence of a cyclic versus linear backbone (**0cG** and **0cGl**), and the influence of aromatic versus aliphatic backbone (**1cAr**). In order to understand the structure-activity relationship (SAR) between the polymers and SR-A, molecular modeling and docking approaches were employed.

The model polymers, described above, were scaled to contain PEG chain repeats of 20 in place of 115, however the aliphatic side chains were full length to better understand the role of the hydrophobic domain. The modeled polymers were docked to SR-A collagen-like domain homology model using GOLD v3.2 [140] and ranked based on each GoldScore. It was noted that all of the unimers appeared to be oriented in a way so as to facilitate some binding in the oxLDL binding pocket, specifically Arg45 and Arg53. The most notable difference between the polymers was the positioning of the aliphatic acid chains. The **1cM**, **1cAr** and **0cGl** hydrophobic arms align with and encircle the SR-A residues. However, in the **1cS** and **0cG**, the arms overlap and a have looser structure that appears to be independent of the binding pocket residues. This is likely due to the spatial positioning of the aliphatic arms on the sugar (saccharic and galacturonic acids) which were not symmetrical in nature. Observed in 3D, the arms of **1cM**, **1cAr**, and **0cGl** wrap closely around the SR-A homology model indicating that there is a significant amount of hydrophobic interactions. The side chains wrap closely around the SR-A protein and seem “locked” in place. This scenario is consistent with more favorable (more negative) binding energies (-29, -26, and -13 kcal/mol in **1cM**, **1cAr**, and **0cGl** respectively). Comparatively, the **0cG** and **1cS** had weaker binding affinities. The

0cG unimer had some hydrophobic interactions, however in **1cS** the hydrophobic interactions are minimal and there was much free space between the arms and the protein. Overall, the **1cAr** was most similar to the "gold standard" **1cM** in terms of binding energy, however only had half as many aliphatic arms. But, as noted in **Figure 3.2** and **Figure 3.3**, the carboxylate group is exposed and available for multiple interactions with SR-A. In **0cGl**, there is no anionic group and binding appears to be mediated primarily though hydrophobic interactions. While the **0cM** and **0cGl** have the same charge, they have drastically different binding affinities, which must be due to the backbone conformation (linear vs. cyclic) and the resulting space-filling of the side chains. These variations begin to yield insights about the unique combination of charge and hydrophobicity that is necessary for efficient SR-A binding. For example, different unimer features could be incorporated in a combinatorial manner to constitute an optimal micelle. A simple way to accomplish this is via mixed micelles without the need for new polymer synthesis, however the equilibration of the constituent unimers needs to be controlled and validated.

The binding energies correlate well with the experimental oxLDL uptake data and were validated by the *in vitro* results. *In vitro* the polymers were compared to the previous gold standard **1cM,** neutral control polymer **0cM**, basal uptake in the presence of no polymers, and basal uptake without tetracycline induction. The role of charge as well as the position and type of polymer backbone on the inhibition of oxLDL uptake in HEK-SRA macrophages was examined via incubation of the cells with 10^{-6} M polymers and fluorescent oxLDL for 24 hr at 37 °C. The uptake inhibition seen was primarily SR-A

mediated as this was the only scavenger receptor expressed in the engineered cell line. It is notable that both the **1cM** and **1cAr** were able to reduce oxLDL accumulation to nearly the same levels seen in the SR-A free control cells. The polymers were able to virtually inhibit all oxLDL uptake associated with SR-A mediated pathways, allowing only a small basal amount of cholesterol to accumulate. These findings could translate to the design of improved polymers for high competitive inhibition of atherogenesis, which will need to be tested further *in vivo*. Polymers that bind with high specificity to scavenger receptors could also be used a carriers for drug delivery.

CHAPTER 4: Scavenger Receptor Targeted Delivery of Hydrophobic Drug to Macrophages

4.1: Specific Aim 3

This aim investigated the multifunctional potential of amphiphilic polymers to target scavenger receptors upregulated on inflamed macrophages and solubilize and deliver a hydrophobic model drug reversing cholesterol accumulation. Two carboxylate-terminated polymers and one neutral control polymer were studied for their SR-A binding and potential to enhance drug loading. The polymers encapsulated hydrophobic agonist (GW3965) against nuclear Liver-X receptor α (LXR), which significantly increased the drug uptake over non-polymer carrier based drug uptake. Alone the polymers reduced SR-A mediated oxLDL uptake by 60% in cultured THP-1 macrophages after 24 hr and showed minimal binding to smooth muscle cells or coronary artery endothelial cells. In combination with the encapsulated LXR-agonist (LXRA), however, the polymers reduced oxLDL accumulation by 88% *in vitro* in macrophages. Thus, these findings suggest that the proposed system of amphiphilic polymers exhibit significant tunability for scavenger receptor targeting, which can be exploited both for inhibition of cholesterol uptake as well as modulating cholesterol intracellular trafficking.

4.2: Rationale

Atherosclerosis, triggered by macrophage, smooth muscle and endothelial cell interactions with low density lipoproteins (LDL) within the vascular wall, is the major

cause of cardiovascular disease and the leading cause of death in developed countries [145]. Elevated LDL plasma levels lead to the accumulation of LDL within the arterial wall, where LDL is oxidized and modified, thus activating endothelial cells, which, in turn recruit circulating monocytes that differentiate into macrophages. This athero-inflammatory cycle is believed to trigger foam cell formation and the advancement of atherosclerosis as macrophages endocytose oxidized LDL (oxLDL) through unregulated scavenger receptors [74, 82, 101, 146].

The localized build-up of cholesterol within the vascular intima and the consequent athero-inflammatory cascade present a major challenge to current therapeutic strategies. Major pharmacologic modalities aim to lower systemic levels of cholesterol through liver-based synthetic pathways. Although systemic therapies may have some impact stabilizing atherosclerotic plaques, their ability to rescue the athero-inflammatory cascade and restore normal anatomy is limited. Further, they are known to cause adverse side effects (from gastrointestinal complaints to liver enzyme elevation and myopathy) [147, 148]. A marked decrease in the progression of advanced necrotic lesions has been noted in ApoE-/- mice through the targeted deletion of scavenger receptors SR-A and CD36, which are upregulated in inflamed macrophages [149], indicating that scavenger receptors play a role in disease progression. Previous investigations have been completed on synthetic compounds that can bind to scavenger receptors, potentially blocking modified LDL entry into cells [102-105]. Synthetic oxidized phospholipids (oxidized phosphocholine) cross-linked to a hexapeptide or bovine serum albumin (BSA) have been used as pattern recognition ligands for CD36 and have been

shown to viably inhibit the binding of oxLDL to CD36 expressing cells [102]. In addition, sulfatide derivatives for the targeting of SR-A have been synthesized and investigated and have been shown to reduce acetylated LDL binding and uptake in a concentration-dependent manner [103]. Atherosclerotic progression may further be controlled through management of atherosclerotic lesion macrophage infiltration, [150] which Yamakawa et al. has recently restricted via the administration of dehydroepiandrosterone (DHEA), independent of systemic cholesterol levels [151].

In this study, the multifunctional nature of nanoscale amphiphilic polymers composed of a sugar backbone with aliphatic side-chains and poly(ethylene glycol) (PEG) was exploited to target inflammatory cells and deliver a hydrophobic drug. The amphiphilic polymers are themselves bioactive; they self-assemble to form nanoscale micelles with the ability to bind to macrophage scavenger receptors with high affinity. At concentrations above the critical micelle concentration (CMC) of 10^{-7} M, these polymers competitively inhibit cellular internalization of oxLDL. Further, the hydrophobic core of the polymer supports good loading efficiency and subsequent release of biologically active hydrophobic drug molecules, enabling the use of the bioactive polymer for drug encapsulation and intracellular delivery [125].

The current study explores the potential of the polymers to inhibit oxLDL accumulation through complementary mechanisms: reduction of cholesterol uptake through binding and blockage of scavenger receptors (intrinsic bioactivity); and delivery of encapsulated hydrophobic drug activating cholesterol efflux channels, exploiting the amphiphilic nature of the polymers. The success of the latter approach is demonstrated

using a model agonist GW3965, a synthetic small molecular weight agonist to nuclear membrane receptor liver-X receptor α [112]. This agonist has been shown to alter cholesterol synthesis, influx and efflux causing an overall decrease of 36% to 39% cellular cholesterol after 96 hrs as well as regulating inflammation and atherosclerosis in animal models [152-154].

I report that the combination of polymer-mediated scavenger receptor binding and intracellular delivery of the liver-X receptor agonist for lipoprotein metabolism was exceptionally effective, with nearly 90% inhibition of cholesterol accumulation after 24 hr in vitro in THP-1 macrophages. This work reveals the potential of polymers to target and rescue inflamed macrophage cells from the atherosclerotic phenotype.

4.3: Materials and Methods

4.3.1: Cell Culture

Human THP-1 monocytes (ATCC) were grown in suspension with RPMI-1640 medium (ATCC) and supplemented with 10 % FBS, in an incubator with 5 % CO_2 at 37 °C. The cells were seeded at a concentration of 10^5 cells/cm^2 and differentiated into macrophage cells by 14 hrs incubation in 16 nM phorbol myristate acetate. After the 14 hr differentiation period the cells were incubated for an additional 58 hrs in RPMI-1640 medium and experiments were performed within three days. Human Aortic Smooth Muscle Cells (HA-SMC) were maintained at 37 °C with 5% CO_2 cultured in F-12K medium (ATCC) supplemented with 0.05 mg/ml ascorbic acid, 0.01 mg/ml insulin, 0.01 mg/ml

transferring, 10 ng/ml sodium selenite, 0.03 mg/ml Endothelial Cell Growth Supplement (ECGS), 10% FBS, and 10 mM TES. The cells were seeded at a concentration of 10^5 cells/cm^2 and experiments were performed within three days. Human Coronary Artery Endothelial Cells (HCAEC) (Lonza) were maintained at 37 °C with 5% CO_2 in endothelial cell basal medium-2 (EBM-2) supplemented with EGM-2-MV singlequots (Lonza). The cells were seeded at a concentration of 10^5 cells/cm^2 and experiments were performed within three days. Activation of cells was achieved though incubation with 1 ng/mL TNF-α (Sigma) for 4 hr prior to experiment.

4.3.2: LDL Oxidation

OxLDL was prepared within five days of each experiment. BODIPY-labeled human plasma derived LDL (Molecular Probes, OR) was oxidized by 18 hr of incubation with 10 µM $CuSO_4$ (Sigma) at 37 °C with 5 % CO_2 [127, 128]. After 18 hr the oxidation was stopped with 0.01 % w/v EDTA.

4.3.3: Polymer Synthesis and Characterization

Structures were prepared as previously described by colleagues in the Dr. Kathryn Uhrich laboratory [106, 108, 124]. The major reactants included 5000 Da heterobifunctional poly(ethylene glycol) (NH2-PEG-COOH) (Nektar, San Carlos, CA), 4-(Dimethylamino)pyridinium p-toluenesulfonate (DPTS) and carboxylate-terminated poly(ethylene glycol) (PEG-COOH 5000 MW) (Sigma, St. Louis, MO). All PEG reagents

were dried by azeotropic distillation with toluene. All other reagents and solvents were purchased from Aldrich and used as received.

Chemical structures and compositions were confirmed by 1H and 13C NMR spectroscopy with samples (~ 5-10 mg/ml) dissolved in CDCl3-d solvent on Varian 400 MHz spectrometers, using tetramethylsilane as the reference signal. IR spectra were recorded on a Mattson Series spectrophotometer (Madison Instruments, Madison, WI) by solvent (methylene chloride) casting on a KBr pellet. Negative ion-mass spectra were recorded with a ThermoQuest Finnigan LCQTMDUO System (San Jose, CA) that includes a syringe pump, an optional divert/inject valve, an atmospheric pressure ionization (API) source, a mass spectrometer (MS) detector, and the Xcalibur data system. Meltemp (Cambridge, Mass) was used to determine the melting temperatures (Tm) of all the intermediates.

Gel permeation chromatography (GPC) was used to obtain molecular weight and polydispersity index (PDI). It was performed on Perkin-Elmer Series 200 LC system equipped with Pl gel column (5 μm, mixed bed, ID 7.8 mm, and length 300 mm) and with a Water 410 refractive index detector, Series 200 LC pump and ISS 200 Autosampler. Tetrahydrofuran (THF) was the eluent for analysis and solvent for sample preparation. Sample was dissolved into THF (~ 5 mg/ml) and filtered through a 0.45 μm PTFE syringe filter (Whatman, Clifton, NJ) before injection into the column at a flow rate of 1.0 ml/min. The average molecular weight of the sample was calibrated against narrow molecular weight polystyrene standards (Polysciences, Warrington, PA).

4.3.4: Polymer Association with Vascular Cells

Texas-red conjugated polymers were prepared as previously described [125, 126]. HCAEC, HA-SMC or differentiated THP-1, cells were incubated with a mixture of 5% Texas red labeled polymers and 95% **1cM** carboxy-terminated polymers or **0cM** uncharged control polymers at 10^{-6} M for 24 hr in 5% serum RPMI-1640 at 37 °C in both basal and activated states with and without 10 ug/ml SR-A antibody blocking (R&D Systems). Cells were washed, fixed with 4% formaldehyde and imaged on a Nikon Eclipse TE2000-S fluorescent microscope to determine fluorescently tagged polymer attachment. The images were analyzed with ImageJ 1.42q (NIH) and fluorescence data was normalized to cell count.

4.3.5: OxLDL Accumulation in Macrophages

The internalization of oxLDL by THP-1 macrophage cells was assayed by incubating BODIPY-labeled oxLDL (10 ug/ml) with cells for 24 hr at 37 °C and 5% CO2. Conditions included a control of RMPI-1640 medium, polymer alone (10^{-6} M), free LXRA (10^{-7} M) admixed with polymer (10^{-6} M), and encapsulated polymer[LXRA] (10^{-6} M/10^{-7} M). Cells were washed, fixed with 4% paraformaldehyde and imaged on a Nikon Eclipse TE2000-S fluorescent microscope to determine fluorescently tagged oxLDL accumulation. The images were analyzed with ImageJ 1.42q (NIH) and fluorescence data was normalized to cell count.

4.3.6: Polymer Encapsulation of Liver-X-receptor Agonist and Characterization

The liver-X-receptor agonist (LXRA), GW3965, was encapsulated within polymers using oil/water emulsion. Specifically, GW3965 in CH_2Cl_2 was added drop wise to a stirring solution of polymer in water. The solution (10^{-4} M polymer and 10^{-5} M GW3965) was stirred continuously in a capped vessel for 24 hr followed by 16 hr uncapped for solvent evaporation. The resulting solution was filtered with a 0.20 μm syringe filter (Fisher Scientific) and diluted to the desired concentration.

Dynamic light scattering (DLS) analyses were performed to determine the diameter of each micellar polymer and LXRA complex to determine encapsulation with the aid of a Malvern Instruments Zetasizer Nano ZS-90 instrument (Southboro, MA). Polymer solutions (1.0 wt %) in water were be prepared and measured at a 90 ° scattering angle at 25 °C.

Encapsulated GW3965 concentration was determined by UV absorption on a UV Mini 1240 UV-vis spectrophotometer (Shimadzu) at 272 nm. Once encapsulated, the drug absorption peak was no longer visible due to micelle shielding. Micelles were disrupted by 1:1 DMA/water and GW3965 concentration quantified by absorption at 273 nm in comparison to a calibration curve.

4.3.7: Macrophage Internalization of Liver-X-receptor Agonist

Differentiated THP-1 macrophages were incubated with polymer at 10^{-6} M and/or 10^{-7} M LXRA for 5 hr in serum-free RPMI at 37 °C. Cells were washed and fixed

and examined under multiphoton microscopy to detect internalized agonist on a Leica TCS SP2 system (Leica Microsystems, Inc., Exton, PA). The cells were illuminated using titanium sapphire femtosecond laser with a tunable wavelength set at 780 nm excitation (Mai Tai, repetition rate 80Mhz, 100 fs pulse duration, 800 mW) and 470-500 nm emission.

4.3.8: Rescue of Cholesterol Pre-loaded Macrophages

The polymer/drug mediated rescue of macrophage cells was quantified following pre-incubation of cells with excess oxLDL. Macrophage cells were incubated with BODIPY-labeled oxLDL (10 μg/mL) and 5 % FBS serum for 2 hr at 37 °C and 5 % CO_2. Excess oxLDL solution was then removed from the cells. Test conditions were added and incubated for 24 hr at 37 °C and 5 % CO_2. A control condition included RMPI-1640 medium with no additional oxLDL added. The remaining conditions each contained LXRA (10^{-7} M) admixed with polymer (10^{-6} M) or encapsulated polymer[LXRA] (10^{-6} M/10^{-7} M). Cells were washed, fixed with 4% paraformaldehyde and imaged on a Nikon Eclipse TE2000-S fluorescent microscope to determine fluorescently tagged oxLDL accumulation. The images were analyzed with ImageJ 1.42q (NIH) and fluorescence data was normalized to cell count.

4.3.9: Statistical Analysis

Each experiment was performed three times and three replicate samples were investigated in each experiment. The results were analyzed using analysis of variance

(ANOVA) performed using Excel's data package software. Significance criteria assumed a 95% confidence level ($P<0.05$). Standard error of the mean is reported in the form of error bars on the graphs of the final data.

4.4: Results

4.4.1: Functionalized Polymers Bind to Activated Macrophages via SR-A

The polymers, composed of poly(ethylene glycol) (PEG) conjugated to a sugar backbone, derivatized with aliphatic side-chains self-assemble in aqueous media to form nanoscale micelles above the critical micelle concentration (10^{-7} M) [106]. Three variants of polymer chemistries were investigated; a carboxy core-terminated amphiphilic polymer (**1cM**), an uncharged control polymer (**0cM**) and a carboxy corona-terminated amphiphilic polymer (**1cP**) (for structures see **Figure 2.1**).

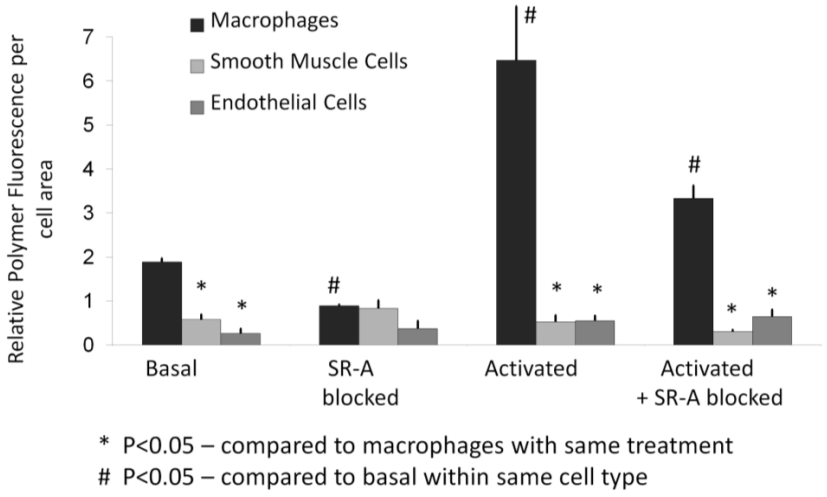

Figure 4.1: Internalization of Texas-red labeled 1cM polymer in THP-1s, HUVECs, and SMCs. 1cM exhibits preferential binding and internalization in human macrophages compared to endothelial and smooth muscle cells .

First, the **1cM** polymer was investigated for its ability to target macrophages compared to two other vascular cell types, human aortic smooth muscle cells (HA-SMC) and human coronary artery endothelial cells (HCAEC). The **1cM** showed enhanced binding to THP-1 macrophages while minimal binding of the polymer was observed in either HA-SMC or HCAEC (**Figure 4.1)**. Significantly greater polymer binding was observed in TNF-α activated macrophage cells (59% increase over basal cells), which have been shown to exhibit increased expression of SR-A [155]. When macrophages were pre-treated with an SR-A antibody, 1cM binding fell to levels seen in the other two cell types. TNF-α treatment and SR-A antibody blocking did not alter polymer binding to cultured human coronary artery endothelial cells or human aortic smooth muscle cells, confirming that preferential carboxy-terminated polymer binding to macrophages can be attributed to SR-A interactions and non-specific binding is consistently minimal among all cell types.

Next, all three polymers were investigated in THP-1 macrophages only. Both of the carboxy-terminated polymers showed enhanced binding in THP-1 macrophages while minimal binding of the uncharged control was observed over all conditions (**Figure 4.2)**. Compared to the basal cells, significantly greater carboxy-terminated polymer binding was observed in TNF-α activated macrophage cells (60% increase), which have been shown to exhibit increased expression of SR-A [155]. When macrophages were pre-treated with an SR-A antibody, the **1cM** and **1cP** polymer binding fell dramatically,

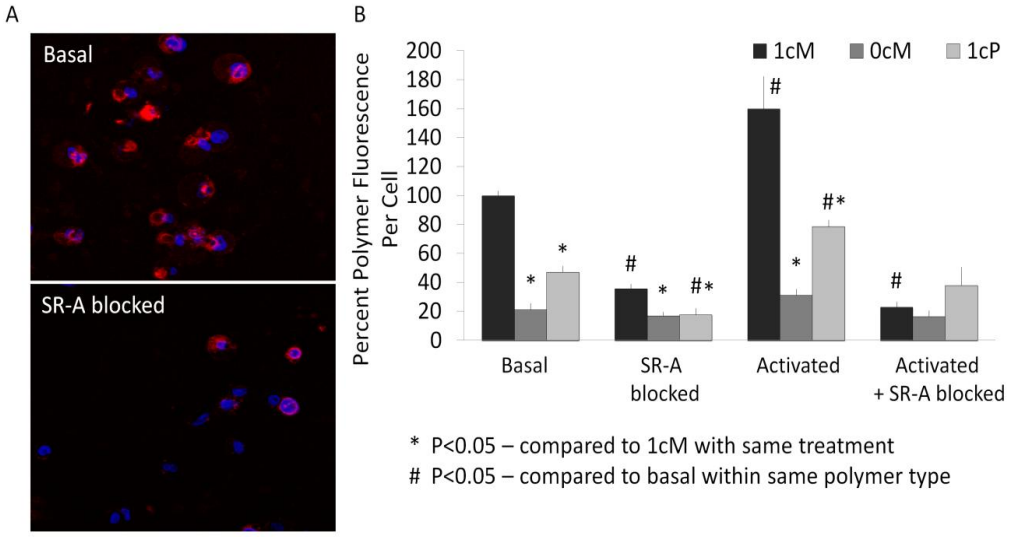

Figure 4.2: A) Accumulation of 1cM polymer in THP-1 cells with and without receptor blocking. THP-1 nuclei are shown in blue and 1cM polymer is shown in red. B) The binding and accumulation of polymer appears to be primarily SR-A mediated and is significantly enhanced in activated (TNFα treated) macrophages.

indicating that both of these polymers bound via SR-A. Moreover, when TNF-α treated THP-1 cells were exposed to SR-A blocking antibodies, the levels of carboxy-terminated polymer (**1cM** and **1cP**) uptake were reduced to non-specific binding levels.

4.4.2: OxLDL Accumulation is Blocked by Polymer Intervention

The polymers were incubated with basal and TNF-α treated THP-1 macrophages in order to elucidate the ability of the polymers to prevent the binding and internalization of oxLDL (**Figure 4.3**). The addition of **1cM** and **1cP** to human macrophage cells in the presence of oxLDL caused a significant decrease in cholesterol uptake after 24 hrs in comparison to control condition of no polymer in both basal and activated conditions. The most significant decrease was observed with the **1cM**

polymer (40% in basal and 58% in treated cells), while very little inhibition was seen with the **0cM** polymer.

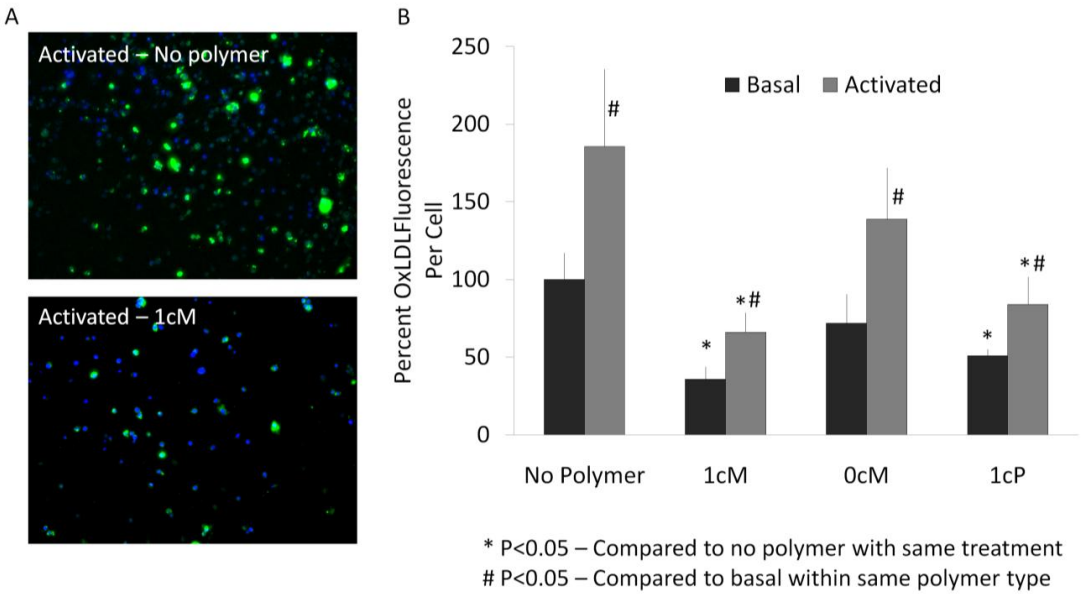

Figure 4.3: A) Reduction of oxLDL accumulation in the presence of various polymers with and without macrophage activation. THP-1 nuclei are shown in blue and oxLDL is shown in green. B) 1cM provided the greatest reduction in both basal and inflamed conditions

2.4.3: Oxidized LDL Accumulation is Reduced by Agonist Delivery

In order to elucidate the ability of the agonist to reduce the accumulation of oxLDL, the GW3965 agonist was encapsulated within each of the three polymers via the oil/water emulsion method (**Figure 4.4**). To ensure that the LXRA was encapsulated, the solution was tested by UV-vis Spectrophotometry and DLS (**Figure 4.5**). While only the results for **1cM** are shown, this verification was also performed with **0cM** and **1cP** encapsulations. The hydrophobic LXRA alone formed large aggregates in water, however after

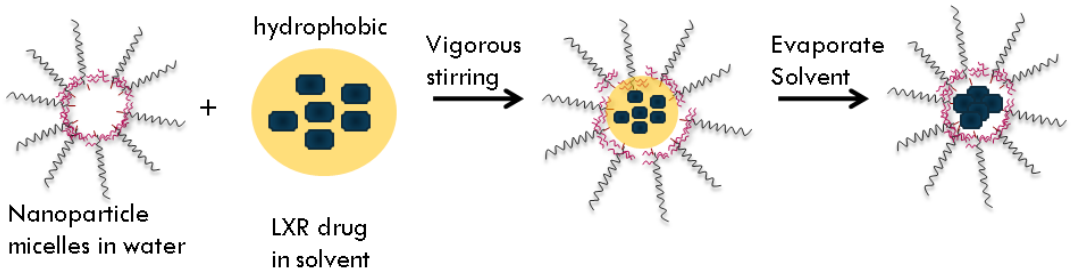

Figure 4.4: Encapsulation of LXR drug agonist within 1cM polymer using the oil-in-water encapsulation method

encapsulation within the **1cM** polymer, the average size fell to around 20 nm, similar to that of **1cM** alone, suggesting that the drug was encapsulated within the micelle core. Furthermore, LXRA alone absorbed light at 272 nm while a sample of encapsulated LXRA did not, as the agonist within the core was shielded by the micelle from UV light. The

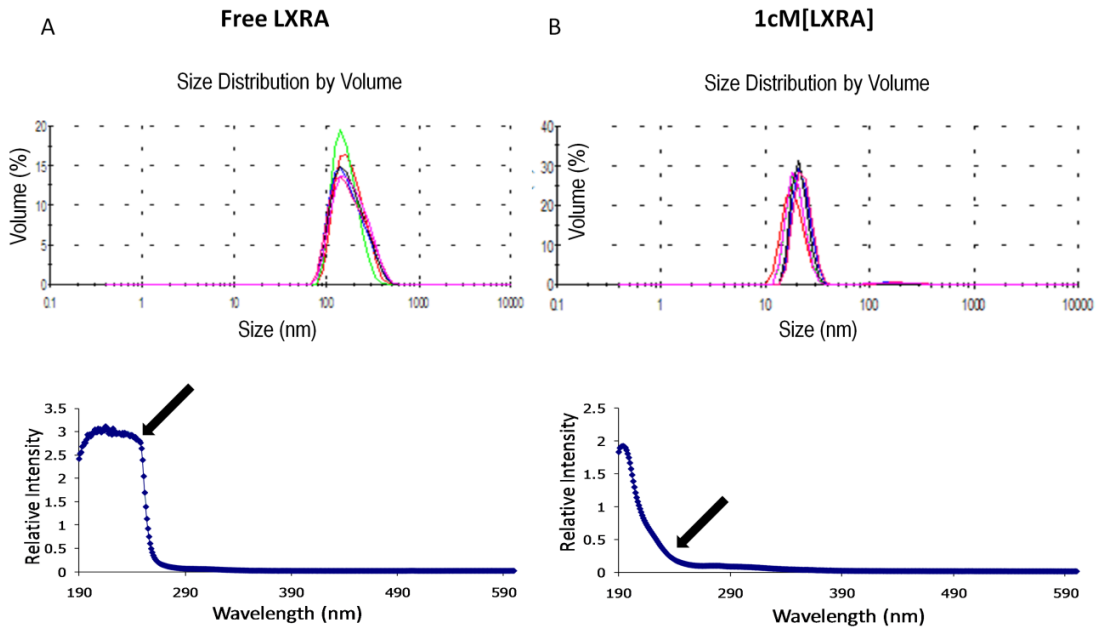

Figure 4.5: The ability of 1cM polymer to encapsulate hydrophobic drug Liver-X receptor agonist (LXRA) was demonstrated. (A) LXRA drug alone forms large aggregates in solution and has a UV peak at 272 nm. (B) LXRA encapsulated in 1cM has an average size close to that of 1cM alone and does not have a UV peak because the drug is shielded by the polymer.

sample was then diluted with dimethylacetamide (DMA) and water 1:1 to disrupt the micelles and release the encapsulated agonist. It was confirmed that the LXRA was indeed encapsulated as the expected absorbance at 272 nm was seen following micelle disruption.

Next, the agonist, free and polymer-encapsulated, was incubated with TNF-α treated THP-1 macrophages in order to elucidate the ability of the polymer-encapsulated agonist to prevent the binding and internalization of oxLDL (**Figure 4.6**). The addition of **1cM** to macrophage cells in the presence of oxLDL caused a significant

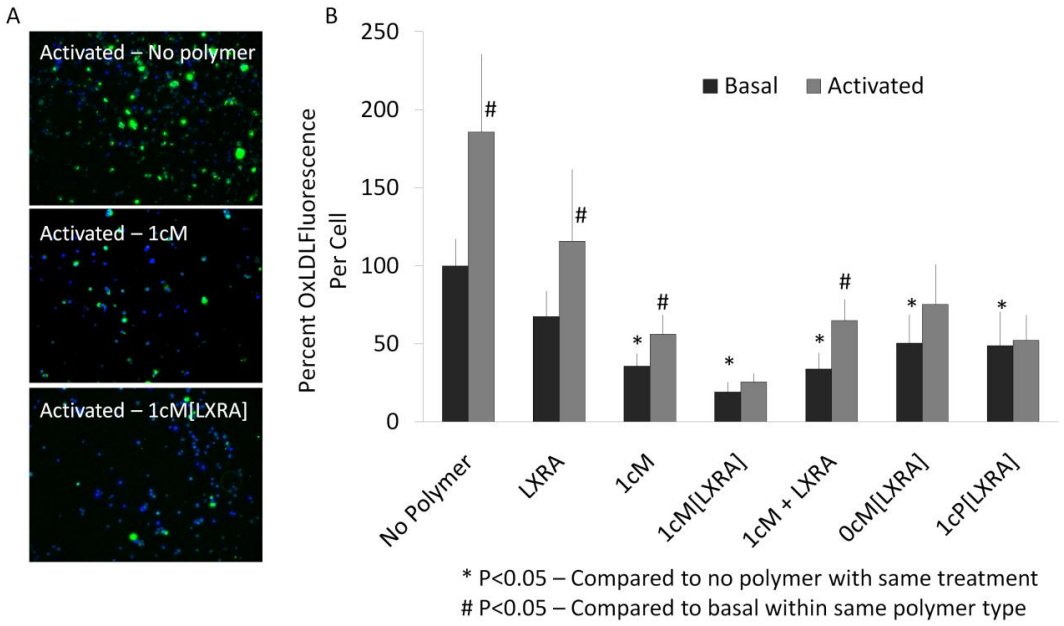

Figure 4.6: A) Reduction of oxLDL accumulation in the presence LXRA encapsulated in various polymer with and without macrophage activation. THP-1 nuclei are shown in blue and oxLDL is shown in green. Encapsulation within 1cM provided the greatest reduction in both basal and inflamed conditions.

decrease in cholesterol uptake after 24 hrs in comparison to control condition of no polymer or drug intervention. Introduction of LXRA alone to cells did not significantly decrease cholesterol content unless polymer was admixed with the agonist (55% less oxLDL than no intervention). The most significant decrease was observed when the agonist was encapsulated within the **1cM** polymer and incubated with macrophages (**1cM**[LXRA]), while LXRA encapsulated in **0cM** or **1cP** was only slightly more effective than LXRA alone.

4.4.4: Polymers Enhance Cellular Uptake of LXR Agonist via SR-A

Free LXRA and polymer-encapsulated agonist (**1cM**[LXRA]) were incubated with THP-1 macrophages in order to elucidate the ability of the cells to bind and internalize the drug agonist (**Figure 4.7)**. Internalization of LXRA in the absence of polymer was over six-fold lower than that quantified with delivery via encapsulated agonist (82% decrease). The uptake of free agonist by cells remained low and was unaffected by SR-A blocking or TNF-α pretreatment. However, polymer-encapsulated agonist delivery increased after TNF-α treatment and was significantly inhibited by the administration of SR-A antibody (37% increase and 88% decrease respectively). This finding paralleled the trends seen for uptake of the polymer alone (**Figure 4.2**) and confirmed that agonist delivery is enhanced through polymer encapsulation and binding via the scavenger receptor SR-A.

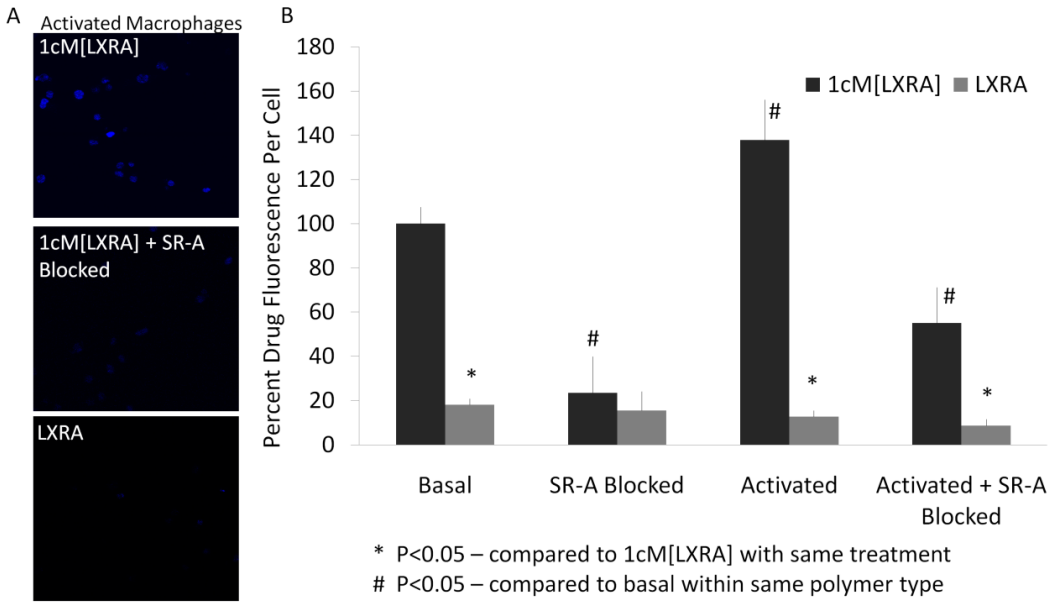

Figure 4.7: Accumulation of LXRA in THP-1 cells when delivered via a 1cM polymer carrier with receptor blocking and macrophage activation. LXRA is shown in blue. B) When encapsulated in 1cM, the GW3965 is taken up by THP-1 macrophages to the greatest extent in both basal and activated macrophages. Drug delivery via the polymers appears to favor activated macrophages, which express increased levels of scavenger receptors.

4.4.5: Cholesterol Efflux from Activated Macrophages is Enhanced by Agonist Delivery

The polymers were incubated with TNF-α treated THP-1 macrophages in order to elucidate the ability of the polymer-drug combinations to reduce the total oxLDL by cholesterol efflux. The cells were pre-loaded with oxLDL before the addition of the polymers (**Figure 4.8**). LXRA encapsulated within **1cM** (**1cM**[LXRA]) caused the most significant efflux (87% decrease in cellular oxLDL compared to no intervention). Polymer admixed with LXRA also displayed significant cholesterol efflux effects, while agonist alone did not result in significant cholesterol efflux. Neither encapsulation in **0cM** or **1cP** provided any additional oxLDL efflux compared to the admixed conditions.

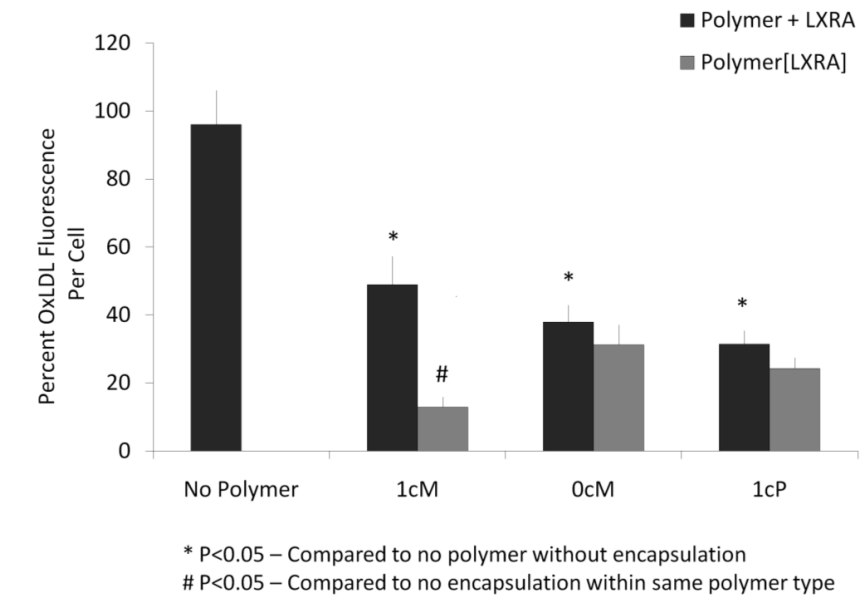

.

Figure 4.8: Reduction of total oxLDL by cholesterol efflux in the presence LXRA encapsulated in various polymer. The cells were pre-loaded with oxLDL before the addition of the polymers. Encapsulation within 1cM provided the greatest efflux of oxLDL.

4.5: Discussion

Major factors underlying the chronic progression of atherosclerotic plaques are the activation and recruitment of macrophages to the vascular injury site, followed by uncontrolled scavenger receptor-mediated internalization of oxLDL. Several different molecular interventional approaches have been proposed including scavenger receptor inhibitors or knockdowns, acyl-CoA cholesteryl acyl transferase (ACAT) inhibitors and knockdown, and inhibitors of macrophage recruitment [109, 112, 156, 157]. In this report, a novel, dual-pronged approach to attenuate cholesterol accumulation was proposed. The approach combines the scavenger receptor-mediated cholesterol blockage potential of the polymers along with anti-atherogenic agonist delivery to inflamed cells.

This agonist has been shown to alter cholesterol synthesis, influx and efflux causing an overall decrease in cellular cholesterol as well as regulating inflammation and atherosclerosis in animal models [152-154].

In vitro studies have previously shown that carboxy-terminated amphiphilic polymers derived from sugar and PEG, can self-assemble into micelles, which bind to macrophage scavenger receptors SR-A and CD36 [108, 143]. These receptors are upregulated in cells at sites of atherosclerotic lesions [155, 158, 159]. The carboxylic acid end groups were hypothesized to mediate electrostatic binding to the positive pocket of residues on the SR-A scavenger receptor [75]. I show that the carboxylate-terminated polymers preferentially bind to scavenger receptor expressing human THP-1 macrophage cells over two other vascular cell types. The increased expression of scavenger receptors in TNF-α activated macrophages further promotes polymer binding. The unique combination of amphiphilicity, geometry and charge was integral to this behavior as none of the control polymers had comparable cholesterol reducing activity. Hence, the carboxylate-terminated polymers act as polymeric therapeutics and may serve as effective candidates for inflamed macrophage targeting *in vivo*.

The liver-X-receptor is implicated in the atherogenic process underlying cardiovascular disease [160]. Since the liver X-receptor agonist (LXRA) GW3965 had been shown to be effective in activating LXR [114, 161], I examined the ability of the polymers to encapsulate and deliver the hydrophobic agonist, GW3965 to activated cells with some degree of specificity. This work demonstrates that increased efficacy of agonist can be achieved via polymer encapsulation. These studies employing direct 2-photon imaging

of cell-internalized agonist confirmed that carboxylate-terminated polymers as well as the LXRA drug are internalized within the cytosol; this cellular internalization allows for drug delivery to the nucleus, where ligand binding is essential for enhanced LXR-signaling and reverse cholesterol transport.

It has been established that effective therapies for cardiovascular disease require the coordinated management of atherogenesis and inflammation [146, 162]. Additional work completed by my colleagues, and included with the results shown above in a future publication, has further explored the anti-inflammatory potential of the polymer-drug complexes both in vitro and in vivo [163]. They found that **1cM** had intrinsic anti-inflammatory activity on both cytokine and MMP-9 secretion, two of the major inflammatory markers of macrophage activation [164-167]. Polymer-based agonist delivery elicited a 9-fold increase in LXRα gene and a 15-fold increase in ABCA after delivery of 10^{-7} M LXRA. Clearly, polymer encapsulation greatly enhanced agonist delivery, via scavenger receptor binding, compared to the non-encapsulated free agonist conditions, resulting in significant alteration in six key atherosclerosis associated genes examined. Typically, elevated SR-A expression is believed to escalate atherosclerosis progression through increased oxLDL accumulation [168]. However, due to enhanced binding of polymer-encapsulated agonist to macrophage SR-A, upregulation allows a route for enhanced polymer and ligand delivery to inflamed cells. These combined results illustrate the potential ability of the polymer-encapsulated agonist complexes to inhibit atherosclerosis at the gene signaling level as well as via receptor blockage, which opens possibilities for depleting as well as retarding the accumulation of cholesterol.

In addition, they used an *in vivo* model to probe the accumulation of cholesterol following localized vascular injury to the carotid artery. Both the polymer and the polymer-encapsulated agonist caused significant inhibition of cholesterol accumulation in comparison to the agonist alone and non-treated samples. A notable finding was that the addition of both polymer alone and polymer-encapsulated agonist significantly inhibited the presence of macrophage cells near the site of injury, which has been reported to be an important atherosclerosis marker independent of cholesterol content [150, 151]. Macrophage recruitment is regulated by factors such as TNF-α and interleukin 1 beta (IL-1β) [150, 169, 170]. This suggests that the polymer therapeutics had an inhibitory effect on the activation of recruited macrophages and possibly the further recruitment of monocytes.

In summary, I show that the polymeric therapeutics significantly lowered total oxLDL accumulation in vitro partially through effective targeted delivering of an LXR agonist. Given the increased bioefficacy and enhanced targeting of activated macrophages, the amphiphilic polymers could be candidates for possible intervention of chronic inflammatory diseases such as sepsis, psoriasis, inflammatory bowel disease, rheumatoid arthritis, and chronic obstructive pulmonary lung disease. As efficient drug carriers, the polymer therapeutics could be used in combination with a broad range of agonists for treatment of various metabolic and neurodegenerative diseases [171].

CHAPTER 5: Conclusions and Future Directions

5.1: Conclusions

This thesis reports findings of a strategy featuring polymeric therapeutics for binding to macrophages expressing SR-A. A self-assembled, amphiphilic polymer based on a poly(ethylene glycol) corona and a hydrophobic core was designed with terminal, carboxylate groups to enhance binding to cationic scavenger receptors on activated human macrophages. The factors necessary for effective binding were not well understood, thus molecular modeling and docking approaches were used to understand the structure-activity relationship (SAR) between the polymers and SR-A. Six polymer models (4 first generation polymers and 2 second generation polymers) were docked to the SR-A homology model to investigate charge placement and clustering, as well as the SR-A residues involved in binding. Polymer models with the most favorable binding energy were also the most effective oxLDL inhibitors in THP-1 macrophages. Mutant SR-A models were generated by replacing charged residues with alanine. All charged residues in the region were necessary, with Lys60, Lys63 and Lys66 having the greatest effect on binding. However, binding was clearly not mediated by charge alone and the polymer hydrophobic domain adjacent to the carboxylate group was found to be essential.

Building upon the success of polymer **1cM** binding studies, together with colleagues, new polymer structures were proposed. Polymer models were designed to investigate the influence of mucic acid backbone stereochemistry, the influence of a cyclic versus linear backbone, and the influence of aromatic versus aliphatic backbone.

Polymer models were docked to the previously constructed SR-A homology model to investigate the significance of the polymer backbone on receptor binding and results indicate the ability of the backbone to position the side chains and "lock" the ligand into position. Polymers were synthesized by our collaborators from the Uhrich laboratory for model validation *in vitro* and results followed those seen in the modeling predictions, with **1cAr** and **0cGl** showing promise. Thus, minute changes in polymer structures can sensitively affect SR-A binding affinities and consequently modulate the competitive inhibition of oxLDL uptake.

Furthermore, the amphiphilic nature of the polymers was exploited to encapsulate a hydrophobic agonist against nuclear Liver-X receptor α (LXR) which significantly increased the drug uptake in the cells. In combination with the encapsulated LXR-agonist (LXRA), the polymers were found to reduce oxLDL accumulation by 88% *in vitro* via the SR-A scavenger receptor. Based on these findings, the system of amphiphilic polymers show the potential to be a multi-functional cardiovascular treatment modality with tunability for receptor targeting.

5.2: Future Directions

5.2.1: Advanced Modeling Efforts

While atomistic models are insightful, they can be somewhat limited in their ability to fully capture the entire nanoparticle dynamics. In the case of the work presented here, only unimer binding could be considered due to limitations in computational time and space, while a more robust model would be necessary to fully

capture micelle aggregation dynamics. A solution to the time and length scale problem in molecular simulation is coarse-graining (CG) the atomistic system studied to one with a lower spatial resolution. Here, the interactions between individual atoms are replaced by interactions between "units". This process dramatically decreases the degrees of freedom of the model, resulting in a speed-up of the simulations by several orders of magnitude [172]. Not surprisingly, the application of such methods to study entirely new problems of biological importance has been rapidly gaining increased attention in the biomolecular simulation community. CG simulations, can result in the construction of models of 10–1000 nm in size [173, 174]. They have been used recently to study modeling of dendrimers and their interactions with bilayers and polyelectrolytes [175], Self-assembly of diblock copolymers into micelles [176], and interactions of polymer-drug conjugates [177]. Additionally, recent research has used CG to aid in investigating polymer–drug interactions, specifically drug encapsulation [178]. This could be used to explore future drugs for possible encapsulation while avoiding a time consuming trial-and-error approach. However, it should be noted that the trade-off is loss of detailed polymer information. In light of the results in Chapter 3, this information might be necessary for understanding binding dynamics as very small changes in the polymer lead to dramatic binding differences.

5.2.2: Multiple Receptor Targeting

A marked decrease in the progression of advanced necrotic lesions has been noted in ApoE-/- mice through the targeted deletion of scavenger receptors SR-A and

CD36, which are upregulated in inflamed macrophages [149]. However, blocking SR-A receptors may not be sufficient to fully inhibit foam cell formation as deletion of one receptor typically results in compensatory over-expression in other scavenger receptors [179]. Utilizing molecular modeling techniques similar to the ones described here, the polymers could be modeled for their interactions with additional scavenger receptors including CD36, SR-BI, SR-PSOX, SREC and LOX-1. Some of these receptors have been crystallized and several would need to be modeled. Designing polymers with binding potential to multiple scavenger receptors could interrupt or suspend the atheroinflammatory cascade, as these receptors trigger atherogenesis and inflammation across both macrophages and endothelial cells. This issue highlights the importance of concerted strategies, such as focusing on anti-inflammatory phenotype of macrophages, reducing monocyte recruitment, and suppressing lipoprotein transport via endothelia. Beside SR-A and CD36, a recent class of scavenger receptors has also emerged as an endothelial cell target, called LOX-1, whose expression is upregulated upon endothelial cell activation [180-184]. LOX-1 activity was recently proposed as a novel predictive marker of coronary heart disease and stroke [65]. Upon recognition of oxLDL, LOX-1 initiates oxLDL internalization and degradation as well as inducing a variety of pro-atherogenic cellular responses, such as reduction of nitric oxide (NO) release [66], secretion of monocyte chemoattractant protein-1 (MCP-1) [67], production of reactive oxygen species [68], expression of matrix metalloproteinase-1 and -3 [69], monocyte adhesion [67], and apoptosis [70].

However, each of these receptors offers slightly different constraints for ligand binding. A characteristic of SR-A is the mediation of uptake and degradation of modified proteins and several polyanionic ligands [32, 117, 118] and binding is thought to be mediated through electrostatic interactions between the Arg and Lys residues in the collagen-like domain of SR-A [75]. Interactions of ligands with CD36 are generally hydrophobic and only somewhat mediated by charge [119]. Further, the incorporation of hydrophobic chains, hydrophilic phosphocholine, and negatively charged carboxylate groups have been shown to contribute to high affinity ligand binding [185]. LOX-1 binding domain, C-type lectin-like domain, contains linearly aligned basic residues, referred to as the basic spine (208 - 248), that are responsible for ligand binding [186]. Others have observed that binding between oxLDL and LOX-1 cannot be solely explained by charge interactions, and because of the receptor's lectin-like structure, sugars on the ApoB portion of oxLDL might play a role in LOX-1 binding [187].

As different receptors offer different binding challenges, the possibility of creating combinatorial micelles by using mixed unimers with different properties is an option. Conceivably three different polymer structures could be optimal for the three different scavenger receptors. Thus, different combinations of these polymer structures can enhance the multiple binding of polymers across the various scavenger receptors. New molecularly designed polymers could present an innovative approach to identify multifaceted biomaterials with cooperative binding affinity toward multiple scavenger receptor targets.

5.2.3: Polymer Fates

Although the role of the polymers in oxLDL uptake and scavenger receptor binding to macrophage cells was explored, further insights are necessary to establish the specific mechanism of action and intracellular fate of the polymers. The binding kinetics and internalization behaviors of polymers, mediated largely by scavenger receptors, needs to be further correlated with the chemistry and architecture of the polymers. Some preliminary work has been done in this area and can be found in the appendices. Endocytosis assays can be performed where the receptors are saturated with fluorescently labeled polymers at 4 °C, then rinsed and brought to 37 °C for specific time intervals in order to quantify the ratio of internalized vs. surface bound ligand. It is possible that beyond the ability of the polymers to bind to the scavenger receptors, the ability of the receptors to endocytose and recycle back to the cell membrane surface is likely affected by polymer design and perhaps plays a larger role in cholesterol accumulation than binding.

Additionally, fluorescently labeled polymers can be tracked and the macrophages counter-stained for co-localization in early endosome (EEA1 [188]), late endosome (Rab7 [189]), and lysosomes (LAMP-1 [190]) at various time points. This will provide information of the intracellular trafficking and kinetics of polymer handling by macrophages.

5.2.4: Polymers for Drug Delivery

The amphiphilic composition of the particles allows for hydrophobic drugs to be protected from solution and increase their solubility, therefore, increasing the drug concentration in a solvent such as blood. Moreover, the nanoscale size of the micelles could potentially allow for delivery that mimics the naturally occurring transport system similar to viruses and lipoproteins [111]. We have recently exploited the amphiphilic nature of the polymers and demonstrated the efficacy of delivery of a liver-X-receptor agonist for cholesterol depletion *in vitro* (Chapter 4). Similar approaches can be combined with other cholesterol trafficking pharmacologic factors (e.g., PPARγ) or anti-inflammatory drugs. In parallel, the polymers could be modified to develop probes for the development and progression of atherosclerotic plaques with increased macrophage activity.

In addition, the molecular modeling platform outlines here could be adapted to include receptors or targets other than scavenger receptors. Efforts are underway to inhibit vascular adhesion molecules including E-selectin, P-selectin, vascular adhesion molecule-1 (VCAM-1) and intercellular adhesion molecule-1 (ICAM-1), as well as chemotactic factors involved in monocyte recruitment to retard atherosclerosis in animal models [191-197]. However, clinical trials have had mixed success [198, 199]. Modeling these receptors and understanding polymer binding could lead to improved formulations of combination polymers as new treatment options. Furthermore, the inclusion of an anti-inflammatory drug could further attenuate the disease progression.

5.2.5: Other Polymer Uses

Because of the scavenger receptor targeting potential exhibited by the polymers, they have the potential to be used for the treatment of many other diseases including, but not limited to, rheumatoid arthritis [200], psoriasis [201], inflammatory bowel disease [202], type 2 diabetes [203], Alzheimer's disease [204] and chronic obstructive pulmonary lung disease [205]. The drug encapsulation capabilities of the polymers could combine to provide a new treatment option for many of these diseases.

This polymer also allows for a disease treatment modality primarily based on its size. Passive targeting of nanoparticles to cancerous tumors due to the gaps found in angiogenic blood vessels [206, 207] is known as the enhanced permeability and retention effect (ERP) [208-211]. The poor lymphatic draining system of tumors [207, 212-214] couples with leaky vessels and allows for an accumulation of nano-scale particles within the growing tissue [215] By encapsulating anti-cancer drugs within these polymers it could be possible to deliver high concentrations of the toxic treatments to tumor cells and while maintaining minimal exposure to healthy tissue.

APPENDIX

A.1: Accumulation of Texas Red Labeled 1cM polymer in THP-1 Macrophages

The accumulation of Texas red labeled **1cM** in THP-1 macrophages in serum containing medium was captured over 12 hr. THP-1 macrophages were seeded in an 8 well lab-tek chamber slides and **1cM** Texas red labeled polymer (5% labeled polymer admixed with 95% unlabeled polymer) was added at time 0. Time lapse images were

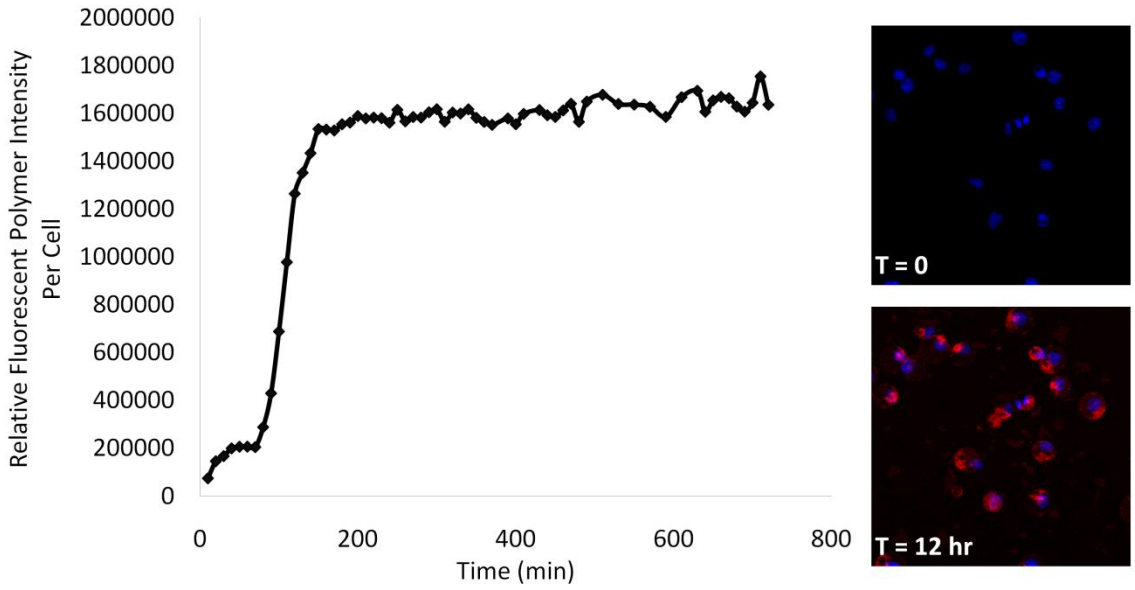

Figure A.1: The accumulation of Texas-red labeled 1cM in THP-1 macrophages over the course of 12 hr in serum containing medium.

taken on the Leica confocal microscope with 63x immersion lens over 12 hr (with the help of Joe Kim). A total of 4 fields were tracked and images were taken at 10 min intervals. The images were compiled into short videos. In addition, the individual

images were analyzed using ImagePro software, and the polymer uptake was quantified as seen in **Figure A.1**.

It appears that over the first hour either binding is predominant over internalization, or the rate of internalization is relatively minimal ($1.3 * 10^5$ fluorescence units per hr). At 70 min, the accumulation rapidly increases at a rate of $8.8 * 10^5$ fluorescence units per hr and the cells are saturated by 3 hr. This, if compared to other polymers could shed light on how binding and uptake of the polymers changes with polymer modification and if there is any correlation to activity. Perhaps efficient polymers not only bind with high affinity, but also affect the rate of receptor internalization and recycling. However, in this study I relied on a mixture of labeled and unlabeled polymers and it is unknown whether these form uniform micelles, each incorporating 5% of the labeled unimers, or if the labeled polymers remain as a separate population.

A.2: Staining of THP-1 Macrophages for EEA1

In order to provide information of the intracellular trafficking and kinetics of polymer handling by macrophages, THP-1 macrophages were stained early endosome marker, EEA1 [188]. THP-1 macrophages were cultured in 8 well lab-tek chamber slides and fixed with 4% paraformaldehyde then stained with 1:50 dilution mouse EEA1 (early endosome marker, Santa Cruz) and 3 ug/mL 488 $1gG_1$ goat anti-mouse secondary (Invitrogen). Images were taken on a Nikon Eclipse TE2000-S fluorescent microscope.

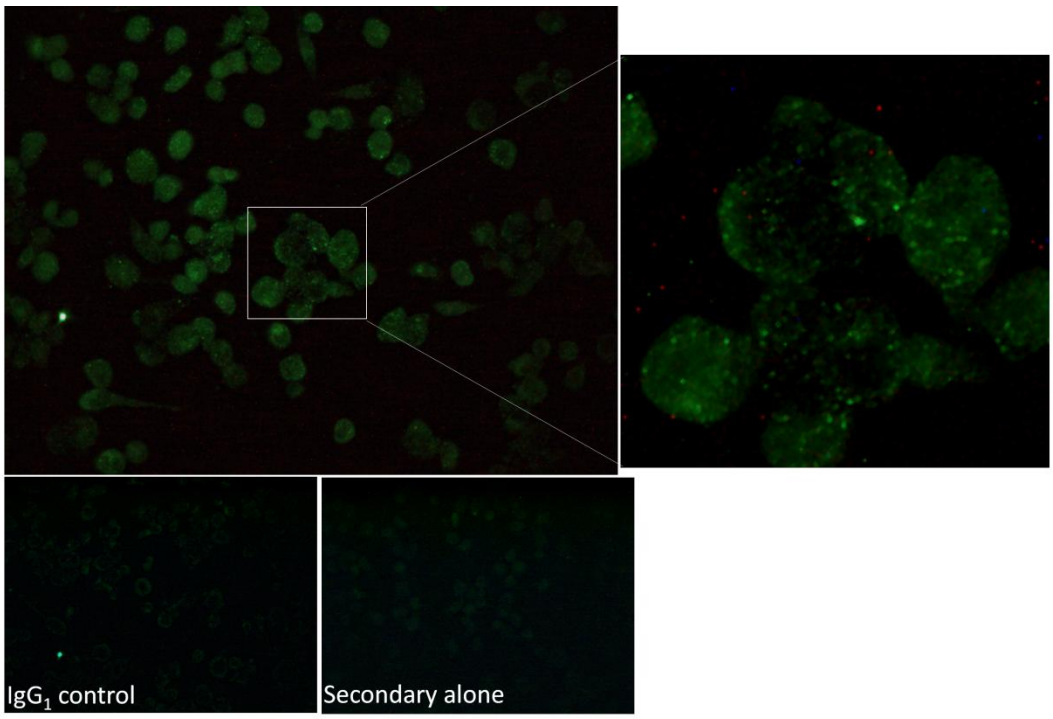

Figure A.2: THP-1 macrophages stained for EEA1, a marker of early endosome. Controls included isotype IgG_1 and 488 goat anti-mouse secondary alone.

Results revealed a typically punctuate staining of EEA1 in the THP-1 cells, while some background fluorescence can be seen in the control conditions. Ideally, fluorescently labeled polymers could be tracked and the macrophages counter-stained for co-localization in early endosome (EEA1 [188]), late endosome (Rab7 [189]), and lysosomes (LAMP-1 [190]) at various time points. This would provide information of the intracellular trafficking and kinetics of polymer handling by macrophages.

A.3: Binding of 1cM to HEK-SRA Cells

Saturation binding experiments measure specific binding at equilibrium at various concentrations of a given ligand. Analysis of such data can determine the

receptor number and binding affinity. In an effort to elucidate the binding of **1cM** to SR-A and exclude all other scavenger receptors, HEK cells inducibly expressing SR-A were employed. After the addition of 0.5 ug/mL tetracycline SR-A is upregulated in the cells. Ordinarily binding can achieved and internalization prevented by performing the experiment at 4 °C, however the conformation of SR-A and thus binding are drastically changed by variations in temperature [121]. Instead, phenylarsine oxide was added to the cell culture medium to inhibit endocytosis [216]. First, both basal and induced HEK cells were incubated with a 10^{-6} M mixture of 5% Texas red labeled and 95% unlabeled **1cM** over 3 hr in order to determine the equilibration time. The binding affinity analyses depend on the assumption that the incubation to proceeded to equilibrium.

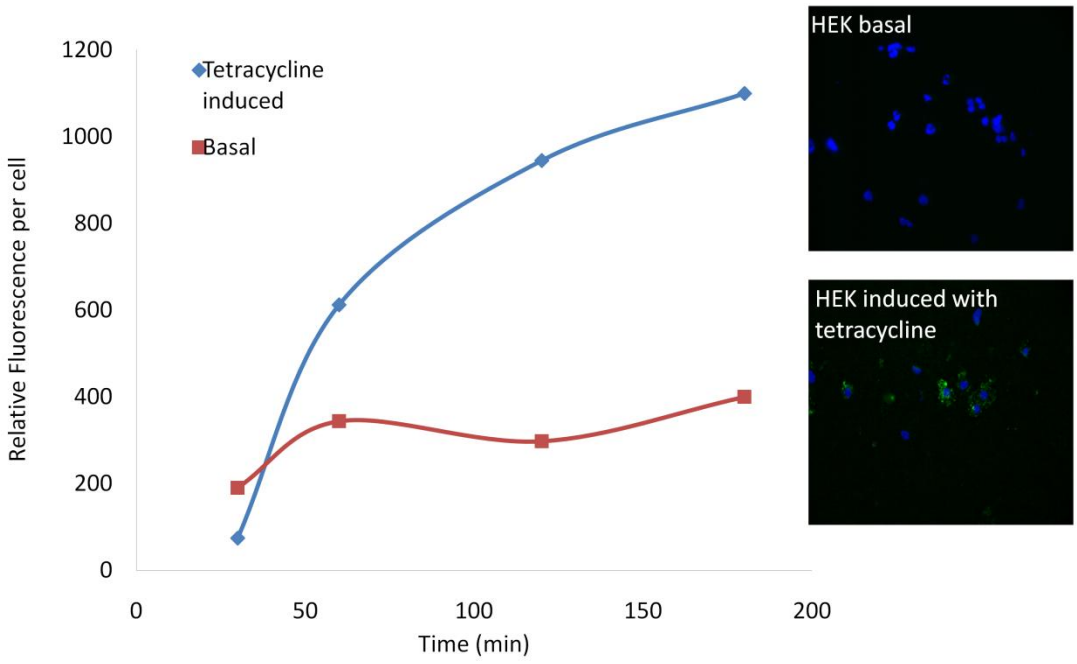

Figure A.3: Binding of fluorescently labeled polymers to HEK-SRA cells over 3 hr. HEK cells do not express SR-A, unless stimulated with tetracycline.

At each timepoint, the cells were washed, fixed with 4% formaldehyde and images were taken on a Nikon Eclipse TE2000-S fluorescent microscope (**Figure A.3**). As expected the basal cells bound significantly less polymer than the induced cells, and 3 hr was deemed sufficient for equilibration.

Next, both basal and induced HEK cells were incubated with a mixture of 5% Texas red labeled and 95% unlabeled **1cM** for 3 hr over a range of polymer concentrations ($5*10^{-5}$ M - 10^{-7} M). After 3 hr, the cells were washed and read on a Cytofluor multi-well plate reader. A standard curve was used to correlate fluorescence intensity to polymer concentration and a Lowry protein assay was run to normalize results to mg protein.

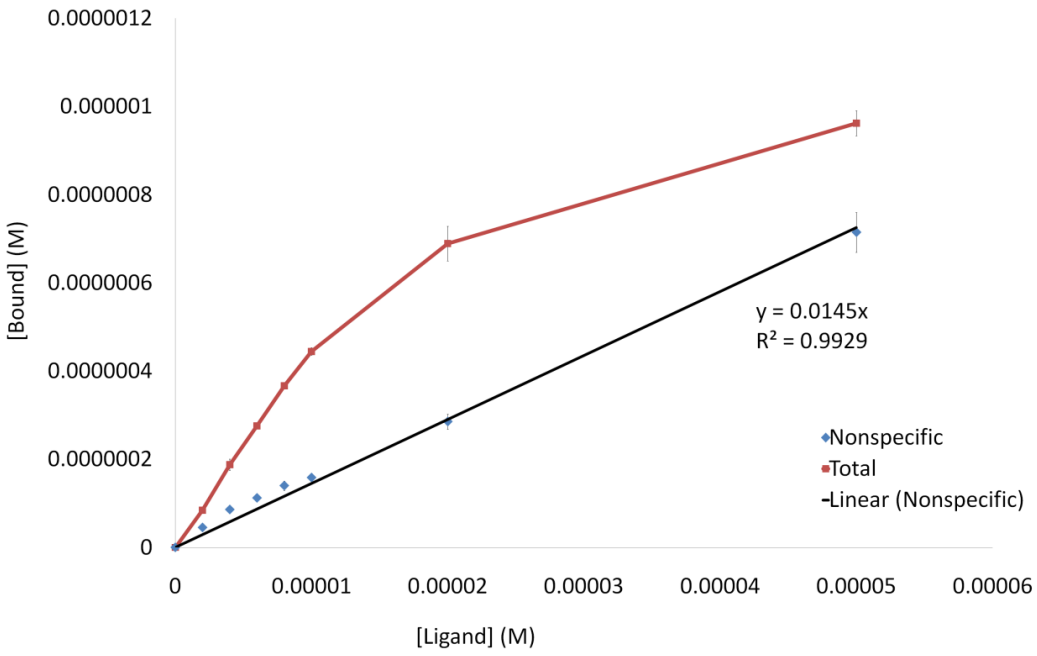

Figure A.4: Binding of fluorescently labeled polymers to HEK-SRA cells. "Total" refers to the amount of binding observed in tetracycline induced cells, which express elevated levels of SR-A and "Non-specific" refers to the binding seen in basal non-induced HEK cells.

In **Figure A.4**, "Total" refers to the amount of binding observed in tetracycline induced cells, which express elevated levels of SR-A and "Non-specific" refers to the binding seen in basal non-induced HEK cells. As expected the nonspecific binding was linear, since nonspecific binding is almost always a linear function of ligand concentration [217]. This data was used to construct a Scatchard plot. In this plot (**Figure A.5**), the X-axis is specific binding and the Y-axis is specific binding divided by free polymer concentration (taken as 10^{-6} M). It is possible to estimate Kd from a Scatchard plot (Kd is the negative reciprocal of the slope).

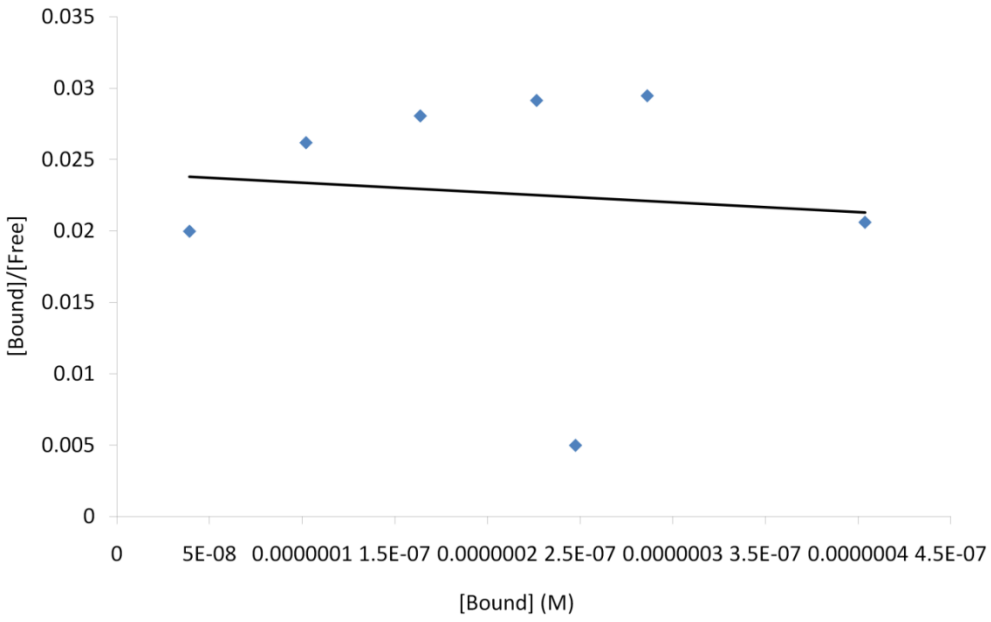

Figure A.5: Scatchard plot representation of the data in Figure A.4.

However, the linear fit is not good. The estimation of Kd from this data would likely be far from the true value. There are several reasons to explain the poor fit. First, more data points may be needed to fill out the curve and better represent the binding of **1cM** to SR-A. Second, Scatchard analysis works on the assumption that binding is 1:1 (for each SR-A receptor there is a single polymer bound). This very well may not be the case as the polymers are above the CMC and would form micelles, and could likely bind as a micelle. Alternatively, multiple SR-A proteins may bind a single, or several polymers. Without additional information on the nature of polymer binding, the results from Scatchard binding analysis may not be accurate.

A.4: Binding Affinity using Surface Plasmon Resonance

The binding affinity of each polymer for SR-A was attempted by surface plasmon resonance (SPR) with the aid of a Biacore 3000 instrument (Biacore AB, Sweden). SPR technology is a label-free method for monitoring biomolecular interactions in real-time. This technique monitors the formation and dissociation of biomolecular complexes on the surface of a coated chip as the interaction occurs [218].

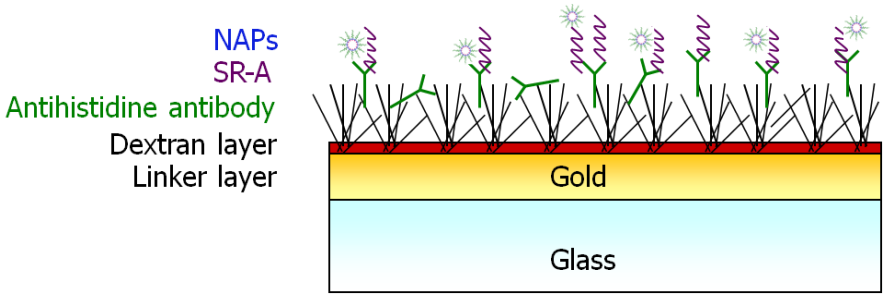

Figure A.6: Schematic of the various layers of the prepared CM5 sensor chip surface used for binding affinity studies.

In order to ensure proper orientation of a scavenger receptor and to conserve material, antibodies were first covalently bound to the sensor chip surface to capture SR-A. A CM5 sensor chip (research grade, Biacore AB, Sweden) was be used. The chip consists of a gold surface coated with a carboxymethylated dextran layer (see **Figure A.6**). All subsequent steps were completed using the Biacore 3000 set at 37 °C and all reagents were injected at a flow rate of 10 μL/min. Monoclonal anti-polyhistidine antibodies were immobilized on the surface of the sensor chip by the standard amine coupling protocol provided by the manufacturer. Briefly, the surface of the chip was activated by exposure to a mixture of 0.1 M *N*-hydroxysuccinimide (NHS) and 0.4 M 1-ethyl-3-(3-dimethylaminopropyl*)* carbodiimide (EDC) for 7 min. Next, 20 μg/mL of anti-polyhistidine antibody (R&D Systems) in sodium acetate buffer (10 mM sodium acetate, 10 mM acetic acid, pH adjusted to 5.0) was added for 5 min. A 1 M solution of ethanolamine (pH 8.5) was injected to deactivate excess reactive groups. Subsequently, 40 μg/mL of recombinant human SR-AI/MSR1 (R&D Systems) in serum-free RPMI was added for 9 min. A reference surface was created by addition of anti-polyhistidine antibody and no SR-A. Lastly, varying concentrations (10^{-3} M -10^{-7} M) of polymer in serum free RPMI were injected.

The curve resulting from the reference surface with anti-polyhistidine antibody alone was subtracted from the binding curves obtained from the flow cell with immobilized scavenger receptors and polymer. Each sensorgram was analyzed by a global fitting procedure using BIAevaluation 3.0 software. The fitting will not only allows for calculation of the binding affinities, but can also explain the binding order. For

example it is able to be determined whether the binding is 1:1, or if multiple receptors bind a single polymer, or if multiple polymers bind to a single receptor. The kinetic analysis of sensorgrams from the interaction of various engineered polymers with the immobilized scavenger receptors is based on the rate equation, $dR/dt = k_a * C * (R_{max} - R_{eq}) - k_d * R_{eq}$, where dR/dt is the rate of change in the SPR signal (RU) due to each polymer-scavenger receptor interaction at time t (s), k_a and k_d are the association and dissociation rate constants, respectively, C is the concentration of the polymers and R_{max} is the maximum polymer binding capacity to scavenger receptors (RU). The affinity constant K_D can be obtained from the ratio of k_d/k_a. A small K_D will indicate that the receptor has a high affinity for the polymer.

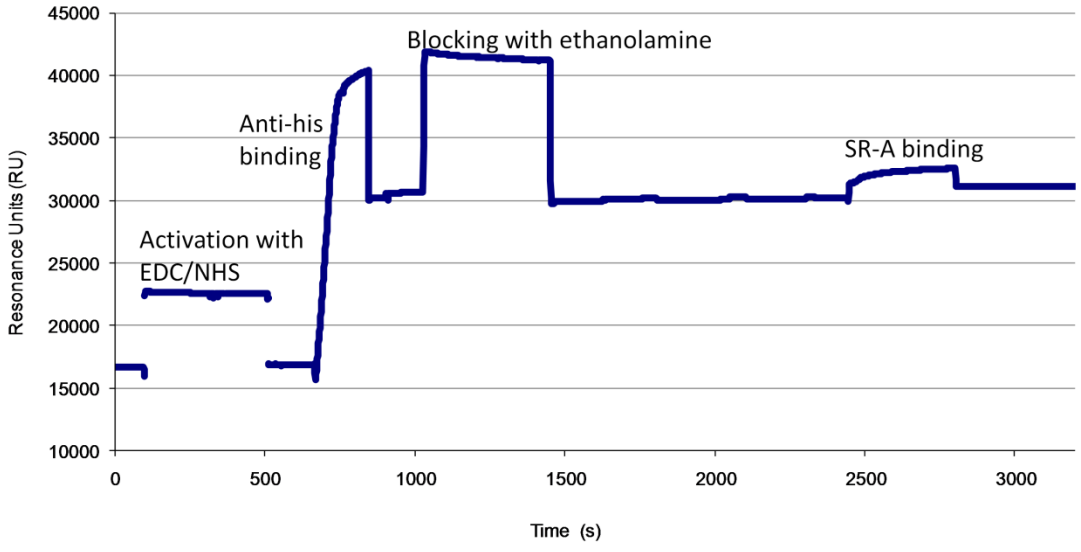

Figure A.7: Sensorgram of surface preparation for SR-A binding affinity studies

Initial SPR studies with the Biacore 3000 have been completed to prepare the surface with recombinant SR-A receptors. The steps required to prepare the CM5 sensor chip surface are described above, and the results are illustrated in Figure A.7. First, the addition of EDC/NHS mixture is completed, which activates the surface by modification of the carboxymethyl groups to N-Hydroxysuccinimide esters. The increase in RU signal throughout the duration of the addition is due to the bulk refractive index of the new solution and not surface binding. Next, the injection of the ligand (anti-histidine antibody) leads to electrostatic attraction and coupling to the CM5 surface and the N-Hydroxysuccinimide esters react spontaneously with the amines on the antibody to form covalent links. The un-reacted NHS-esters are then blocked and deactivated with ethanolamine. Lastly, SR-A is added. The SR-A used has an N-terminal polyhistidine tag, which, when bound to the anti-histidine antibody, will orient the SR-A as it would be on the cell membrane. In addition, a reference surface without anti-histidine was run in parallel and no SR-A binding was seen, thus ensuring a specific interaction between the anti-histidine antibody and SR-A.

Next, in order to ensure that the SR-A protein was not inactivated during the immobilization, anti-SR-A was used as a positive control. This can be seen in **Figure A.8**, starting from the addition of recombinant SR-A. The SR-A (40 μg/mL) was sent through the system a second time to guarantee enough receptor was on the surface to see noticeable antibody binding. The anti-SR-A bound to the surface and produced a signal

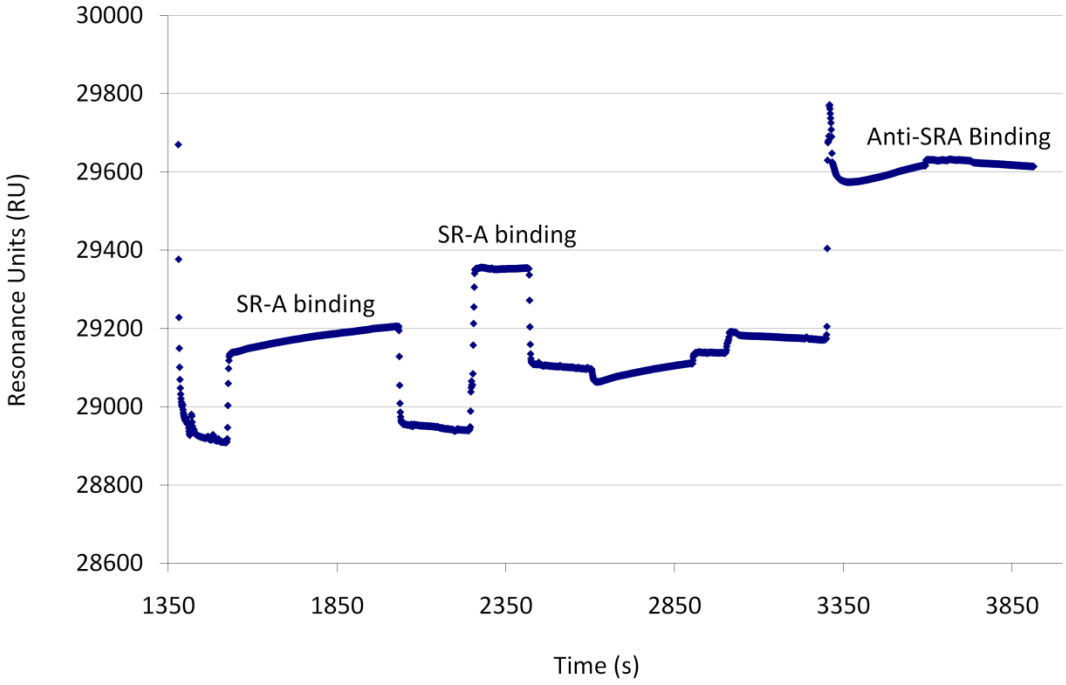

Figure A.8: Sensorgram of SR-A binding to SR-A antibody to ensure activity of the immobilized ligand.

of 440.9 RU, which is equivalent to 440.9 pg/mm2 of bound antibody. In addition, a reference surface without anti-histidine was run in parallel and no SR-A or SR-A antibody binding was noted, thus ensuring a specific interaction between SR-A and anti-SRA.

Unfortunately, this promising preliminary data never translated into polymer binding results. **Figure A.9** is representative of the results of polymer binding to immobilized SR-A. The concentrations of both SR-A and 1cM were varied as well as the buffer pH, however, binding was never detected. This is not to say that polymer did not bind to the chip surface. The Biacore 3000 may not have the level of sensitivity needed

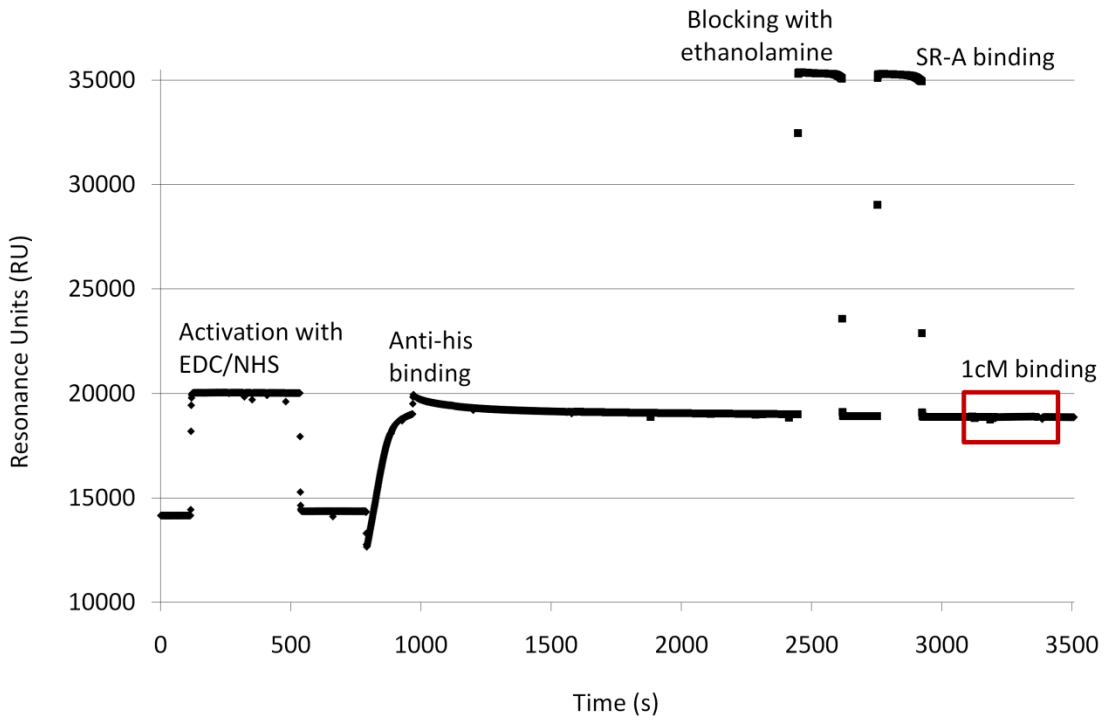

Figure A.9: Sensorgram of 1cM binding to surface immobilized SR-A

to detect the binding of the small polymers, particularly if the mode of binding is through unimers and not micelle aggregates.

A.5: Binding Affinity using Isothermal Titration Calorimetry

Isothermal Titration Calorimetry (ITC) directly measures the energetics of binding interactions. A VP-ITC microcalorimeter (MicroCal) was employed to better study the binding of our multi-functional polymers to SR-A. Interactions are detected from the change in heat (binding enthalpy) of the interaction.

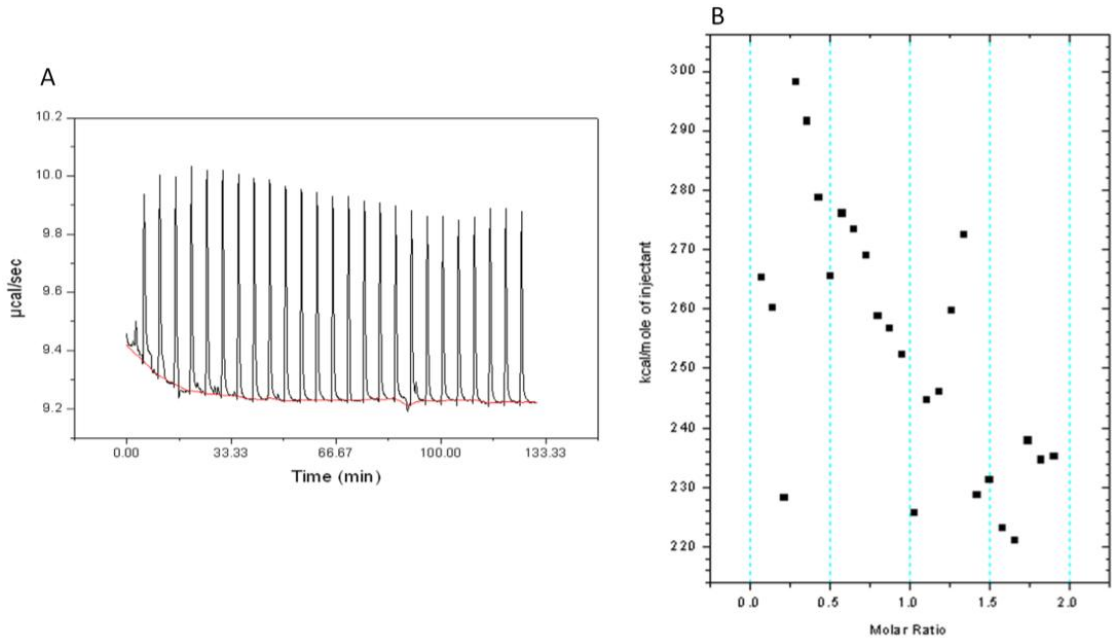

Figure A.10: Representative data from ITC detection of SR-A binding to 1cM

An isothermal titration calorimeter is composed of two identical cells, surrounded by an adiabatic jacket. Sensitive thermopile/ thermocouple circuits are used to detect temperature differences between the reference cell (filled with water) and the sample cell containing the molecule complex. Twenty-five 10 uL injections of recombinant human SR-AI/MSR1 (R&D Systems) were made each 400 s at 37 °C into the cell containing **1cM**.

A representative experiment is shown in **Figure A.10**. Part **A** is a graph of power versus time created using Origin 7.0 (MicroCal). The area under each spike is proportional to the heat of binding. Because the values are positive, binding is endothermic, as power was applied to maintain the temperature between the experimental and reference cells. The low values and that binding does not change with

concentration indicate binding is low or negligible. Further, part **B** illustrates the amount of heat measured at each injection normalized to the number of moles of SR-A. The results in **B** should show a smooth curve, but indicate again that the binding affinity is too low to effectively measure.

REFERENCES

1. Hegyi, L.; Hardwick, S. J.; Siow, R. C.; Skepper, J. N., Macrophage death and the role of apoptosis in human atherosclerosis. *J Hematother Stem Cell Res* **2001,** 10, (1), 27-42.
2. Ross, R., Atherosclerosis--an inflammatory disease. *N Engl J Med.* **1999,** 340, (2), 115-126.
3. Sadeghi, M. M.; Glover, D. K.; Lanza, G. M.; Fayad, Z. A.; Johnson, L. L., Imaging atherosclerosis and vulnerable plaque. *J Nucl Med* **2010,** 51 Suppl 1, 51S-65S.
4. Camejo, G.; Hurt-Camejo, E.; Wiklund, O.; Bondjers, G., Association of apo B lipoproteins with arterial proteoglycans: Pathological significance and molecular basis. *Atherosclerosis* **1998,** 139, 205-222.
5. Simionescu, M.; Simionescu, N., Proatherosclerotic events: pathobiochemical changes occuring in the arterial wall before monocyte migration. *FASEB J.* **1993,** 7, 1359-1366.
6. Schwenke, D. C.; Carew, T. E., Inititation of atherosclerotic lesions in cholesterol-fed rabbits. II. Selective retention of LDL vs. selective increases in LDL permeability in susceptible sites of arteries. *Arteriosclerosis* **1989,** 9, 908-918.
7. Lusis, A. J., Atherosclerosis. *Nature* **2000,** 407, 233-241.
8. Williams, K. J.; Tabas, I., The response-to-retention hypothesis of atherogenesis reinforced. *Curr Opin Lipidol* **1998,** 9, (5), 471-4.
9. Camejo, G.; Hurt, E.; Wiklund, O.; Rosengren, B.; Lopez, F.; Bondjers, G., Modifications of low density lipoprotein induced by arterial proteoglycans and chondroitin-6-sulfate. *Biochim. Biophys. Acta* **1991,** 1096, 253-261.
10. Hurt-Camejo, E.; Camejo, G.; Rosengren, B.; Lopez, F.; Ahlstrom, C.; Fager, G.; Bondjers, G., Effect of arterial proteoglycans and glycosaminoglycans on low density lipoprotein oxidation and its uptake by human macrophages and arterial smooth muscle cells. *Arteriosclerosis & Thrombosis* **1992,** 12, (5), 569-83.
11. Oorni, K.; Pentikainen, M. O.; Annila, A.; Kovanen, P. T., Oxidation of low density lipoprotein particles decreases their ability to bind to human aortic proteoglycans. *J Biol Chem* **1997,** 272, 21303-21311.
12. Haberland, M. E.; Fong, D.; Cheng, L., Malondialdehyde-altered protein occurs in atheroma of Watanabe heritable hyperlipidemic rabbits. *Science* **1988,** 241, (4862), 215-218.
13. Palinski, W.; Rosenfeld, M. E.; Yla-Herttuala, S.; Gurtner, G. C.; Socher, S. S.; Butler, S. W.; Parthasarathy, S.; Carew, T. E.; Steinberg, D.; Witztum, J. L., Low density lipoprotein undergoes oxidative modification in vivo. *Proc Natl Acad Sci U S A* **1989,** 86, (4), 1372-1376.
14. Steinberg, D.; Parthasarathy, S.; Carew, T. E.; al., e., Beyond cholesterol. Modifications of low-density lipoprotein that increase its atherogenicity. *N Engl J Med.* **1989,** 320, 915-924.
15. Rosenfeld, M. E., Cellular mechanisms in the development of atherosclerosis. *Diabetes Res. and Clin. Practice* **1996,** 30, 1-11.

16. Niemann-Jonsson, A.; Dimayuga, P.; Jovinge, S.; Calara, F.; Ares, M. P.; Fredrikson, G. N.; Nilsson, J., Accumulation of LDL in rat arteries is associated with activation of tumor necrosis factor-alpha expression. *Arteriosclerosis, Thrombosis & Vascular Biology* **2000,** 20, (10), 2205-11.
17. Stary, H. C.; Chandler, A. B.; Glagov, S.; Guyton, J. R.; Insull, W., Jr.; Rosenfeld, M. E.; Schaffer, S. A.; Schwartz, C. J.; Wagner, W. D.; Wissler, R. W., A definition of initial, fatty streak, and intermediate lesions of atherosclerosis. A report from the Committee on Vascular Lesions of the Council on Arteriosclerosis, American Heart Association. *Circulation* **1994,** 89, (5), 2462-78.
18. Brown, M. S.; Goldstein, J. L., Regulation of the activity of the low density lipoprotein receptor in human fibroblasts. *Cell* **1975,** 6, (3), 307-16.
19. Goldstein, J. L.; Ho, Y. K.; Basu, S. K.; Brown, M. S., Binding site on macrophages that mediates uptake and degradation of acetylated low density lipoprotein, producing massive cholesterol deposition. *Proceedings of the National Academy of Sciences of the United States of America* **1979,** 76, (1), 333-337.
20. Brown, M. S.; Goldstein, J. L., Lipoprotein metabolism in the macrophage: implications for cholesterol deposition in atherosclerosis. *Annu Rev Biochem* **1983,** 52, 223-261.
21. Ross, R., The pathogenesis of atherosclerosis--an update. *N Engl J Med* **1986,** 314, (8), 488-500.
22. Ohashi, R.; Mu, H.; Yao, Q.; Chen, C., Atherosclerosis: immunopathogenesis and immunotherapy. *Med. Sci. Monit.* **2004,** 10, (11), RA255-260.
23. Robbins, R. C., Effect of flavonoids on survival time of rats fed thrombogenic or atherogenic regimens. *J Atheroscler Res* **1967,** 7, (1), 3-10.
24. Sniderman, A. D.; Pedersen, T.; J., K., Putting Low-Density Lipoproteins at Center Stage in Atherogenesis,. *The American Journal of Cardiology* **1997,** 79, 64-67.
25. Alberts, G. F.; Brogi, E.; Libby, P.; Li, H., An atherogenic diet rapidly induces VCAM-1, a cytokine-regulatable mononuclear leukocyte adhesion molecule, in rabbit aortic endothelium. *Biochemical & Biophysical Research Communications* **1993,** 191, (3), 1081-8.
26. Hatch, F. T.; Lees, R. S., Practical methods for plasma lipoprotein analysis. *Adv. Lipid Res.* **1968,** 6, 1-.
27. Hevonoja, T.; Pentikaeinen, M. O.; Hyvonen, M. T.; Kovanen, P. T.; Ala-Korpela, M., Structure of low density lipoprotein (LDL) particles: Basis for understanding molecular changes in modified LDL. *Biochimica et Biophysica Acta* **2000,** 1488, 189-210.
28. Wight, T. N., Cell biology of arterial proteoglycans. *Arteriosclerosis* **1989,** 9, 1-20.
29. Wight, T. N., The extracellular matrix and atherosclerosis. *Curr. Opin. Lipidol.* **1995,** 6, 326-334.
30. Hurt-Camejo, E.; Olsson, U.; Wiklund, O.; Bondjers, G.; Camejo, G., Cellular consequences of the association of apoB lipoproteins with proteoglycans. Potential contribution to atherogenesis. *Arteriosclerosis, Thrombosis & Vascular Biology* **1997,** 17, (6), 1011-7.

31. Kaplan, M.; Aviram, M., Macrophage plasma membrane chondrotin sulfate proteoglycan binds oxidized low-density lipoprotein. *Atherosclerosis* **2000,** 149, 5-17.
32. Zhang, H.; Yang, Y.; Steinbrecher, U. P., Structural requirements for the binding of modified proteins to the scavenger receptor of macrophages. *J Biol Chem* **1993,** 268, 5535-5542.
33. Hessler, J. R.; Roberston, A. L.; Chisolm, G. M., LDL-induced cytoxicity and its inhibition by HDL in humas vascular scmooth muscle cells and endothelial cells in culture. *Atherosclerosis* **1979,** 32, 213-229.
34. Martens, J. S.; Lougheed, M.; Gomez-Munoz, A.; Steinbrecher, U., A modification of apolipoprotein B accounts for most of the induction of macrophage growth by oxidized low density lipoprotein. *J Biol Chem* **1999,** 274, 10903-10910.
35. Petit, L.; Lesnik, P.; Dachet, C.; al., e., Tissue factor pathway inhibitor is expressed by human monocyte-derived macrophages: relationship to tissue factor induction by cholesterol and oxidized LDL. *Arterioscler Thromb Vasc Biol* **1999,** 19, 309-315.
36. Li, W.; Yuan, X. M.; Brunk, U. T., OxLDL-induced macrophage cytotoxicity is mediated by lysosomal rupture and modified by intralysosomal redox-active iron. *Free Radic. Res. Commun.* **1998,** 29, 389-398.
37. Huang, Y. H.; Mironova, M.; Lopes-Virella, M. F., Oxidized LDL stimulates matrix metalloproteinase-1 expression in human vascular endothelial cells. *Arterioscler Thromb Vasc Biol* **1999,** 19, 2640-2647.
38. Huang, A.; Li, C.; Kao, R. L.; Stone, W. L., Lipid hydroperoxides inhibit nitric oxide production in RAW264.7 macrophages. *Free Radic Biol Med* **1999,** 26, 526-537.
39. Wang, X.; Reape, T. J.; Li, X.; al., e., Induced expression of adipophilin mRNA in human macrophages stimulated with oxidized low-density lipoprotein and in atherosclerotic lesions. *FEBS Lett* **1999,** 462, 145-150.
40. Gomez-Munoz, A.; Martens, J. S.; Steinbrecher, U., Stimulation of phospholipase D activity by oxidized LFL in mouse peritoneal macrophages. *Arterioscler Thromb Vasc Biol* **2000,** 20, 135-143.
41. Jessup, W.; Kritharides, L., Metabolism of oxidized LDL by macrophages. *Curr. Opin. Lipidol.* **2000,** 11, 473-481.
42. Quinn, M. T.; Parthasarathy, S.; Fong, L. G.; Steinberg, D., Oxidatively modified low density lipoproteins: a potential role in recruitment and retention of monocyte/macrophages during atherogenesis. *Proc Natl Acad Sci U S A* **1987,** 84, (9), 2995-2998.
43. Rajavashisth, T. B.; Andalibi, A.; Territo, M. C.; Berliner, J. A.; Navab, M.; Fogelman, A. M.; Lusis, A. J., Induction of endothelial cell expression of granulocyte and macrophage colony-stimulating factors by modified low-density lipoproteins. *Nature* **1990,** 344, (6263), 254-257.
44. Hessler, J. R.; Morel, D. W.; Lewis, L. J.; Chisolm, G. M., Lipoprotein oxidation and lipoprotein-induced cytotoxicity. *Arteriosclerosis* **1983,** 3, (3), 215-222.
45. Xu, X. P.; Jovinge, S.; Meisel, S.; Xu, X. O.; Chai, N. N.; Fishbein, M. C.; Kaul, S.; Cercek, B.; Sharifi, B.; Shah, P. K., Oxidized low-density lipoprotein regulates matrix

metalloproteinase-9 and its tissue inhibitor in human monocyte-derived macrophages. *Circulation* **1999,** 99, (24), 3103-9.
46. Divchev, D., Bernhard Schieffer, The secretory phospholipase A2 group IIA: a missing link between inflammation, activated renin-angiotensin system, and atherogenesis? *Vasc Health Risk Manag* **2008,** 4, (3), 597-604.
47. Kudo, I., Murakami M, Phospholipase A2 enzymes. *Prostaglandins Other Lipid Mediat.* **2002,** 68-69, 3-58.
48. Six, D., Dennis EA, The expanding superfamily of phospholipase A2 enzymes: classification and characterization. *Biochimica et Biophysica Acta* **2000,** 1488, 1-19.
49. Kockx, M., Wendy Jessup; Leonard Kritharides Regulation of Endogenous Apolipoprotein E Secretion by Macrophages. *Arteriosclerosis Thrombosis Vascular Biology* **2008,** 28, 1060-1067.
50. Gafencu, A., Robciuc MR, Fuior E, Zannis VI, Kardassis D, Simionescu M, Inflammatory signaling pathways regulating ApoE gene expression in macrophages. *J Biol Chem* **2007,** 282, 21776-21785.
51. Singh, N., Ramji DP, Transforming growth factor-beta-induced expression of the apolipoprotein E gene requires c-Jun N-terminal kinase, p38 kinase, and casein kinase 2. *Arteriosclerosis Thrombosis Vascular Biology* **2006,** 26, 1323-1329.
52. Galetto, R., Albajar M, Polanco JI, Zakin MM, Rodriguez-Rey JC, Identification of a peroxisome-proliferator-activated-receptor response element in the apolipoprotein E gene control region. *Biochem J* **2001,** 357, 521-527.
53. Laffitte, B., Repa JJ, Joseph SB, Wilpitz DC, Kast HR, Mangelsdorf DJ, Tontonoz P, LXRs control lipid-inducible expression of the apolipoprotein E gene in macrophages and adipocytes. *Proceedings of the National Academy of Science U S A* **2001,** 98, 507-512.
54. Silverstein, S. C.; Steinman, R. M.; Cohn, Z. A., Endocytosis. *Ann. Rev. Biochem.* **1977,** 46, 669-722.
55. Brown, M. S.; Ho, Y. K.; Goldstein, J. L., The cholesteryl ester cycle in macrophage foam cells. Continual hydrolysis and re-esterification of cytoplasmic cholesteryl esters. *J Biol Chem* **1980,** 255, (19), 9344-9352.
56. Brown, M. S.; Goldstein, J. L.; Krieger, M.; Ho, Y. K.; Anderson, R. G. W., Reversible accumulation of cholesteryl esters in macrophages incubated with acetylated lipoproteins. *J Cell Biol.* **1979,** 82, (3), 597-613.
57. Hoppe, G.; O'Neil, J.; Hoff, H., Inactivation of lysosomal proteases by oxidized low density lipoprotein is partially responsible for its poor degradation by mouse peritoneal macrophages. *J. Clin. Invest.* **1994,** 94, (4), 1506-1512.
58. Jessup, W.; Mander, E. L.; Dean, R. T., The intracellular storage and turnover of apolipoprotein B of oxidized LDL in macrophages. *Biochim. Biophys. Acta* **1992,** 1126, 167-177.
59. Lougheed, M.; Zhang, H. F.; Steinbrecher, U. P., Oxidized low density lipoprotein is resistant to cathepsins and accumulates within macrophages. *J biol Chem* **1991,** 266, 14519-14525.

60. Mander, E. L.; Dean, R. T.; Stanley, K. K.; Jessup, W., Apolipoprotein B of oxidized LDL accumulates in the lysosomes of macrophages. *Biochim. Biophys. Acta* **1994,** 1212, 80-92.
61. Krieger, M., Acton, S., Ashkenas, J., Pearson, A., Penman, M., Resnick, D., Molecular Flypaper, Host Defense, and Atherosclerosis: structure, binding properties, and functions o macrophage scavenger receptors. *J Biol Chem* **1993,** 268, (7), 4569-4572.
62. Moore, K. J.; Freeman, M. W., Scavenger receptors in atherosclerosis: beyond lipid uptake. *Arterioscler Thromb Vasc Biol* **2006,** 26, (8), 1702-11.
63. Kunjathoor, V. V.; Febbraio, M.; Podrez, E. A.; Moore, K. J.; Andersson, L.; Koehn, S.; Rhee, J.; Silverstein, R.; Hoff, H. F.; Freeman, M. W., Scavenger receptors Class A-I/II and CD36 are the principal receptors responsible for the uptake of modified low density lipoprotein leading to lipid loading in macrophages. *J Biol Chem* **2002,** 277, 49982-49988.
64. Nakagawa-Toyama, Y.; Yamashita, S.; Miyagawa, J.; Nishida, M.; Nozaki, S.; Nagaretani, H.; Sakai, N.; Hiraoka, H.; Yamamori, K.; Yamane, T.; Hirano, K.; Matsuzawa, Y., Localization of CD36 and scavenger receptor class A in human coronary arteries--a possible difference in the contribution of both receptors to plaque formation. *Atherosclerosis* **2001,** 156, (2), 297-305.
65. Inoue, N.; Okamura, T.; Kokubo, Y.; Fujita, Y.; Sato, Y.; Nakanishi, M.; Yanagida, K.; Kakino, A.; Iwamoto, S.; Watanabe, M.; Ogura, S.; Otsui, K.; Matsuda, H.; Uchida, K.; Yoshimoto, R.; Sawamura, T., LOX Index, a Novel Predictive Biochemical Marker for Coronary Heart Disease and Stroke. *Clin Chem* **2010,** 56, (4), 550-558.
66. Cominacini, L.; Rigoni, A.; Pasini, A. F.; Garbin, U.; Davoli, A.; Campagnola, M.; Pastorino, A. M.; Lo Cascio, V.; Sawamura, T., The binding of oxidized low density lipoprotein (ox-LDL) to ox-LDL receptor-1 reduces the intracellular concentration of nitric oxide in endothelial cells through an increased production of superoxide. . *J. Biol. Chem.* **2001,** 276, 13750-13755.
67. Li, D.; Mehta, J. L., Antisense to Lox-1 inhibits oxidized LDL-mediated upregulation of monocyte chemoattractant protein-1 and monocyte adhesion to human coronary artery endothelial cells. . *Circulation* **2000,** 101, 2889-2895.
68. Cominacini, L.; Pasini, A. F.; Garbin, U.; Davoli, A.; Tosetti, M. L.; Campagnola, M.; Rigoni, A.; Pastorino, A. M.; Lo Cascio, V.; Sawamura, T., Oxidized low density lipoprotein (ox-LDL) binding to ox-LDL receptor-1 in endothelial cells induces the activation of NF-kB through an increased production of intracellular reactive oxygen species. . *J. Biol. Chem.* **2000,** 275, 12633-12638.
69. Li, D.; Liu, L.; Chen, H.; Sawamura, T.; Ranganathan, S.; Mehta, J. L., LOX-1 Mediates Oxidized Low-Density Lipoprotein-Induced Expression of Matrix Metalloproteinases in Human Coronary Artery Endothelial Cells. *Circulation* **2003,** 107, (4), 612-617.
70. Li, D.; Mehta, J. L., Upregulation of endothelial receptor for oxidized LDL (Lox-1) by oxidized LDL and implications in apoptosis of human coronary artery endothelial cells: evidence from use of antisense Lox-1 mRNA and chemical inhibitors. . *Arterioscler Thromb Vasc Biol* **2000,** 20, 1116-1122.

71. Murphy, J. E.; Tedbury, P. R.; Homer-Vanniasinkam, S.; Walker, J. H.; Ponnambalam, S., Biochemistry and cell biology of mammalian scavenger receptors. *Atherosclerosis* **2005,** 182, (1), 1-15.
72. Dhaliwal, B. S.; Steinbrecher, U. P., Scavenger receptors and oxidized low density lipoproteins. *Clin Chim Acta* **1999,** 286, (1-2), 191-205.
73. Suzuki, H.; Kurihara, Y.; Takeya, M.; Kamada, N.; Kataoka, M.; Jishage, K.; Ueda, O.; Sakaguchi, H.; Higashi, T.; Suzuki, T.; Takashima, Y.; Kawabe, Y.; Cynshi, O.; Wada, Y.; Honda, M.; Kurihara, H.; Aburatani, H.; Doi, T.; Matsumoto, A.; Azuma, S.; Noda, T.; Toyoda, Y.; Itakura, H.; Yazaki, Y.; Kodama, T., A role for macrophage scavenger receptors in atherosclerosis and susceptibility to infection. *Nature* **1997,** 386, 292-296.
74. Babaev, V. R.; Gleaves, L. A.; Carter, K. J.; Suzuki, H.; Kodama, T.; Fazio, S.; Linton, M. F., Reduced atherosclerotic lesions in mice deficient for total or macrophage-specific expression of scavenger receptor-A. *Arterioscler Thromb Vasc Biol* **2000,** 20, 2593-2599.
75. Platt, N.; Gordon, S., Is the class A macrophage scavenger receptor (SR-A) multifunctional? - The mouse's tale. *J Clin Invest* **2001,** 108, (5), 649-54.
76. Doi, T.; Higashino, K.; Kurihara, Y.; Wada, Y.; Miyazaki, T.; Nakamura, H.; Uesugi, S.; Imanishi, T.; Kawabe, Y.; Itakura, H., Charged collagen structure mediates the recognition of negatively charged macromolecules by macrophage scavenger receptors. *J Biol Chem* **1993,** 268, (3), 2126-2133.
77. Mori, T.; Takahashi, K.; Naito, M.; Kodama, T.; Hakamata, H.; Sakai, M.; Miyazaki, A.; Horiuchi, S.; Ando, M., Endocytic pathway of scavenger receptors via trans-Golgi system in bovine alveolar macrophages. *Lab Invest* **1994,** 71, (3), 409-16.
78. In *Consensus conference. Lowering blood cholesterol to prevent heart disease.*, JAMA, 1985; 1985.
79. LaRosa, J. C.; Hunninghake, D.; Bush, D.; Criqui, M. H.; Getz, G. S.; Gotto, A. M. J.; Grundy, S. M.; Rakita, L.; Roberston, R. M.; Weisfeldt, M. L.; al., e., The cholesterol facts. A summary of the evidence relating dietary fats, serum cholesterol, and coronary heart disease. A joint statement by the American Heart Association and the National Heart, Lung, and Blood Institute. The Task Force on Cholesterol Issues, American Heart Association. *Circulation* **1990,** 81, (5), 1721-1733.
80. Law, M. R.; Wald, N. J.; Wu, T.; Hackshaw, A.; Bailey, A., Systematic underestimation of association between serum cholesterol concentration and ischaemic heart disease in observational studies: data from the BUPA study. *BMJ* **1994,** 308, 363-366.
81. Olsson, A. G.; Molgaard, J.; Von Scnek, H., Synvinolin in hypercholesterolemia. *Lancet.* **1986,** 2, (390-393).
82. McKenney, J. M., Lipid management: tools for getting to the goal. *Am J Manag Care* **2001,** 7, (9 Suppl), S299-306.
83. van Heek, M.; France, C. F.; Compton, D. S.; Mcleod, R. L.; Yumibe, N. P.; Alton, K. B.; Sybertz, E. J.; Davis, H. R. J., In vivo metabolism-based discovery of a potent cholesterol absorption inhibitor, SCH58235, in the rat and rhesus monkey through the identification of the active metabolites of SCH48461. *J Pharmacol Exp Ther.* **1997,** 283, 157-163.
84. DeNoon, D., Cholesterol Drugs Have Painful Problem. *WebMD Medical News* May 13, 2002.

85. Reuters *Men file lawsuits claiming Lipitor side effects*; New York, Jun 8, 2006.
86. Stolcpart, R. S.; Olson, K. L.; Delate, T.; Rasmussen, J.; Rehring, T. F.; Merenich, J. A., The risk for significant creatine kinase elevation with statins. *Am J Cardiovasc Drugs* **2010,** 10, (3), 187-92.
87. Law, M.; Rudnicka, A. R., Statin Safety: A Systematic Review. *Am J Cardiol.* **2006,** 97, (8A), 52C-60C.
88. Oliver, M. F., Might treatment of hypercholesterolaemia increase non-cardiac mortality? *Lancet.* **1991,** 337, 1529-1531.
89. Davey Smith, G.; Pekkanen, J., Should there be a moratorium on the use of cholesterol lowering drugs? *BMJ* **1992,** 304, 431-434.
90. Malinski, T., Understanding nitric oxide physiology in the heart: a nanomedical approach. *Am J Cardiol.* **2005,** 96, (7B), 13i-24i.
91. Carella, M.; Volinia, S.; Gasparini, P., Nanotechnologies and microchips in genetic diseases. *J Nephrol* **2003,** 16, (4), 597-602.
92. He, W.; Yong, T.; Teo, W.; Ma, Z.; Ramakrishna, S., Fabrication and endothelialization of collagen-blended biodegradable polymer nanofibers: potential vascular graft for blood vessel tissue engineering. *Tissue Eng* **2005,** 11, (9-10), 1574-1588.
93. He, W.; Ma, Z.; Yong, T.; Teo, W. E.; Ramakrishna, S., Fabrication of collagen-coated biodegradable polymer nanofiber mesh and its potential for endothelial cells growth. *Biomaterials* **2005,** 26, (36), 7606-7615.
94. Ma, Z.; He, W.; Yong, T.; Ramakrishna, S., Grafting of gelatin on electrospun poly(caprolactone) nanofibers to improve endothelial cell spreading and proliferation and to control cell Orientation. *Tissue Eng* **2005,** 11, (7-8), 1149-1158.
95. Meng, J.; Kong, H.; Xu, H. Y.; Song, L.; Wang, C. Y.; Xie, S. S., Improving the blood compatibility of polyurethane using carbon nanotubes as fillers and its implications to cardiovascular surgery. *J Biomed Mater Res A* **2005,** 74, (2), 208-214.
96. Endo, M.; Koyama, S.; Matsuda, Y.; Hayashi, T.; Kim, Y. A., Thrombogenicity and blood coagulation of a microcatheter prepared from carbon nanotube-nylon-based composite. *Nano Lett* **2005,** 5, (1), 101-105.
97. Buxton, D. B.; Lee, S. C.; Wickline, S. A.; Ferrari, M., Recommendations of the National Heart, Lung, and Blood Institute Nanotechnology Working Group. *Circulation* **2003,** 108, (22), 2737-42.
98. Kolodgie, F. D.; John, M.; Khurana, C.; Farb, A.; Wilson, P. S.; Acampado, E.; Desai, N.; Soon-Shiong, P.; Virmani, R., Sustained reduction of in-stent neointimal growth with the use of a novel systemic nanoparticle paclitaxel. *Circulation* **2002,** 106, (10), 1195-8.
99. Finkelstein, A.; McClean, D.; Kar, S.; Takizawa, K.; Varghese, K.; Baek, N.; Park, K.; Fishbein, M. C.; Makkar, R.; Litvack, F.; Eigler, N. L., Local drug delivery via a coronary stent with programmable release pharmacokinetics. *Circulation* **2003,** 107, (5), 777-84.
100. Steinberg, D., Low density lipoprotein oxidaton and its pathobiological significance. *J Biol Chem* **1997,** 272, 20963-20966.
101. Febbraio, M.; Sheibani, N.; Schmitt, D.; Silverstein, R. L.; Hajjar, D. P.; Cohen, P. A.; Frazier, W. A.; Hoff, H. F.; Hazen, S. L., Targeted disruption of the class B scavenger

receptor CD36 protects against atherosclerotic lesion development in mice.[see comment]. *Journal of Clinical Investigation* **2000,** 105, (8), 1095-108.
102. Boullier, A., Friedman, P., Harkewicz, R., Hartvigsen, K., Green, S.R., Almazan, F., Dennis, E.A., Steinberg, D., Witztum, J.L., Quehenberger, O., Phosphocholine as a pattern recognition ligand for CD36. *J Lipid Res* **2005,** 46, 969-976.
103. Yoshiizumi, K.; Nakajima, F.; Dobashi, R.; Nishimura, N.; Ikeda, S., 2,4-Bis(octadecanoylamino)benzenesulfonic acid sodium salt as a novel scavenger receptor inhibitor with low molecular weight. *Bioog Med Chem Lett* **2004,** 14, (11), 2791-2795.
104. Guaderrama-Diaz, M.; Solis, C. F.; Velasco-Loyden, G.; Laclette, J. P.; Mas-Oliva, J., Control of scavenger receptor-mediated endocytosis by novel ligands of different length. *Mol Cell Biochem* **2005,** 271, (1-2), 123-132.
105. Broz, P.; Benito, S. M.; Saw, C.; Burger, P.; Heider, H.; Pfisterer, M.; Marsch, S.; Meier, W.; Hunziker, P., Cell targeting by a generic receptor-targeted polymer nanocontainer platform. *J Control Release* **2005,** 102, (2), 475-488.
106. Tian, L.; Yam, L.; Zhou, N.; Tat, H.; Uhrich, K. E., Amphiphilic Scorpion-like Macromolecules:Design, Synthesis, and Characterization. *Macromolecules* **2004,** 37, (2), 538-543.
107. Chnari, E.; Nikitczuk, J. S.; Uhrich, K. E.; Moghe, P. V., Nanoscale anionic macromolecules can inhibit cellular uptake of differentially oxidized LDL. *Biomacromolecules* **2006,** 7, (2), 597-603.
108. Chnari, E.; Nikitczuk, J. S.; Wang, J.; Uhrich, K. E.; Moghe, P. V., Engineered polymeric nanoparticles for receptor-targeted blockage of oxidized low density lipoprotein uptake and atherogenesis in macrophages. *Biomacromolecules* **2006,** 7, (6), 1796-805.
109. Tao, L.; Uhrich, K. E., Novel amphiphilic macromolecules and their in vitro characterization as stabilized micellar drug delivery systems. *J Colloid Interface Sci* **2006,** 298, (1), 102-10.
110. Chnari, E.; Tian, L.; Uhrich, K.; Moghe, P. V., Nanoscale anionic macromolecules for selective retention of low-density lipoproteins. *Biomaterials* **2005,** 26, 3749-3758.
111. Tian, L. Novel Amphiphilic Macromolecules for Drug Delivery Applications: Design, Synthesis and Characterization. Rutgers, The State University of New Jersey, New Brunswick, 2004.
112. Geyeregger, R.; Zeyda, M.; Stulnig, T. M., Liver X receptors in cardiovascular and metabolic disease. *Cell Mol Life Sci* **2006,** 63, (5), 524-39.
113. Li, Y.; Schwabe, R. F.; DeVries-Seimon, T.; Yao, P. M.; Gerbod-Giannone, M. C.; Tall, A. R.; Davis, R. J.; Flavell, R.; Brenner, D. A.; Tabas, I., Free cholesterol-loaded macrophages are an abundant source of tumor necrosis factor-alpha and interleukin-6: model of NF-kappaB- and map kinase-dependent inflammation in advanced atherosclerosis. *J Biol Chem* **2005,** 280, (23), 21763-72.
114. Joseph, S. B.; McKilligin, E.; Pei, L.; Watson, M. A.; Collins, A. R.; Laffitte, B. A.; Chen, M.; Noh, G.; Goodman, J.; Hagger, G. N.; Tran, J.; Tippin, T. K.; Wang, X.; Lusis, A. J.; Hsueh, W. A.; Law, R. E.; Collins, J. L.; Willson, T. M.; Tontonoz, P., Synthetic LXR

ligand inhibits the development of atherosclerosis in mice. *Proc Natl Acad Sci U S A* **2002,** 99, (11), 7604-9.
115. Joseph, S. B.; Castrillo, A.; Laffitte, B. A.; Mangelsdorf, D. J.; Tontonoz, P., Reciprocal regulation of inflammation and lipid metabolism by liver X receptors. *Nat Med* **2003,** 9, (2), 213-9.
116. Li, A. C.; Glass, C. K., The macrophage foam cell as a target for therapeutic intervention. *Nature Med* **2002,** 8, (11), 1235-42.
117. Yla-Herttuala, S.; Hiltunen, T. P., Expression of LDL receptor, VLDL receptor, LDL receptor-related protein, and scavenger receptor in rabbit atherosclerotic lesions: marked induction of scavenger receptor and VLDL receptor expression during lesion development. *Atherosclerosis* **1998,** 137 Suppl, S81-8.
118. de Winther, M. P.; van Dijk, K. W.; Havekes, L. M.; Hofker, M. H., Macrophage scavenger receptor class A: A multifunctional receptor in atherosclerosis. *Arterioscler Thromb Vasc Biol* **2000,** 20, (2), 290-7.
119. Wang, X.; Greilberger, J.; Ratschek, M.; Juergens, G., Oxidative modifications of LDL increase its binding to extracellular matrix from human aortic intima: influence of lesion development, lipoprotein lipase and calcium. *J Pathol* **2001,** 195, 244-250.
120. Yamada, H.; Kazumi, Y.; Doi, N.; Otomo, K.; Aoki, T.; Mizuno, S.; Udagawa, T.; Tagawa, Y.; Iwakura, Y.; Yamada, Y., Scavenger receptor family proteins: roles for atherosclerosis, host defence and disorders of the central nervous system. *J Med Microbiol* **1998,** 47, (10), 871-7.
121. Andersson, L.; Freeman, M. W., Functional changes in scavenger receptor binding conformation are induced by charge mutants spanning the entire collgaen domain. *J Biol Chem* **1998,** 273, 19592019601.
122. Acton, S.; Resnick, D.; Freeman, M.; Ekkel, Y.; Ashkenas, J.; Krieger, M., The collagenous domains of macrophage scavenger receptors and complement component C1q mediate their similar, but not identical, binding specificities for polyanionic ligands. *J Biol Chem* **1993,** 268, (5), 3530-7.
123. Dejager, S.; Mietus-Snyder, M.; Friera, A.; Pitas, R. E., Dominant negative mutations of the scavenger receptor. Native receptor inactivation by expression of truncated variants. *J Clin Invest* **1993,** 92, (2), 894-902.
124. Wang, J.; Plourde, N. M.; Iverson, N.; Moghe, P. V.; Uhrich, K. E., Nanoscale amphiphilic macromolecules as lipoprotein inhibitors: the role of charge and architecture. *Int J Nanomedicine* **2007,** 2, (4), 697-705.
125. Tao, L.; Uhrich, K. E., Novel amphiphilic macromolecules and their in vitro characterization as stabilized micellar drug delivery systems. *J. Colloid Interface Sci.* **2006,** 298, (1), 102-110.
126. Chnari, E.; Nikitczuck, J.; Wang, J.; Uhrich, K.; Moghe, P., Engineered Polymeric Nanoparticles for Receptor-Targeted Blockage of Oxidized Low Density Lipoproteins Uptake and Atherogenesis in Macrophages. *Biomacromolecules* **2006,** 7, 1796-1805.
127. Chang, M.; Potter-Perigo, S.; Wight, T.; Chait, A., Oxidized LDL bind to nonproteoglycan components of smooth muscle extracellular matrices. *J. Lipid Res.* **2001,** 42, 824-833.

128. Oorni, K., et al., Oxidation of low density lipoprotein particles decreases their ability to bind to human aortic proteoglycans. Dependence on oxidative modification of the lysine residues. *Journal of Biological Chemistry* **1997,** 272, (34), 21303-11.
129. Wang, J. M.; Cieplak, P.; Kollman, P. A., How well does a restrained electrostatic potential (RESP) model perform in calculating conformational energies of organic and biological molecules? *J Comput Chem* **2000,** 21, (12), 1049-1074.
130. Altschul, S. F.; Madden, T. L.; Schaffer, A. A.; Zhang, J.; Zhang, Z.; Miller, W.; Lipman, D. J., Gapped BLAST and PSI-BLAST: a new generation of protein database search programs. *Nucleic Acids Res* **1997,** 25, (17), 3389-402.
131. Thompson, J. D.; Higgins, D. G.; Gibson, T. J., CLUSTAL W: improving the sensitivity of progressive multiple sequence alignment through sequence weighting, position-specific gap penalties and weight matrix choice. *Nucleic Acids Res* **1994,** 22, (22), 4673-80.
132. Orgel, J. P.; Irving, T. C.; Miller, A.; Wess, T. J., Microfibrillar structure of type I collagen in situ. *Proc Natl Acad Sci U S A* **2006,** 103, (24), 9001-5.
133. Jones, D. T., Protein secondary structure prediction based on position-specific scoring matrices. *J Mol Biol* **1999,** 292, (2), 195-202.
134. McGuffin, L. J.; Bryson, K.; Jones, D. T., The PSIPRED protein structure prediction server. *Bioinformatics* **2000,** 16, (4), 404-5.
135. Sali, A.; Blundell, T. L., Comparative protein modelling by satisfaction of spatial restraints. *J Mol Biol* **1993,** 234, (3), 779-815.
136. MacKerell, A. D.; Bashford, D.; Bellott, M.; Dunbrack, R. L.; Evanseck, J. D.; Field, M. J.; Fischer, S.; Gao, J.; Guo, H.; Ha, S.; Joseph-McCarthy, D.; Kuchnir, L.; Kuczera, K.; Lau, F. T. K.; Mattos, C.; Michnick, S.; Ngo, T.; Nguyen, D. T.; Prodhom, B.; Reiher, W. E.; Roux, B.; Schlenkrich, M.; Smith, J. C.; Stote, R.; Straub, J.; Watanabe, M.; Wiorkiewicz-Kuczera, J.; Yin, D.; Karplus, M., All-atom empirical potential for molecular modeling and dynamics studies of proteins. *J Phys Chem B* **1998,** 102, (18), 3586-3616.
137. Braun, W.; Go, N., Calculation of protein conformations by proton-proton distance constraints. A new efficient algorithm. *J Mol Biol* **1985,** 186, (3), 611-26.
138. Case, D. A.; Cheatham, T. E., 3rd; Darden, T.; Gohlke, H.; Luo, R.; Merz, K. M., Jr.; Onufriev, A.; Simmerling, C.; Wang, B.; Woods, R. J., The Amber biomolecular simulation programs. *J Comput Chem* **2005,** 26, (16), 1668-88.
139. Yamamoto, K.; Nishimura, N.; Doi, T.; Imanishi, T.; Kodama, T.; Suzuki, K.; Tanaka, T., The lysine cluster in the collagen-like domain of the scavenger receptor provides for its ligand binding and ligand specificity. *FEBS Lett* **1997,** 414, (2), 182-6.
140. Jones, G.; Willet, P.; Glen, R. C.; Leach, A. R.; Taylor, R., Development and validation of a genetic algorithm for flexible docking. *J. Mol. Biol.* **1997,** 267, 727-748.
141. Hakansson, K.; Lim, N. K.; Hoppe, H. J.; Reid, K. B., Crystal structure of the trimeric alpha-helical coiled-coil and the three lectin domains of human lung surfactant protein D. *Structure* **1999,** 7, (3), 255-64.
142. Otsuka, H.; Nagasaki, Y.; Kataoka, K., Self-assembly of poly(ethylene glycol)-based block copolymers for biomedical applications. *Curr Opin in Colloid In* **2001,** 6, (1), 3-10.

143. Plourde, N. M.; Kortagere, S.; Welsh, W.; Moghe, P. V., Structure-activity relations of nanolipoblockers with the atherogenic domain of human macrophage scavenger receptor A. *Biomacromolecules* **2009,** 10, (6), 1381-91.
144. Chang, M. Y.; Potter-Perigo, S.; Wight, T. N.; Chait, A., Oxidized LDL bind to nonproteoglycan components of smooth muscle extracellular matrices. *J Lipid Res* **2001,**42, 824-833.
145. Lloyd-Jones, D.; Adams, R.; Carnethon, M.; De Simone, G.; Ferguson, T.; Flegal, K.; Ford, E.; Furie, K.; Go, A.; Greenlund, K.; Haase, N.; Hailpern, S.; Ho, M.; Howard, V.; Kissela, B.; Kittner, S.; Lackland, D.; Lisabeth, L.; Marelli, A.; McDermott, M.; Meigs, J.; Mozaffarian, D.; Nichol, G.; O'Donnell, C.; Roger, V.; Rosamond, W.; Sacco, R.; Sorlie, P.; Stafford, R.; Steinberger, J.; Thom, T.; Wasserthiel-Smoller, S.; Wong, N.; Wylie-Rosett, J.; Hong, Y.; Subcommittee, A. H. A. S. C. a. S. S., Heart disease and stroke statistics--2009 update: a report from the American Heart Association Statistics Committee and Stroke Statistics Subcommittee. *Circulation* **2009,** 119, (3), 480-486.
146. Gotto, A. M., Jr., The cardiology patient page. Statins: powerful drugs for lowering cholesterol: advice for patients. *Circulation* **2002,** 105, (13), 1514-6.
147. McKenney, J. M., Lipid Management: Tools for Getting to the Goal. *Am. J. Man. Care* **2001,** 7, (9), S299-S306.
148. Gotto, A. M., Statins: Powerful Drugs for Lowering Cholesterol. *Circulation* **2002,** 105, 1514-1516.
149. Manning-Tobin, J. J.; Moore, K. J.; Seimon, T. A.; Bell, S. A.; Sharuk, M.; Alvarez-Leite, J. I.; Winther, M. P. J. d.; Tabas, I.; Freeman, M. W., Loss of SR-A and CD36 Activity Reduces Atherosclerotic Lesion Complexity Without Abrogating Foam Cell Formation in Hyperlipidemic Mice. *Arterioscler., Thromb., Vasc. Biol.* **2009,** 29, (1), 19-26.
150. Ross, R., Cell biology of atherosclerosis. *Annu. Rev. Physiol.* **1995,** 57, 791-804.
151. Yamakawa, T.; Ogihara, K.; Nakamura, M.; Utsunomiya, H.; Kadonosono, K.; Kishikawa, S.; Terauchi, Y., Effect of Dehydroepiandrosterone on Atherosclerosis in Apolipoprotein E-Deficient Mice. *J. Atheroscler. Thromb.* **2009,** 16, 501-508.
152. Aravindhan, K.; Webb, C.; Jaye, M.; Ghosh, A.; Willette, R.; DiNardo, N. J.; Jucker, B. M., Assessing the effects of LXR agonists on cellular cholesterol handling: a stable isotope tracer study. *J. Lipid Res.* **2006,** 47, 1250-1260.
153. Tangirala, R., Bischoff, ED, Joseph, SB, Wagner, BL, Walczak, R, Laffitte, BA, et al., Identification of macrophage liver X receptors as inhibitors of atherosclerosis. *Proc Natl Acad Sci USA 2002* **2002,** 99, (18), 11896-11901.
154. Tontonoz, P., and Mangelsdorf, DJ, Liver x receptor signaling pathways in cardiovascular disease. *Mol Endocrinol* **2003,** 17, (6), 985-993.
155. Virella, G.; Munoz, J.; Galbraith, G.; Gissinger, C.; Chassereau, C.; Lopes-Virella, M., Activation of human monocyte-derived macrophage by immune complexes containing low density lipoprotein. *Clin. Immunol. Immunopathol.* **1995,** 75, 179-189.
156. Yamakawa, T.; Ogihara, K.; Nakamura, M.; Utsunomiya, H.; Kadonosono, K.; Kishikawa, S.; Terauchi, Y., Effect of dehydroepiandrosterone on atherosclerosis in apolipoprotein E-deficient mice. *J Atheroscler Thromb* **2009,** 16, (4), 501-8.

157. Tontonoz, P.; Mangelsdorf, D. J., Liver X receptor signaling pathways in cardiovascular disease. *Mol Endocrinol* **2003,** 17, (6), 985-93.
158. Geng, Y. J.; Holm, J.; Nygren, S.; Bruzelius, M.; Stemme, S.; Hansson, G. K., Expression of the macrophage scavenger receptor in atheroma. Relationship to immune activation and the T-cell cytokine interferon-gamma. *Arterioscler Thromb Vasc Biol* **1995,** 15, (11), 1995-2002.
159. Luoma, J.; Hiltunen, T.; Sarkioja, T.; Moestrup, S. K.; Gliemann, J.; Kodama, T.; Nikkari, T.; Yla-Herttuala, S., Expression of alpha 2-macroglobulin receptor/low density lipoprotein receptor-related protein and scavenger receptor in human atherosclerotic lesions. *J Clin Invest* **1994,** 93, (5), 2014-21.
160. Bradley, M. N.; Hong, C.; Chen, M.; Joseph, S. B.; Wilpitz, D. C.; Wang, X.; Lusis, A. J.; Collins, A.; Hseuh, W. A.; Collins, J. L.; Tangirala, R. K.; Tontonoz, P., Ligand activation of LXRβ reverses atherosclerosis and cellular cholesterol overload in mice lacking LXRα and apoE. *J. Clin. Invest.* **2007,** 117, 2337-2346.
161. Castrillo, A.; Joseph, S. B.; Marathe, C.; Mangelsdorf, D. J.; Tontonoz, P., Liver X receptor-dependent repression of matrix metalloproteinase-9 expression in macrophages. *J Biol Chem* **2003,** 278, (12), 10443-9.
162. Lloyd-Jones, D.; Adams, R.; Carnethon, M.; De Simone, G.; Ferguson, T. B.; Flegal, K.; Ford, E.; Furie, K.; Go, A.; Greenlund, K.; Haase, N.; Hailpern, S.; Ho, M.; Howard, V.; Kissela, B.; Kittner, S.; Lackland, D.; Lisabeth, L.; Marelli, A.; McDermott, M.; Meigs, J.; Mozaffarian, D.; Nichol, G.; O'Donnell, C.; Roger, V.; Rosamond, W.; Sacco, R.; Sorlie, P.; Stafford, R.; Steinberger, J.; Thom, T.; Wasserthiel-Smoller, S.; Wong, N.; Wylie-Rosett, J.; Hong, Y., Heart disease and stroke statistics--2009 update: a report from the American Heart Association Statistics Committee and Stroke Statistics Subcommittee. *Circulation* **2009,** 119, (3), 480-6.
163. Iverson, N.; Plourde, N. M.; Sparks, S. M.; Wang, J.; Patel, E.; Nackman, G. B.; Uhrich, K. E.; Moghe, P. V., Bioactive Polymers for Multimodal Inhibition of Inflammation and Atherogenesis in Activated Macrophages. *to be submitted to Circulation Research* **2010**.
164. Khanna, A. K., Enhanced susceptibility of cyclin kinase inhibitor p21 knockout mice to high fat diet induced atherosclerosis. *Journal of Biomedical Science* **2009,** 16, (66).
165. Hansson, G., Inflammation, atherosclerosis and coronary artery disease. *N Engl J Med* **2005,** 352, 1685-1695.
166. Schreyer, S. A., Jacques J Peschon, Renee C LeBoeuf, Accelerated Atherosclerosis in Mice Lacking Tumor Necrosis Factor Receptor p55. *The Journal of Biological Chemistry* **1996,** 271, (42), 26174-26178.
167. Dinarello, C., Biologic basis for interleukin-1 in disease. *Blood* **1996,** 87, 2095-2147.
168. Kunjathoor, V.; Febbraio, M.; Podrez, E.; Moore, K.; Andersson, L.; Koehn, S.; Rhee, J.; Silverstein, R.; Hoff, H.; Freeman, M., Scavenger receptors class A-I/II and CD36 are the principal receptors responsible for the uptake of modified low density lipoprotein leading to lipid loading in macrophages. *J. Biol. Chem.* **2002,** 277, (51), 49982-49988.
169. Lusis, A. J., Atherosclerosis. *Nature* **2000,** 407, (6801), 233-241.

170. Hansson, G. K., Immune mechanisms in atherosclerosis. *Arterioscler., Thromb., Vasc. Biol.* **2001,** 21, (12), 1876-1890.
171. Zelcer, N.; Khanlou, N.; Clare, R.; Jiang, Q.; Reed-Geaghan, E. G.; Landreth, G. E.; Vinters, H. V.; Tontonoz, P., Attenuation of neuroinflammation and Alzheimer's disease pathology by liver X receptors. *Proc. Natl. Acad. Sci. USA.* **2007,** 104, 10601-6.
172. Frenkel, D.; Smit, B., *Understanding molecular simulations: from algorithms to applications*. Academic Press: San Diego, CA, 2002.
173. Groot, R. D.; Warren, P. B., Dissipative particle dynamics: bridging the gap between atomistic and mesoscopic simulation. *J Chem Phys* **1997,** 107, 4423-4435.
174. Maiti, A.; McGrother, S., Bead–bead interaction parameters in dissipative particle dynamics: relation to bead-size, solubility parameter, and surface tension. *J Chem Phys* **2004,** 120, 1594-1601.
175. Lee, H.; Larson, R. G., Multiscale modeling of dendrimers and their interactions with bilayers and polyelectrolytes. *Molecules* **2009,** 14, (1), 423-38.
176. Srinivas, G.; Discher, D. E.; Klein, M. L., Self-assembly and properties of diblock copolymers by coarse-grain molecular dynamics. *Nat Mater* **2004,** 3, (9), 638-44.
177. Peng, L. X.; Ivetac, A.; Van, S.; Zhao, G.; Chaudhari, A. S.; Yu, L.; Howell, S. B.; McCammon, J. A.; Gough, D. A., Characterization of a clinical polymer-drug conjugate using multiscale modeling. *Biopolymers* **2010**.
178. Ahmad, S.; Johnston, B. F.; Mackay, S. P.; Schatzlein, A. G.; Gellert, P.; Sengupta, D.; Uchegbu, I. F., In silico modelling of drug-polymer interactions for pharmaceutical formulations. *J R Soc Interface* **2010**.
179. Moore, K. J.; Kunjathoor, W.; Koehn, S. L.; Manning, J. J.; Tseng, A. A.; Silver, J. M.; McKee, M.; Freeman, M. W., Loss of receptor-mediated lipid uptake via scavenger receptor A or CD36 pathways does not ameliorate atherosclerosis in hyperlipidemic mice. *J. Clin. Invest.* **2005,** 115, 2192-2201.
180. Holvoet, P.; Harris, T. B.; Tracy, R. P.; Verhamme, P.; Newman, A. B.; Rubin, S. M.; Simonsick, E. M.; Colbert, L. H.; Kritchevsky, S. B., Association of high coronary heart disease risk status with circulating oxidized LDL in the well-functioning elderly: findings from the Health, Aging, and Body Composition study. *Arterioscler Thromb Vasc Biol* **2003,** 23, (8), 1444-8.
181. Li, D.; Liu, L.; Chen, H.; Sawamura, T.; Ranganathan, S.; Mehta, J. L., LOX-1 mediates oxidized low-density lipoprotein-induced expression of matrix metalloproteinases in human coronary artery endothelial cells. *Circulation* **2003,** 107, (4), 612-7.
182. Mehta, J. L.; Sanada, N.; Hu, C. P.; Chen, J.; Dandapat, A.; Sugawara, F.; Satoh, H.; Inoue, K.; Kawase, Y.; Jishage, K.; Suzuki, H.; Takeya, M.; Schnackenberg, L.; Beger, R.; Hermonat, P. L.; Thomas, M.; Sawamura, T., Deletion of LOX-1 reduces atherogenesis in LDLR knockout mice fed high cholesterol diet. *Circ Res* **2007,** 100, (11), 1634-42.
183. Ogura, S.; Kakino, A.; Sato, Y.; Fujita, Y.; Iwamoto, S.; Otsui, K.; Yoshimoto, R.; Sawamura, T., Lox-1: the multifunctional receptor underlying cardiovascular dysfunction. *Circ J* **2009,** 73, (11), 1993-9.

184. Sawamura, T.; Kume, N.; Aoyama, T.; Moriwaki, H.; Hoshikawa, H.; Aiba, Y., An endothelial receptor for oxidized low-density lipoprotein. *Nature* **1997,** 386, 73-77.
185. Gao, D.; Ashraf, M. Z.; Kar, N. S.; Lin, D.; Sayre, L. M.; Podrez, E. A., Structural basis for the recognition of oxidized phospholipids in oxidized low density lipoproteins by class B scavenger receptors CD36 and SR-BI. *J Biol Chem* 285, (7), 4447-54.
186. Ohki, I.; Ishigaki, T.; Oyama, T.; Matsunaga, S.; Xie, Q.; Ohnishi-Kameyama, M.; Murata, T.; Tsuchiya, D.; Machida, S.; Morikawa, K.; Tate, S., Crystal structure of human lectin-like, oxidized low-density lipoprotein receptor 1 ligand binding domain and its ligand recognition mode to OxLDL. *Structure* **2005,** 13, (6), 905-17.
187. Moriwaki, H.; Kume, N.; Sawamura, T.; Aoyama, T.; Hoshikawa, H.; Ochi, H.; Nishi, E.; Masaki, T.; Kita, T., Ligand specificity of LOX-1, a novel endothelial receptor for oxidized low density lipoprotein. *Arterioscler Thromb Vasc Biol* **1998,** 18, (10), 1541-7.
188. Mu, F. T.; Callaghan, J. M.; Steele-Mortimer, O.; Stenmark, H.; Parton, R. G.; Campbell, P. L.; McCluskey, J.; Yeo, J. P.; Tock, E. P.; Toh, B. H., EEA1, an early endosome-associated protein. EEA1 is a conserved alpha-helical peripheral membrane protein flanked by cysteine "fingers" and contains a calmodulin-binding IQ motif. *J Biol Chem* **1995,** 270, (22), 13503-11.
189. Chen, Y. T.; Holcomb, C.; Moore, H. P., Expression and localization of two low molecular weight GTP-binding proteins, Rab8 and Rab10, by epitope tag. *Proc Natl Acad Sci U S A* **1993,** 90, (14), 6508-12.
190. Febbraio, M.; Silverstein, R. L., Identification and characterization of LAMP-1 as an activation-dependent platelet surface glycoprotein. *J Biol Chem* **1990,** 265, (30), 18531-7.
191. Veillard, N. R.; Kwak, B.; Pelli, G.; Mulhaupt, F.; James, R. W.; Proudfoot, A. E.; Mach, F., Antagonism of RANTES receptors reduces atherosclerotic plaque formation in mice. *Circ Res* **2004,** 94, (2), 253-61.
192. Morand, E. F., New therapeutic target in inflammatory disease: macrophage migration inhibitory factor. *Intern Med J* **2005,** 35, (7), 419-26.
193. Kalinowska, A.; Losy, J., Investigational C-C chemokine receptor 2 antagonists for the treatment of autoimmune diseases. *Expert Opin Investig Drugs* **2008,** 17, (9), 1267-79.
194. Guo, J.; Van Eck, M.; Twisk, J.; Maeda, N.; Benson, G. M.; Groot, P. H.; Van Berkel, T. J., Transplantation of monocyte CC-chemokine receptor 2-deficient bone marrow into ApoE3-Leiden mice inhibits atherogenesis. *Arterioscler Thromb Vasc Biol* **2003,** 23, (3), 447-53.
195. Gu, L.; Okada, Y.; Clinton, S. K.; Gerard, C.; Sukhova, G. K.; Libby, P.; Rollins, B. J., Absence of monocyte chemoattractant protein-1 reduces atherosclerosis in low density lipoprotein receptor-deficient mice. *Mol Cell* **1998,** 2, (2), 275-81.
196. Duffy, S. J.; Dart, A. M., Novel cardiac therapies and innocent by standers. *Lancet* **2008,** 371, (9626), 1726-8.
197. Besemer, J.; Harant, H.; Wang, S.; Oberhauser, B.; Marquardt, K.; Foster, C. A.; Schreiner, E. P.; de Vries, J. E.; Dascher-Nadel, C.; Lindley, I. J., Selective inhibition of

cotranslational translocation of vascular cell adhesion molecule 1. *Nature* **2005,** 436, (7048), 290-3.
198. Duffy, S. J.; Dart, A. M., Novel cardiac therapies and innocent bystanders. *Lancet* **2008,** 371, 1726-1728.
199. Tardif, J. C.; McMurray, J. J.; Klug, E.; Small, R.; Schumi, J.; Choi, J.; Cooper, J.; Scott, R.; Lewis, E. F.; L'Allier, P. L.; Pfeffer, M. A., Effects of succinobucol (AGI-1067) after an acute coronary syndrome: a randomized, double-blind, placebo-controlled trial. *Lancet* **2008,** 371, 1761-1768.
200. van Lent, P. L.; Hofkens, W.; Blom, A. B.; Grevers, L.; Sloetjes, A.; Takahashi, N.; van Tits, L. J.; Vogl, T.; Roth, J.; de Winther, M. P.; van den Berg, W. B., Scavenger receptor class A type I/II determines matrix metalloproteinase-mediated cartilage destruction and chondrocyte death in antigen-induced arthritis. *Arthritis Rheum* **2009,** 60, (10), 2954-65.
201. Begany, A.; Simon, M., Jr.; Dehmel, N.; Hunyadi, J., Expression of thrombospondin-1 (TSP1) and its receptor (CD36) in healthy and diseased human skin. *Acta Derm Venereol* **1994,** 74, (4), 269-72.
202. Oz, H. S.; Zhong, J.; de Villiers, W. J., Pattern Recognition Scavenger Receptors, SR-A and CD36, Have an Additive Role in the Development of Colitis in Mice. *Dig Dis Sci* **2009**.
203. Sun, Y.; Scavini, M.; Orlando, R. A.; Murata, G. H.; Servilla, K. S.; Tzamaloukas, A. H.; Schrader, R.; Bedrick, E. J.; Burge, M. R.; Abumrad, N. A.; Zager, P. G., Increased CD36 Expression Signals Monocyte Activation Among Patients with Type 2 Diabetes Mellitus. *Diabetes Care* **2010**.
204. Pellicano, M.; Bulati, M.; Buffa, S.; Barbagallo, M.; Di Prima, A.; Misiano, G.; Picone, P.; Di Carlo, M.; Nuzzo, D.; Candore, G.; Vasto, S.; Lio, D.; Caruso, C.; Romano, G. C., Systemic Immune Responses in Alzheimer's Disease: In Vitro Mononuclear Cell Activation and Cytokine Production. *J Alzheimers Dis* **2010**.
205. Ohar, J. A.; Hamilton, R. F., Jr.; Zheng, S.; Sadeghnejad, A.; Sterling, D. A.; Xu, J.; Meyers, D. A.; Bleecker, E. R.; Holian, A., COPD is associated with a macrophage scavenger receptor-1 gene sequence variation. *Chest* **2010,** 137, (5), 1098-107.
206. Allen, T., Cullis PR, Drug delivery systems: entering the mainstream. *Science* **2004,** 303, 1818-1822.
207. Edens, H., Levi BP, Jaye DL, et al., Neutrophil transepithelial migration: evidence for sequential, contact-dependent signaling events and enhanced paracellular permeability independent of transjunctional migration. *J Immunol* **2002,** 169, 476-486.
208. Gao, X., Cui Y, Levenson RM, et al, In vivo cancer targeting and imaging with semiconductor quantum dots. *Nat Biotechnol* **2004,** 22, 969-976.
209. Jain, T., Morales MA, Sahoo SK, et al, Iron oxide nanoparticles for sustained delivery of anticancer agents. *Mol Pharm* **2005,** 2, 194-205.
210. Pelicano, H., Martin DS, Xu RH, Huang P., Glycolysis inhibition for anticancer treatment. *Oncogene* **2006,** 25, 4633-4646.
211. Deryugina, E., Quigley JP, Matrix metalloproteinases and tumor metastasis. *Cancer Metastasis Rev* **2006,** 25, 9-34.

212. Brannon-Peppas, L., Blanchette JO, Nanoparticle and targeted systems for cancer therapy. *Adv. Drug Delivery Rev* **2004,** 56, 1649-1659.
213. Sledge, G. J., Miller KD., Exploiting the hallmarks of cancer: the future conquest of breast cancer. *Eur J Cancer* **2003,** 39, 1668-1675.
214. Jain, R., Transport of molecules across tumor vasculature. *Cancer Metastasis Rev* **1987,** 6, 559-593.
215. Cuenca, A., Jiang H, Hochwald SN, et al, Emerging implications of nanotechnology on cancer diagnostics and therapeutics. *Cancer* **2006,** 107, 459-466.
216. Gibson, A. E.; Noel, R. J.; Herlihy, J. T.; Ward, W. F., Phenylarsine oxide inhibition of endocytosis: effects on asialofetuin internalization. *Am J Physiol* **1989,** 257, (2 Pt 1), C182-4.
217. Motulsky, H., and Christopoulos, A, *Fitting Models to Biological Data using Linear and Nonlinear Regression*. GraphPad Software Inc.: San Diego, 2003.
218. *Biacore 3000 Instrument Handbook*. Biacore: 2003.

CURRICULUM VITAE

Nicole M. Plourde

EDUCATION

Ph.D. in Chemical and Biochemical Engineering, September 2004 - October 2010
Rutgers University, NJ

- Thesis: *Nanoscale Amphiphilic Polymers for Modulation of Macrophage-LDL Interactions Underlying Atherogenesis*

B.S. in Chemical Engineering with a minor in Chemistry, September 2000 - May 2004
University of Massachusetts Amherst, MA

- Cum laude
- Commonwealth College Honors Program

RESEARCH AND PROFESSIONAL EXPERIENCE

Graduate Assistant, September 2004 – August 2010
Rutgers University, Department of Chemical and Biochemical Engineering
PhD Thesis advisor: Professor Prabhas V. Moghe

- Investigated the effect of biocompatible amphiphilic polymers on modulating oxidized LDL accumulation in macrophages through receptor blocking, and the ability of the polymer to encapsulate a cholesterol reducing agonist and selectively deliver it to activated macrophages.
- Studied the binding of various nanopolymer configurations toward the key scavenger receptors mediating oxLDL binding and uptake in order to elucidate and assess correlations between polymer architecture, chemistry and binding affinity and thereby to establish the most effective nanopolymer construction for targeting macrophage cells.
- Developed molecular modeling approaches to describe the major domains within modeled scavenger receptors and studied binding behavior for screening polymers with varying chemistries.

Intern in the Merck Future Talent Program, May 2007 – August 2007
Merck & Co, Inc., Rahway, NJ

- Worked in the department of Cardiovascular New Targets on Research and Development

Teaching Assistant, Spring 2005 – Fall 2006
Rutgers University, Department of Chemical and Biochemical Engineering

Head teaching assistant for two senior level courses: Chemical Engineering Analysis II (Fall 2005) and Transport Phenomena II (Spring 2006)

- Conducted office hours and review sessions
- Graded homework

PATENT

- Moghe PV, Uhrich KE, Iverson N, Plourde N, Wang JZ. Compositions and Methods for Treating Cardiovascular Conditions. PCT International Patent Application: 08/077247. Filing Date: September 22, 2008.

PUBLICATIONS

- Plourde, N; Hehir, S; Kamisoglu, K; Welsh, W; Moghe, P "Sterereochemical Requirements of Nanoscale Amphiphilic Polymers for Inhibition of Cholesterol Trafficking via Scavenger Receptors SR-A and LOX-1 (in preparation).

- Iverson, N; Plourde, N; Sparks, S; Wang, J; Patel, E; Nackman, G; Uhrich, KE; Moghe, PV "Bioactive Polymers for Inhibition of Inflammation and Atherogenesis in Activated Macrophages" (submitted to Circulation Research, 2010)

- Plourde, N; Kortagere, S; Welsh, W; Moghe, P "Structure Activity Relations of Nanolipoblockers with the Atherogenic Domain of Human Macrophage Scavenger Receptor A", Biomacromolecules, 10(6):1381-91 (2009)

- Iverson, N; Plourde, N; Chnari, E; Nackman, GB; Moghe, PV "Convergence of Nanotechnology and Cardiovascular Medicine: Progress and emerging prospects", BioDrugs, 22 (1) 1-10 (2008).

- Wang, J; Plourde, NM; Iverson, N; Moghe, PV and Uhrich, KE "Nanoscale Amphiphilic Macromolecules as Lipoprotein Inhibitors: The role of charge and architecture", Intern. J. Nanomedicine, 2 (4) 697-705 (2007).